

**Identification of antioxidant active trace element  
proteins in animal cells and human cell lines using  
bioanalytical methods**

Dissertation zur Erlangung des akademischen Grades des  
Doktors der Naturwissenschaften (Dr. rer. nat.)

eingereicht im Fachbereich Biologie, Chemie, Pharmazie  
der Freien Universität Berlin

vorgelegt von

Elżbieta Charkiewicz

2012

Diese Arbeit wurde in der Arbeitsgruppe „Elementanalytik (F-A1)“ am Helmholtz – Zentrum Berlin für Materialien und Energie unter der Leitung von Herrn Dr. Kyriakopoulos angefertigt.

1. Gutachter: Prof. Dr. Ulrich Abram
2. Gutachter: Prof. Dr. Nora Graf

Disputation am: 25.06.2012

# Contents

<b>1. Main aims .....</b>	<b>4</b>
<b>2. Introduction.....</b>	<b>5</b>
2.1. Antioxidants .....	5
2.1.1. The function of antioxidants .....	5
2.1.2. Antioxidants in biological systems .....	6
2.2. Oxidants .....	7
2.2.1. The role of oxidants in the living organism .....	8
2.2.2. Free Radicals .....	8
2.2.3. Reactive oxygen species .....	8
2.2.4. Oxidative stress .....	9
2.3. Trace elements .....	10
2.4. Selenium .....	11
2.4.1. Selenium-containing proteins in mammals .....	12
2.5. Skeletal muscle .....	13
2.6. Lung .....	14
<b>3. Materials and Methods.....</b>	<b>17</b>
3.1. Materials .....	17
3.1.1. Experimental animals.....	17
3.1.2. Cell lines.....	17
3.1.3. Antibodies .....	18
3.1.4. Radiotracer <sup>75</sup> Se .....	19
3.1.5. Chemicals.....	19
3.1.6. Buffer and solutions .....	19
3.1.7. Equipment .....	20
3.1.8. Software .....	20
3.1.9. Bioinformatics.....	20
3.1.10. Text and data converting.....	21
3.2. Methods.....	21
3.2.1. Sample preparation.....	21
3.2.1.1. Homogenization of tissues .....	21
3.2.1.2. Homogenization of cells.....	22
3.2.1.3. Subcellular fractionation .....	22
3.2.1.3.1. Separation by ultracentrifugation .....	22

3.2.1.3.2. Separation by density-gradient centrifugation.....	23
3.2.1.3.3. Identification of separated organelles.....	24
3.2.2. Protein chemistry .....	25
3.2.2.1. Bradford protein assay.....	25
3.2.2.2. Polyacrylamide gel electrophoresis.....	25
3.2.2.3. Two-dimensional gel electrophoresis.....	26
3.2.2.3.1. First dimension (NEpHGE).....	27
3.2.2.3.2. Second dimension.....	28
3.2.2.4. Staining of polyacrylamide gels.....	28
3.2.2.4.1. Coomassie staining.....	28
3.2.2.4.2. Silver staining of Blum.....	29
3.2.2.5. Western blotting.....	29
3.2.2.6. Immunoassays .....	30
3.2.2.7. Gel drying.....	30
3.2.2.8. Autoradiography.....	31
3.2.3. Immunocytochemistry.....	31
3.2.3.1. Glutathione peroxidase activity assay .....	32
3.2.4. ABTS assay .....	33
3.2.5. Paraoxonase Purification.....	33
3.2.5.1. Plasma pre-treatment.....	33
3.2.5.2. DEAE-Sephadex A-50 column chromatography .....	34
3.2.5.3. Sephadex G 200 gel filtration chromatography .....	34
3.2.5.4. Paraoxonase activity.....	35
3.2.6. Analytical method .....	35
3.2.6.1. Neutron activation analysis .....	35
3.2.6.2. Speciation Analysis .....	37
3.2.6.2.1. Inductively coupled plasma mass spectrometry .....	37
3.2.6.2.2. Size exclusion chromatography.....	38
<b>4. Results.....</b>	<b>40</b>
4.1. Elemental analysis.....	40
4.1.1. Determination of trace element concentration by means of INAA.....	40
4.1.1.1. Determination of element concentration in selected tissues of the rat .....	41
4.1.1.2. Distribution of trace element in the subcellular fractions of the skeletal muscle, lung and spleen.....	43
4.1.2. Summary .....	46
4.2. Trace experiments with <sup>75</sup> Se in the cultured cells .....	47
4.2.1. Selenium – containing proteins in the cell lines C2C12 with SDS- PAGE .....	48

4.2.2. Selenium – containing proteins in the cell lines A549 with SDS-PAGE.....	49
4.2.3. Characterization and identification of selenium containing proteins in the cell lines C2C12 and A549 with SDS-PAGE.....	50
4.2.4. Selenium – containing proteins in the subcellular fractions of the cell lines C2C12 by two - dimensional gel electrophoresis .....	52
4.2.5. Selenium – containing proteins in the subcellular fractions of the cell lines A549 by two - dimensional gel electrophoresis.....	55
4.2.6. Study on the selenium-containing proteins in the cell lines C2C12 and A549 by two-dimensional gel electrophoresis.....	57
4.2.7. Summary .....	60
4.3. Antioxidant activity .....	61
4.3.1. The total antioxidant status in cytosolic fraction .....	61
4.3.2. AOS-scavenging enzymes .....	63
4.3.2.1. GPx 1 activity in the cytosol .....	63
4.3.2.2. Detection and localization of antioxidants proteins .....	65
4.3.2.2.1. TrxR1.....	66
4.3.2.2.2. GPx1 .....	68
4.3.2.2.3. Selenoprotein 15 kDa .....	69
4.3.2.2.4. Cu/Zn SOD .....	71
4.3.2.2.5. Catalase.....	73
4.3.2.2.6. PON 1 .....	75
4.3.2.2.7. Effect of the selenium status on the distribution of antioxidants proteins in the tissues of the skeletal muscle, lung and spleen.....	77
4.3.3. Speciation analysis of the trace element – containing proteins.....	79
4.3.3.1. Column calibration.....	87
4.3.3.2. Summary .....	88
4.3.4. Effect of selenium status of the proteome of skeletal muscle, lung and spleen.....	90
4.3.5. Summary .....	92
4.4. Paraoxonase 1 .....	94
4.4.1. Purification.....	94
4.4.1.1. Activity.....	94
4.4.1.2. Detection and localization of Paraoxonase 1 in the human plasma .....	96
4.4.2. Speciation analysis of the Paraoxonase 1.....	97
4.4.3. PON 1 localization in the cell lines.....	99
4.4.4. Localization of lanthanum-binding proteins .....	101
4.4.5. Summary .....	103
<b>5. Discussion .....</b>	<b>105</b>
<b>6. Summary.....</b>	<b>114</b>

<b>7. Zusammenfassung .....</b>	<b>117</b>
<b>8. References.....</b>	<b>120</b>
<b>9. Appendix.....</b>	<b>132</b>
9.1. List of abbreviations.....	132
9.2. Publication .....	133
9.3. Acknowledgements.....	136
9.4. Curriculum Vitae.....	137
9.5. Selbständigkeitserklärung .....	138

# 1. Main aims of the present work

Function and role of antioxidants are important for several fields of science. For example the better knowledge can help to prevent a lot of diseases.

The skeletal muscle and the lung, with regard to their function, are influenced by many exogenous and endogenous factors such as changes in energy supply, oxygen flux during contraction, atmospheric pollutants like ozone, nitrogen peroxide, cigarette smoke, asbestos, herbicides and many metals and metalloids obtained in the aerosolic particular matter. The lung contains the largest endothelial surface area, which therefore makes it a major target site for circulating oxidants. Exposure to this factors lead to the alteration of the skeletal muscle and lung. Therefore both organs require a specific antioxidant system.

Previous studies have suggested that numerous trace elements are involved in oxidative stress [1-3, 23]. Most of the trace elements occur in the cells in protein-bound form.

The function of trace elements in the cells and tissues is strongly dependent on their concentrations and chemical species. To this day it is not known how and how many of these elements are involved in oxidative stress. It is therefore of great interest:

- to determine the trace elements present in the skeletal muscle and lung,
- to obtain information on their subcellular distribution,
- to obtain information on their antioxidative effect

Numbers of experiments were carried out. Using elemental analytical methods the concentrations of several trace elements in the skeletal muscle, lung and their subcellular fractions were determined. For studies on the trace element protein binding, speciation analysis was applied in order to find patterns in the investigated tissues. The combination of biochemical methods and tracer techniques was used for investigation of selenium – containing proteins, their localization, characterisation and identification. For the detection and localization of antioxidative proteins immunoassays were applied. In this work the total antioxidant status and the action of individual elements of them was analyzed. The spleen, its important roles with regard to red blood cells and the immune system was used in this study as comparison tissue.

## **2 Introduction**

### **2.1 Antioxidants**

The living organism is exposed to many exogenous and endogenous factors, which can affect the balance between oxidants and antioxidants. As a consequence of this process many diseases occur.

The antioxidants can be defined as substances, which in comparatively low concentration can delay or decrease the oxidation of a substrate [4].

#### **2.1.1 The function of antioxidants**

Antioxidants have a very important function for the cellular protection against the deleterious effects of reactive oxidants generated in the aerobic metabolism. The principles of the antioxidant defense strategy include three essential levels of protection: prevention, disconnection and repair [5].

The first step of defense is prevention, which protects against oxidants formation. Early studies have shown that cells and body fluids have many enzymatic systems to control the level of oxidants. They can generate a cascade of products, which are able to attack oxidants. The prevention of initiation of chain reactions includes the binding of metal in form of ions, especially copper and iron. Metal chelation is a major way of controlling lipid peroxidation and DNA fragmentation. Therefore, metal-binding proteins, like ferritin, transferrin, metallothionein and others, take a central role in the control of potential radical-generating reactions. Another way to increase the resistance against metal ion-dependent oxidation is to modify the potential target site [1, 6].

The second step of the antioxidant defense strategy is disconnection. This is the process of deactivation. The radical compounds are transformed to non-radical and non-reactive end products.

When prevention and disconnection processes are not effective, the body has several cellular repair systems. Continuously formed oxidants can cause DNA damage and can break single-strand or double-strand of DNA. They can also cause membrane damage



in form of phospholipids oxidation and can damage proteins and other compounds. This can lead to dysfunction of organism or diseases [7, 8].

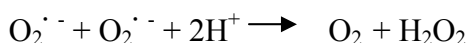
## 2.1.2 Antioxidants in biological systems

The antioxidant defense can be potentiated by combination of lipid- and water-soluble antioxidants. In general, lipid-soluble antioxidants protect cell membranes from lipid peroxidation. Water-soluble antioxidants react with oxidants in the cell cytosol and the body plasma.

These compounds are synthesized in the body or obtained from diet.

These two groups consist of many enzymic and non-enzymic systems, which control the level of oxidants. The major enzymic antioxidants are superoxide dismutase, glutathione peroxidase and catalase [9-11]. The important antioxidants are presented in the Table 2.1.

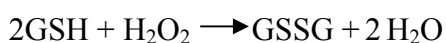
Superoxide dismutase (SOD) transforms superoxide radicals ( $O_2^{\cdot -}$ ) to molecular oxygen ( $O_2$ ) and hydrogen peroxide ( $H_2O_2$ ).



SOD with different catalytic metal ions Cu, ZnSOD, MnSOD/FeSOD and NiSOD are found in Eukaryotes and some prokaryotes. The last-mentioned protein had been found in bacteria only. All classes of SOD are characterized by disproportionation reaction, occurring through alternate oxidation and reduction of their catalytic metal ions. SOD catalysis takes place at rates close to diffusion limits [12].

In mammals three types of SOD had been described. One cytoplasmatic and extracellular enzyme possesses Cu – Zn atoms and one mitochondrial enzyme possesses Mn atom [13, 14].

Glutathione peroxidase (GPx) catalyzes the reduction of  $H_2O_2$  or organic hydroperoxides to water or the corresponding alcohols using reduced glutathione [15].



The mammalian GPx family consists of eight proteins. The known selenium-containing GPxs are GPx1, GPx2, GPx3, GPx4 and, depending on species, GPx6 [16].

Catalase generates molecular oxygen as a consequence of oxidation of hydrogen peroxide. The activity of the enzyme catalase is dependent on the structural conformation of three essential domains. The heme moiety at the active site reduces NADPH bound in the NADPH-binding domain and a complex secondary structure formed by the threading and intertwining of long peptide loops during tetramerization [17].

<b>System</b>	<b>Examples of antioxidants</b>
Non-enzymic	$\alpha$ -tocopherol (vitamin E), $\beta$ -carotene, ascorbate (vitamin C), glutathione (GSH), urate, bilirubin, ubiquinone plasma proteins (metal binding, e.g. ceruloplasmin, albumin, etc.)
Enzymic (direct)	superoxide dismutase (SOD), catalase, glutathione peroxidase (GPx)
Enzymic (indirect)	conjugation enzymes (glutathione-S-transferase, UDP-glucuronosyl-transferase NADPH-oxidoreductase, NADPH (pentose phosphate pathway), Glutathione reductase (GR)
Repair systems	DNA repair systems, oxidized protein turnover

Table 2.1 Important antioxidants in biological systems [5]

## 2.2 Oxidants

Oxidants occur naturally as part of normal body processes. They cause extensive damage to DNA, proteins and lipids. This damage is a major contributor to aging and degenerative diseases such as cancer, cardiovascular disease, immune-system decline and brain dysfunction.

### **2.2.1 The role of oxidants in the living organism**

In the living organism, oxidants are generated in many ways. The famous oxidants like superoxide, hydrogen peroxide and hydroxyl radical are known as mutagens produced by radiation but they are also produced as by-product in the normal metabolism [18].

As a consequence of normal aerobic respiration mitochondria consume oxygen, which is reduced to water. Unavoidable by-products in this process are  $O_2^-$ ,  $H_2O_2$  and  $HO^{\cdot}$  [19, 20].

Another way oxidants are generated is in the defense system against pathogens. Phagocytes cells damage bacteria or virus infected cells with an oxidative burst of nitric oxide, superoxide anion radical, hydrogen peroxide and  $OCl^-$  [21].

Oxidants can also be produced in peroxisomes, in which the fat acid and other molecules are degraded [22].

### **2.2.2 Free Radicals**

Free radicals can be defined as atoms or molecules with at least one unpaired electron.

In this extremely unstable configuration, the radicals react with other molecules or radicals in order to achieve a stable configuration by capturing missing electrons.

### **2.2.3 Reactive oxygen species**

Reactive oxygen species (ROS) are generated through normal processes of the live of aerobic organisms as consequence of electron transport processes in aerobic respiration and photosynthesis. They can be formed by other mechanisms like the interaction of ionizing radiation or synthesized by dedicated enzymes in phagocytes cells like neutrophils and macrophages.

Under correct physiological conditions these harmful species are generally neutralized by the cellular antioxidants system, which consists of antioxidants enzymes, vitamins, glutathione and thiols [23, 24].

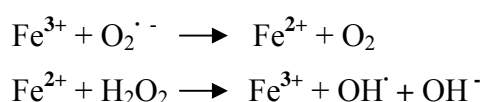
The production of ROS is assumed to be the fundamental mechanism for the biochemical and physiological changes that occur during exercise and are indicative of oxidative stress.

The known ROS and their half-live are present in Table 2.2.

<b>ROS</b>	<b>Half-life [s]</b>
HO <sup>•</sup> hydroxyl radical	10 <sup>-9</sup>
RO <sup>•</sup> alkoxy radical	10 <sup>-6</sup>
ROO <sup>•</sup> peroxy radical	7
H <sub>2</sub> O <sub>2</sub> hydrogen peroxide	- (enzymic)
O <sub>2</sub> <sup>•-</sup> superoxide anion radical	- (enzymic)
<sup>1</sup> O <sub>2</sub> singlet oxygen	10 <sup>-5</sup>
NO <sup>•</sup> nitric oxide radical	1-10
ONOO <sup>-</sup> peroxynitrite	0.05-1

Table 2.2 Reactive oxygen species and their half-lives [5]

Long-living ROS such as O<sub>2</sub><sup>•-</sup> or H<sub>2</sub>O<sub>2</sub> can diffuse into other cells, where they also generate aggressive radicals like OH<sup>•</sup>. The reactive OH<sup>•</sup> in this way can oxidate the cells structure [5, 25]. It occurs in the Haber-Weiss reaction by catalysis of the free iron and copper ions from superoxide anion radical and hydrogen peroxide.



## 2.2.4 Oxidative stress

Imbalance between reactive oxygen species (ROS) and antioxidants, with disadvantage for the second, is referred to as oxidative stress. The effect of oxidative stress can damage all components of the cells, including DNA, proteins and lipids, which can trigger apoptosis. Long-time intense stress may cause necrosis. In this case the cell is not able to control the biochemical and biological functions and therefore is the oxidative stress responsible for many diseases in humans such as atherosclerosis,

Parkinson's disease, Alzheimer's disease, heart failure, myocardial infarction, muscular dystrophy and has role of aging processes [26-29].

## **2.3 Trace elements**

The trace elements for a long time were regarded only as causal existent components of the body. In the further development of the examinations in this matter it was assessed that these elements with their small concentration are not only hazard but the elements have a very important function in the body.

The important essential trace elements are iron, copper, iodine, zinc, selenium, manganese, chromium and cobalt. The other elements, which are continuously established in tissues, but are not known as essential, are cadmium, arsenic, mercury, vanadium, rubidium, aluminum, fluorine and lead. For these elements the nutritional value is not known and some of them are found as toxic. Previous studies have demonstrated the toxic effect of mercury or cadmium in comparatively low level of concentration [30, 31]. The effect of the trace elements is strongly dependent on their specific concentration and chemical forms. In the living organism this is important for two reasons. First, because metabolic deficit of essential metal impairs the function of the synthesized biomolecules. Second, a local excess of trace elements could be toxic.

The living organism transports and stores elements in many ways. These elements can be delivered in accurate concentration and to an exact location in the body. In these processes many proteins are involved.

In the living organism essential trace elements are important functional, structural and regulatory components of numerous biomolecules. These elements have both catalytic and structural roles in enzymes and are critical for the function of a number of metalloproteins. They are also involved in the function of membrane transport, nerve conduction, muscle contraction and the antioxidative defense system.

## 2.4 Selenium

The trace element selenium was discovered by Swedish chemist Jöns Jacob Berzelius in 1817, who named it after Selene, the Greek moon goddess. The element was found in a Swedish factory as an impurity in the waste from the production of sulfuric acid. Selenium occurs in almost all rocks, soils and water bodies and is usually combined with sulfur in copper, nickel, lead and silver minerals. In the Periodic Table of Elements, selenium is found in the VI group together with oxygen, sulfur, tellurium and polonium. It is a chemical element with atomic number of 34, an atomic weight of 78.96 g/mol and chemical symbol Se. It is a metalloid, whose chemical properties are related to sulfur and tellurium. In compounds its most common valence states are 6, 4, 2 and -2. A number of allotropic forms of this element exist. This element can be prepared with either an amorphous or crystalline structure. The color of amorphous selenium is red in powder form, or black in vitreous form. Crystalline hexagonal selenium is colored metallic gray and it is the most stable variety. Crystalline monoclinic selenium is deep red. Selenium has six naturally occurring isotopes:  $^{74}\text{Se}$ ,  $^{76}\text{Se}$ ,  $^{77}\text{Se}$ ,  $^{78}\text{Se}$ ,  $^{80}\text{Se}$ , and  $^{82}\text{Se}$ . About fifteen other isotopes have been characterized.

Actually selenium is used in the electronic industry (photocopying, photocells, solar cells), in photography, in the glass industry and as a component of pigments of plastics, paints, inks and rubber. Radioactive selenium is used in diagnostic medicine.

Selenium is also an important element for many live forms, but only in small concentration, because in higher concentration it can be toxic. About fifty years ago, it was reported for the first time about the essentiality of selenium. Schwarz and Foltz reported that selenium administered to vitamin E deficient rats prevented liver necrosis [32]. The trace element selenium plays many vital roles in the human and the animal body, including antioxidants, cancer protection, DNA repair, production of sperm cells, detoxification of poisonous metals, antibody synthesis, immunity, cellular respiration and energy transfer. Human selenium deficiency is associated with low levels of selenium in the soil in countries or regions (North and East Asia) [33]. For example the Keshan disease is a cardiomyopathy that affects young women and children in a selenium deficient region of China. The incidence of this disease is closely associated with very low dietary intakes of selenium and a poor selenium nutritional status. Another disease which is associated with low selenium status in areas of northern China, North Korea and eastern Siberia, is the Kashin-Back Disease [34].

On the other hand high level of selenium can result in a condition called selenosis. Symptoms of selenosis include gastrointestinal upsets, garlic breath odor, hair loss, white blotchy nails, irritability, and mild nerve damage [35].

### **2.4.1 Selenium-containing proteins in mammals**

Mammals require selenium for the function of many selenium-dependent proteins. In the human selenoproteome 25 selenium-containing proteins are known [36]. The following proteins belong to the family of glutathione peroxidase. This protein group includes the ubiquitously expressed cytosolic GPx1 which can metabolize hydrogen peroxide [37]. Gastrointestinal GPx2 has a specific function in protecting the gastrointestinal tract against inflammation and cancer development [38]. Plasma GPx3 is an efficient antioxidant [39]. Phospholipid hydroperoxide GPx4 can reduce phospholipid and cholesterol hydroperoxides [40]. The sperm nuclei-specific enzyme snGPx4 [41] and a new discovered glutathione peroxidase GPx6 is located in olfactory epithelium and embryonic tissues [42]. The iodothyronine deiodinases (DIOs) consist of three different distributed Se-containing oxidoreductases. DIO1 and DIO2 catalyze the activation and DIO3 the inactivation of the thyroid hormones thyroxine ( $T_4$ ), 3,5,3'-triiodotyronine ( $T_3$ ) and reverse-3,5,3'-triiodotyronine ( $rT_3$ ) by removing distinct iodine moieties [43]. Thioredoxin reductases have a function in the regeneration of several antioxidant systems [44].

The second important selenoprotein in plasma is Selenoprotein P, which is estimated to contain 50% of the plasma selenium [45]. The function of 15 kDa protein is unknown, it was suggested that it could play a role in regulation of apoptosis [46]. The biological function of Selenoprotein N and W is not known as well. It is clear that the SelN plays a vital role in muscle tissues and SelW probably has antioxidant function [47-49]. Selenophosphate synthetase 2 is involved in the Sec (selenocysteine) biosynthesis and catalyzes the conversion of selenide to selenophosphate [50]. The nucleus and cytoplasm localized Sel R is a redox-active selenoprotein with a specific enzymatic function for the repair of oxidative damaged proteins [51]. Another selenoprotein is the Sel K. Overexpression of it decreases the levels of intracellular ROS and protects cardiomyocytes against oxidative stress [52].

Further selenium-containing proteins with unknown function are SelM, SelH, SelO, SelI, SelT, SelV.

## **2.5 Skeletal muscle**

Skeletal muscle constitutes 40 – 50% of the total body weight and is considered the largest single organ of the body. The tissue is voluntarily controlled under the somatic nervous system and in addition to cardiac and smooth muscle, the skeletal muscle is one of the three major muscle types.

Skeletal muscle is formed from spindle-shaped muscle precursor cells – myoblasts. The cells fuse together to form a new cell with more nuclei and in this fusion process elongated tubular cells are formed, which are the mature multinucleated skeletal muscle cells or muscle fiber. The muscle fibers are composed of myofibrils. Cross-section of myofibrils expose existence of two types of filaments- thick and thin. Thick filaments with radius of about 15 nm are composed of myosin and the thin filaments with radius of about 9 nm are composed of actin, tropomyosin and troponin complex. Both filaments are composed of repeating sections of sarcomere. The borders of the sarcomere are formed from actin, which molecules are bound to the Z line. The Z line appears as series of dark lines. Surrounding the Z-line is the region of the I-band, in which the actin filaments are the major components and extend into the A-band. The major component in the A-band constitutes a myosin filament. The central region of the A-band is a paler from the rest band and is called H-band. Inside the H-zone is a thin M-line formed of cross-connecting elements of the cytoskeleton [53, 54].

The bands can be seen very good under polarization microscope when the sarcomere is relaxed. The sarcomere model is presented in Figure 2.1.



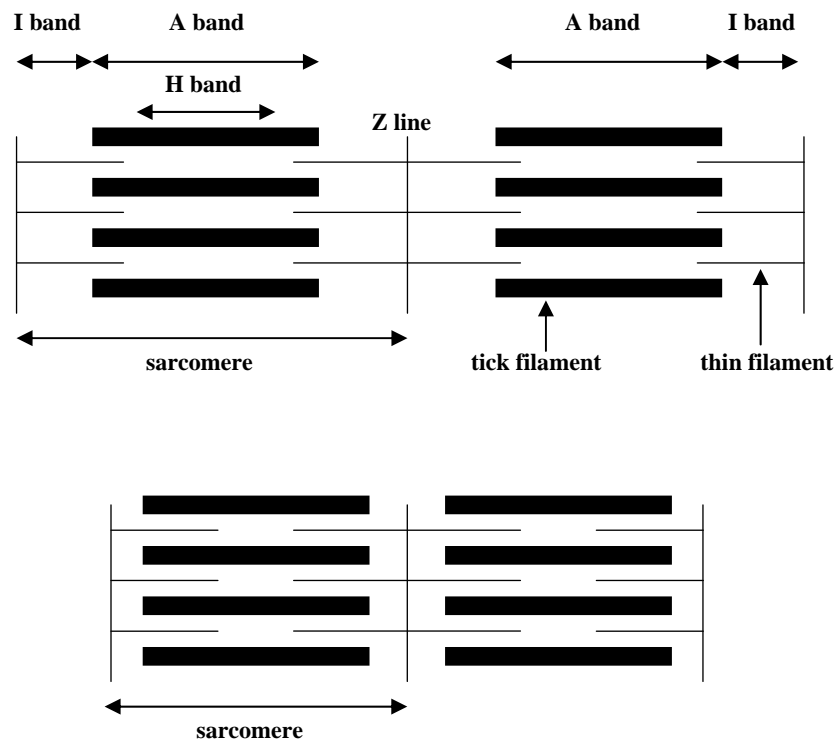


Figure 2.1 Model of the skeletal muscle by vertebrate seen under polarization microscope. Above: relaxed; below: contracted

The function and build of skeletal muscle is unique. The muscle must be able to undertake very rapid and coordinated changes in energy supply and oxygen flux during contraction. A number of studies have suggested that the tissues due to its physiological function could be prone to oxygen radical-mediated damage. Free radicals have been suggested to play a role in muscle damage, which are induced by different forms of exercise and in various pathological disorders, such as the muscular dystrophy, inflammatory myopathies or malignant hyperthermia [55].

## 2.6 Lung

The lung is a vital respiration organ in many air breathing vertebrates, which belongs to the respiratory system. In mammals and other higher live forms the lung are located in thorax on either side of the heart. Both lobes are encircled by a pleural cavity which consists of serous membrane. This membrane forms the parietal pleura that lies against the rib cage and the visceral pleura lies on the surface of the lungs.

In the rat the right lung consists of four lobes and the left lung of only one lobe. The lungs of mammals have a bright pink, spongy and soft texture. The inhaled air is transported further to bronchi. The bronchi then divide into smaller bronchioles, which end in clusters of microscopic air sacs called alveoli. In the alveoli oxygen from the air is absorbed into the blood and carbon dioxide, which produce metabolisms processes, is passages from blood to alveoli and there can be exhaled. Between the alveoli is a thin layer of cells called the interstitium, which contain blood vessels and cells that help support the alveoli [56].

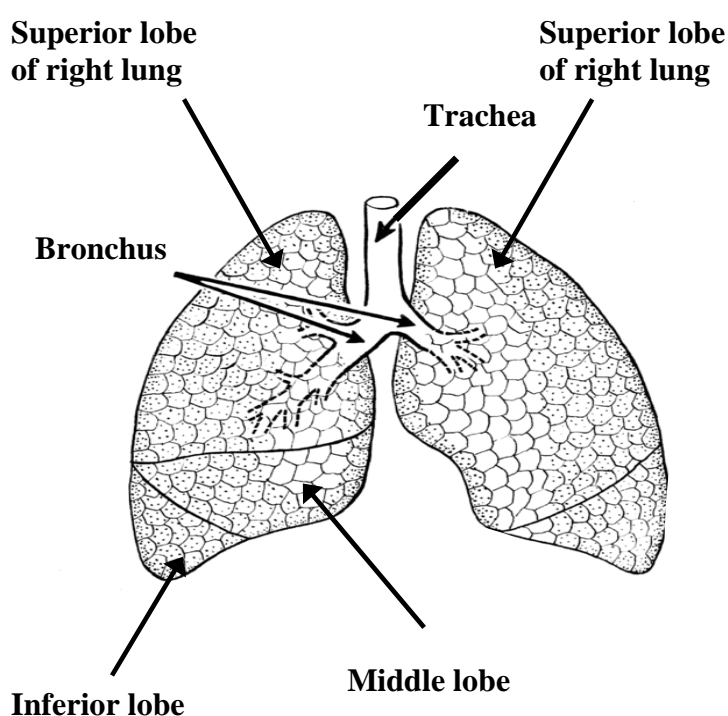


Figure 2.2 Anatomy of the lung

On account of its function, the lung can be exposed to exogenous oxidants. The inhaled air can contain air pollutions like nitrogen dioxide and ozone or cigarette smoke which also contain high concentrations of nitrogen oxides. Exposure to this gases lead to the alteration of the respiratory system [57, 58]. In Table 2.3 examples of reactive oxygen species are shown, which lead to characteristic lesions or diseases of the lung.

<b>Factor</b>	<b>Mediators/influences (diseases)</b>
Air pollutants	ROS, lipid peroxidation, activated PMN's, (ARDS, hyperreactivity in asthmatics)
Asbestos, silica	Activated macrophages, Fe <sup>2+</sup> , ROS, (asbestosis)
Cigarette smoke	NO <sub>x</sub> , peroxy radical, stimulated macrophages and PMN's, ROS (emphysema, cancer)
Herbicide (paraquat)	Redox cycling, ROS, (oedema, lung fibrosis)

Table 2.3 Factor examples causing lung influences and diseases [59]

## **3 Materials and Methods**

### **3.1 Materials**

#### **3.1.1 Animal experiments**

Tissues from six months old male Wistar rats (Charles River, Sulzfeld, Germany) were used for investigations. The animals were kept in a simulated 12+12 hours day-night rhythm and were nourished with special diets and deionised water.

The selenium deficient animal group was fed with a chemically well defined diet containing about  $10 \mu\text{g Se kg}^{-1}$  for several generations and the selenium sufficient group was fed with the same basal diet, but containing  $300 \mu\text{g Se kg}^{-1}$  as sodium selenite.

For experiments where the diet was not critical for the results, the animals were nourished with a non-defined diet and tap-water.

#### **3.1.2 Cell lines**

Mouse myoblasts cell line C2C12, human lung carcinoma cell line A-549 and human hepatocellular carcinoma cell line HepG2 were cultured for the experiments. All cell lines were purchased at the Deutsche Sammlung von Mikroorganismen und Zellkulturen GmbH (DSMZ GmbH, Braunschweig, Germany).

C2C12 cells were established from mouse strain C31+. The cells grow adherently as monolayers in 90% RPMI 1640 medium with 10% fetal bovine serum (FBS),  $100 \text{ U ml}^{-1}$  penicillin and  $100 \mu\text{g ml}^{-1}$  streptomycin. The cultures were splitted 1:10 to 1:50 every 2-4 days using trypsin-EDTA. The cells were incubated at  $37^\circ\text{C}$  in 5%  $\text{CO}_2$  in a humidified air atmosphere until they were ready to be subcultured.

The human lung carcinoma cell line A-549 was established from an explanted lung tumor. The cells are epithelial cells, growing as monolayers in 90% Dulbecco's

Modified Eagle Medium (DMEM) with 10% FBS, 100 U ml<sup>-1</sup> penicillin and 100 µg ml<sup>-1</sup> streptomycin, in a humidified atmosphere containing 5% CO<sub>2</sub> at 37°C. The cells were divided 1:5 to 1:10 every 4-7 days using trypsin-EDTA.

HepG2 is a human hepatocellular carcinoma cell line and morphologically classified as epithelial cells. The cells were cultivated in RPMI 1640 supplemented with 10% FBS, 100 U ml<sup>-1</sup> penicillin and 100 µg ml<sup>-1</sup> streptomycin at 37°C in 5% CO<sub>2</sub> in a humidified air atmosphere. Every 4-7 days subcultures were prepared 1:5 to 1:10 using trypsin-EDTA.

### **3.1.3 Antibodies**

The following antibodies were used for the immunoassays:

#### Primary antibody

- Anti-thioredoxin reductase 1 (TrxR 1) polyclonal antibody from Abcam (Cambridge, United Kingdom)
- Anti-glutathione peroxidase 1 (GPx 1) polyclonal antibody from Lab Frontier (Seoul, Korea)
- Anti-15 kDa-selenoprotein (Sep 15) monoclonal antibody from Bio Genes (Berlin, Germany)
- Anti-Cu/Zn Superoxide dismutase (Cu/Zn SOD) polyclonal antibody from Bio Genes (Berlin, Germany)
- Anti-Catalase (CAT) polyclonal antibody from Bio Genes (Berlin, Germany)
- Anti-Paraoxonase 1 (PON 1) polyclonal antibody from Sigma-Aldrich (Hamburg, Germany)

#### Secondary antibody

- IRDye 800CW goat anti-rabbit IgG secondary antibody from LI-COR (Lincoln, USA)
- IRDye 680CW goat anti-rabbit IgG secondary antibody from LI-COR (Lincoln, USA)

- IRDye 800CW goat anti-mouse IgG secondary antibody from LI-COR (Lincoln, USA)
- IRDye 680CW goat anti-mouse IgG secondary antibody from LI-COR (Lincoln, USA)

### 3.1.4 Radiotracer $^{75}\text{Se}$

The [ $^{75}\text{Se}$ ]-selenite was used for the *in vivo* labeling of the cultured cells. The nuclide has a half-life of 120.6 days and decays by electron capture to  $^{75}\text{As}$ . The excited  $^{75}\text{As}$  emits  $\gamma$ -rays with energy of 121.1 keV, 136.0 keV, 264.7 keV and 279.5 keV which can be detected autoradiographically or measured by  $\gamma$ -spectrometry.

For the production of the radionuclide  $^{75}\text{Se}$ , enriched  $^{74}\text{Se}$  was irradiated for several months with neutrons in the nuclear reactor BER II of Helmholtz Zentrum Berlin (Berlin, Germany). The elemental selenium was dissolved in nitric acid and in this way oxidized to selenite, the [ $^{75}\text{Se}$ ]-selenite solution was neutralized with sodium hydroxide and diluted in saline solution.

### 3.1.5 Chemicals

Analytically grade chemicals from Merck (Darmstadt, Germany), USB Corporation (Cleveland, USA), Calbiochem (San Diego, USA), Sigma-Aldrich (Taufkirchen, Germany), Serva (Heidelberg, Germany) and Carl Roth GmbH (Karlsruhe, Germany) were used.

### 3.1.6 Buffer and solutions

The buffer and solutions used in this work were prepared using ultra-pure deionised water (conductance  $\geq 10 \text{ M}\Omega\cdot\text{cm}^{-1}$ ) from a Milli-Q system (Millipore, Eschborn, Germany).

### **3.1.7 Equipment**

Particular equipment is mentioned in the method-section (3.2) at the according procedures. The further equipment used for this work was from Eppendorf (Hamburg, Germany), Beckman Coulter (Palo Alto, USA), Carl Roth (Karlsruhe, Germany), BioStep (Jahnsdorf, Germany), and Bio-Rad (Brussels, Belgium).

### **3.1.8 Software**

In this work following software was used:

- Odyssey 2.1 Software (Li-COR Biosciences) was used for the detection of IR-dye-labeled antibodies following immunochemistry
- Scan Wizard Pro 7.132 (Mikrotek, Hsinchu, Taiwan) was used for the documentation of polyacrylamide gels
- Aida Image Analyzer v.4.27 (Raytest Isotopenmeßgeräte GmbH, Straubenhardt, Germany) was used for the analysis and documentation of gel images
- Melanie 8.0 was used for the analysis of protein patterns after gel electrophoresis
- Cell-F 2.8 (Olympus soft Imaging Solutions, Münster, Germany) was used for recording the fluorescence microscopy images
- Prime View (GE Healthcare, Freiburg, Germany) was used for programming and monitoring of Äkta-FPLC runs

### **3.1.9 Bioinformatics**

Different computer programs freely available in internet were employed to obtain bioinformatic informations about proteins. All the programs used for this work were accessed either through ExPASy Proteomics tools for protein classification and characterization (<http://www.expasy.org>) or through PubMed (<http://www.ncbi.nlm.nih.gov/guide/>).

### **3.1.10 Text and data converting**

Text processing was carried out using Microsoft Word 2003. For the editing of data, tables, figures and photos a Microsoft Excel 2003 and Origin Pro 8G were used.

## **3.2 Methods**

### **3.2.1 Sample preparation**

#### **3.2.1.1 Homogenization of tissues**

The tissues of skeletal muscle, lung and spleen from rat were homogenized in an isotonic medium. Firstly the tissues were washed in a tris-HCl buffer (homogenization buffer, composition below) and then were cut into coarse pieces with scissors in the step after. Finally for homogenization a hand homogenizer, a sonifier (Branson Sonifier W-450 with a parabolic beaker resonator; Heinemann, Schwäbisch Gmünd, Germany) or an electric disperser (Polytron PT 1300, Kinematica AG, Littau-Luzern, Switzerland) was used. All steps were carried out at 4°C.

#### Homogenization buffer

0.25 M sucrose

5 mM MgCl<sub>2</sub>

10 mM tris HCl pH 7.4

1 mM phenylmethylsulfonyl fluoride (PMSF)

0.8% protease inhibitor cocktail



### **3.2.1.2 Homogenization of cells**

Homogenisation of the cells was done after harvesting (by utilizing cell scrapers) and cell lysis in a lysis buffer. The cells were homogenized by means of hand homogenizers or sonifier. The steps of homogenization were carried out at 4°C.

#### Lysis buffer

20 mM tris HCl pH 8.0

137 mM NaCl

10% glycerol

1% Nonidet P-40 (NP-40, Sigma)

2 mM EDTA

0.8% protease inhibitor cocktail

### **3.2.1.3 Subcellular fractionation**

To investigate low abundant proteins an enrichment step by prefractionation of cell compartments can be applied.

#### **3.2.1.3.1 Separation by ultracentrifugation**

Differential pelleting was applied for separation of the homogenate components into: nuclei, mitochondria, microsomes and cytosol by centrifugation at 600×g for 10 minutes, 8000×g for 20 minutes and 186000×g for 60 minutes, respectively (Optima MAX with MLA-55 rotor, Beckman Instruments GmbH, Munich, Germany):

The tissue homogenate is placed in a centrifuge tube and centrifuged for sufficient time to sediment the largest groups of cell organelles. The supernatant is then poured off and recentrifuged to collect the next fraction [60].

All these operations were carried out at 4°C. To minimize contamination the pellets were washed by resuspending in homogenization buffer and recentrifuged under the same conditions.

### 3.2.1.3.2 Separation by density-gradient centrifugation

Because with the above mentioned protocol nuclei can not sufficiently be purified, separation by density-gradient centrifugation was applied for their isolation. The separation of organelles on the basis of their density was carried out by layering the organelles over or under a density gradient formed by a series of buffer containing different sucrose concentrations and centrifugation to equilibrium.

#### **Purification of nuclei from spleen and lung**

For the purification of lung and spleen nuclei the method of Windell and Tata [61] was used. The tissue was homogenized in nine volumes of the cold homogenization buffer. The homogenate was centrifuged at 600×g for ten minutes at 4°C and the pellet was resuspended in half the original volume of the homogenization buffer. The suspension was centrifuged again as described above. A pellet of the nuclei was resuspended and homogenized in the washing buffer to remove membrane contamination. Afterwards the nuclei were centrifuged 80 minutes at 80000×g and 4°C.

To remove the nuclear membrane the cream-colored nuclei pellet was washed with the homogenization buffer containing 0.5% Triton X-100.

#### Homogenization buffer

0.25 M sucrose

5 mM MgCl<sub>2</sub>

10 mM tris HCl pH 7.4

1 mM PMSF (phenylmethylsulfonyl fluoride)

#### Wash puffer

2.2 M sucrose

1 mM MgCl<sub>2</sub>

10 mM tris HCl pH 7.4

0.8% protease inhibitor cocktail

#### **Purification of nuclei from skeletal muscle**

The purification of nuclei from skeletal muscle represents several challenges. The number of nuclei per gram in skeletal muscle is very low compared with other tissues. The next problem is that muscle fibers are extremely tough and homogenization procedure must be chosen with care to balance maximum disruption of the tissue with a minimum of damage to nuclei. For the purification of nuclei the modified method of Wielkie *et al.* was used [62].

The muscle tissue was initially broken down by scissors and then homogenized. The homogenate was filtered to remove the bulk of the fibrous material and poorly disrupted tissue pieces. The resulting filtrate was centrifuged at 1000×g for ten minutes, then the pellet was diluted with ice-cold 0.25 M SHKM buffer and centrifuged again at 4000×g for 20 minutes. After this the pellet was resuspended with ice-cold 0.25 M SHKM buffer and was homogenized to break up aggregated nuclei. A volume of ice-cold 2.3 M SHKM buffer was added to the nuclei solution that the end concentration of sucrose was 1.85M. Next the nuclei were spun through a tree-step sucrose gradient (1.85 M, 2.15 M, 2.8 M) in the ultracentrifuge at 82000×g for 60 minutes. The nuclei was diluted in ice-cold HKM buffer and centrifuged at 4000×g for 20 minutes and finally, the pellet with nuclei was resuspended in 0.25 M SHKM buffer and was stored at -40°C. All steps in this procedure were carried out at 4°C.

Homogenization buffer

10 mM Hepes pH 7.4  
 60 mM KCl  
 2 mM EDTA  
 300 mM sucrose  
 0.8% protease inhibitor cocktail  
 2 mM DTT

x\* M SHKM buffer

x\* M sucrose  
 50 mM Hepes pH 7.4  
 25 mM KCl  
 5 mM MgCl<sub>2</sub>  
 0.8% protease inhibitor cocktail  
 2 mM DTT

HKM buffer

50 mM Hepes pH 7.4  
 5 mM MgCl<sub>2</sub>  
 25 mM KCl  
 0.8% protease inhibitor cocktail  
 2 mM DTT

x\* = 0.25 M, 2.15 M, 2.3 M, 2.5 M, 2.8 M sucrose

**3.2.3.3.3 Identification of separated organelles**

For the identification and purity control of the separated organelles biochemical methods (Western Blotting) or light and fluorescence microscopy were applied.

## **3.2.2 Protein chemistry**

### **3.2.2.1 Bradford protein assay**

The Bradford protein assay was used for the measurement of the protein concentration in the samples. This colorimetric assay is based on the shift in the absorbance maximum when coomassie brilliant blue G-250 dye reacts with proteins. In this method the Beer's Law is applied for quantitation of protein by selecting an appropriate ratio between the fixed dye volume and the sample concentration, which is changed by using an adequate volume. At the assay pH, the dye molecules are doubly protonated and are present as the red cationic form. Binding of the dye to protein stabilizes the blue anionic form, detected at 595nm. Dye binding requires a protein containing active basic or aromatic residues.

The measurement procedure involved the pipetting of sample or standard, distilled water and diluted reagent (volumes are given below) in a cuvette made from poly(methyl methacrylate), an incubation at room temperature for about 5 minutes and the determination of the absorbance in a spectrophotometer. For the calibration curve, the bovine serum albumin standard solution was used and for each assay was prepared freshly. The concentration of the measured samples was determined from its absorbance by interpolation using the standard curve [63].

#### Volumes per measurement:

800 µl Bradford reagent (1:5 in aqua dest.)

x µl sample or standard

(200 - x) µl aqua dest.

### **3.2.2.2 Polyacrylamide gel electrophoresis**

Sodium dodecylsulfate-polyacrylamide gel electrophoresis (SDS-PAGE) according to the Laemmli method [64] was used to separate complex mixtures of proteins.

The electrophoresis was carried out using the vertical apparatus from Pharmacia (Freiburg, Germany). The polyacrylamide gel consisted of a stacking and a separating

gel. The composition of both gel solutions is presented in the Table 3-1. The separating gel was cast, overlaid with a mixture of water and butanol and was allowed to polymerize for at least 45 minutes. Then the stacking gel was prepared on the top of the separating gel and polymerized for a minimum of 15 minutes. For the application of multiple samples in a one-dimensional separation it usually contained five or ten sample slots.

The samples were prepared by adding a defined volume of loading buffer and subsequent denaturation at 95°C for five minutes. The loading buffer consists of 4% SDS, 20 mM DTT, 20% (v/v) glycerol, 0.2% (w/v) bromophenol blue, 125 mM tris-HCl pH 6.8.

The protein separation was carried out in the SDS-running buffer for 12 h at a current of 12 mA or for 3 h at 50 mA per gel.

	Stacking gel	Separating gel
Acrylamide	5% (w/v)	15% (w/v)
N,N'-methylenebisacrylamide	0.13% (w/v)	0.4% (w/v)
SDS	0.1% (w/v)	0.1% (w/v)
Tris – HCl	125 mM pH 6.8	375mM pH 8.8
TEMED	0.03% (v/v)	
APS	0.025% (v/v)	

Table 3.1 The composition of the solution used for casting of polyacrylamide gels

#### SDS-running buffer

50 mM Tris – HCl pH 8.3

196 mM glycine

0.1 % (w/v) SDS

### **3.2.2.3 Two-dimensional gel electrophoresis**

Two-dimensional electrophoresis (2DE) was used to separate complex protein mixtures (e.g. cell homogenates) into several protein spots. This spots could be visualized by

different staining techniques (see below) and the patterns could be used to analyze protein expression. In this method mixtures of proteins are separated by two independent properties in two isolated steps: the first dimension step is isoelectric focusing in order to separate the proteins according to their isoelectric points. The second dimension step is SDS-PAGE in which the proteins are separated by differences in their molecular masses.

### **3.2.2.3.1 First dimension (NEpHGE)**

The Non-Equilibrium-pH Gradient Electrophoresis (NEpHGE) as the first separation step depends on the isoelectric point of the proteins. The procedure involves a tub gel system, sample application and focusing. The gels were cast and run in glass capillary-tubes which were 1.5 mm wide and 110 mm long. The gel solution was prepared according to the O'Farrell [65] method.

#### Gel solution

10% acrylamide/ bisacrylamide (v/v)

8 M urea

2% ampholytes 3-10 (v/v)

2% NP-40 (v/v)

0.2 % APS (v/v)

0.14% TEMED (v/v)

A short gel at the end of the tube (0.5 cm), the cap-gel, was composed of 50% gel solution and 50% AA/PDA. The much higher acrylamide concentration prevented from the loss of highly basic proteins which otherwise could be lost during extended focusing times.

The samples were solubilized in the rehydration solution containing 8 M urea, 2% ampholytes, 2% Triton X-100, 10 mM DTT. The gel with sample was running at 500 V, 70 mA, 300 W for 3.0 kVh. After the focusing the gel was removed from the glass capillary-tubes and incubated in equilibration buffer for 15 minutes. The SDS-PAGE as second dimension was carried out directly or the gels were frozen at -40°C and stored for later analysis.

#### Equilibration buffer

62.5 mM tris HCl pH 6.8

2.3% (w/v) SDS

40 mM DTT

0.02% bromophenol blue

#### Anode buffer

3 M urea

5% (v/v) phosphoric acid

#### Cathode buffer

9 M urea

5% (w/v) glycerin

5% (w/v) ethylenediamine

### **3.2.2.3.2 Second dimension**

The second dimension step was performed as described in chapter 3.2.2.2. Instead of preparing a stacking gel, the gel was overlaid with 1-2 ml of agarose to prevent moving.

### **3.2.2.4 Staining of polyacrylamide gels**

#### **3.2.2.4.1 Coomassie staining**

Coomassie staining was used to visualize proteins after electrophoretic separation in a polyacrylamide gel. With this staining down to 6-8 ng protein per band with a linear dynamic range of one order of magnitude can be detected, depending on the applied protocol.

After electrophoresis, the gels were incubated in the gel-fixing solution for 60 minutes and subsequently incubated for 30 minutes in the staining solution. To remove unbound dye, the gels were then washed in distilled water and finally kept for 20-30 minutes in the fixing solution to destain the background.

#### Fixing solution

30% (v/v) ethanol

10% (v/v) acetic acid

#### Color solution

30% (v/v) ethanol

10% (v/v) acetic acid

0.2% (w/v) coomassie Blue G 250

#### **3.2.2.4.2 Silver staining of Blum**

The detection limit of coomassie staining is sufficient to detect a large number of protein bands in one-dimensional separations. However, in 2DE the protein amount per spot is often below. Therefore, some gels were stained with the more sensitive silver staining according to Blum [66]. With this method as little as 0.1 ng protein can be detected, but the linear dynamic range is worse and the protocol is more time consuming.

After electrophoresis, the gels were incubated for 30 minutes in fixing solution, then for 20 minutes in 20% (v/v) ethanol and washed for 20 minutes in distilled water. Afterwards the gels were impregnated for 1 minute with the sensitizer solution. They were shortly washed (three times for 20 seconds each) in distilled water and next incubated for 20 minutes in silver solution. Before the gels were developed with the development solution they were rinsed with water to remove excess silver ions. The developing procedure was stopped with a solution containing 5% (v/v) acetic acid and finally the gels were stored in 1% (v/v) acetic acid solution.

##### Fixing solution

30% (v/v) ethanol

10% (v/v) acetic acid

##### Sensitizer solution

0.02% sodium thiosulfate

##### Silver solution

0.2% (w/v) silver nitrate

##### Development solution

3% (w/v) sodium carbonate

0.05% (v/v) formaldehyde

0.0004% sodium thiosulfate

#### **3.2.2.5 Western blotting**

To make proteins available for further analysis after electrophoresis (such as immunochemical detection), they were transferred from the polyacrylamide matrix to the surface of a nitrocellulose membrane (Whatman, GE Healthcare) using a semidry blotting system (Bio-Rad).

The membrane and blot paper were soaked in blotting buffer. The transfer was carried out for 60 minutes at 18V.



### Blot buffer

192 mM glycine

25 mM tris

20% (v/v) ethanol

### **3.2.2.6 Immunoassays**

SDS-PAGE can be used to determine the apparent molecular weight of a protein band. However, in a complex sample this information is not precise enough to identify a certain protein, especially if its presence in the sample is uncertain. A protein of interest can hence be identified and under some conditions also relatively quantified by its binding to specific antibodies. These primary antibodies bind species specific, secondary antibodies which can be detected due to enzymatically active or fluorescence group, bind the primary antibody.

Subsequently to the western blotting, the nitrocellulose membrane was washed in TBS buffer and then incubated with 10% non-fat dry milk to block non-specific binding of the primary antibody. The membrane was washed again in the TBS-T buffer and incubated for 2 hours at room temperature or over night at 4°C with the diluted primary antibody. Following the washing steps the membrane was incubated with the diluted secondary antibody, which was detected finally with the Odyssey IR-Imaging System (Li-COR).

#### TBS

10 mM tris HCl pH 8.0

150 mM NaCl

#### TBS-T

0.1% (v/v) Tween 20 in TBS

### **3.2.2.7 Gel drying**

The colored gels were incubated for 5-10 minutes in dehydrating solution and after that the gels were dried at 65°C for 12 hour in a vacuum using a gel drying system (Biometra D62, Göttingen, Germany).

### Dehydrating solution

80% (v/v) ethanol

20% (v/v) glycerin

### **3.2.2.8 Autoradiography**

For the visualization of radioactive labeled proteins in the gel after electrophoresis, an “Imaging Plate” (Fuji Photo Film, Kanagawa, Japan), a film like radiation image sensor, was used. The plate is an image sensor with bunches of small crystals of photo-stimulable barium fluorobromide containing a trace amount of bivalent europium (BaFBr: Eu<sup>2+</sup>) as a luminescence center. When a radioactively labeled sample is exposed to an IP, the energy from the sample is transferred to the phosphors and stored as trapped electron. The stored energy is stable until scanned with a laser beam (Dürr Medical CR 35 Bio), which then releases the energy as luminescence [67].

### **3.2.2.9 Immunocytochemistry**

The immunocytochemistry is a technique used to detect the presence of a protein and its localisation in cells by use of an immunofluorescence staining. The cells were diluted in medium to a concentration of  $1 \times 10^5 \text{ ml}^{-1}$ . Muscle myoblasts cell line C2C12 (mouse), the lung epithelial cell line A549 (human) and hepatocellular carcinoma cell line HepG2 (human) were cultured on coverslips in 12 well plates over night. After obtaining 50 - 60% confluence, the cells were washed 3 times with PBS buffer and then 10 minutes fixed in 4% formaldehyde (v/v) in PBS at room temperature. Subsequently the cells were washed 3 times and blocked for 1 hour at room temperature. The blocking buffer was used to block non-specific binding of the primary antibody. The cells were then 2 times washed in PBS and 5 minutes permeabilized with 0.5% Triton X-100 (w/v). Afterwards the cells were incubated with the primary antibody over night at 4°C and then were washed with PBS and incubated for 1 hour at room temperature with the secondary antibody. The cells were washed with PBS and the nuclei were stained with

1  $\mu\text{g ml}^{-1}$  Hoechst 3342 (Invitrogen) in PBS for 5 minutes at room temperature. Finally, the cells were washed and stored at 4°C in the dark till acquisition of the pictures.

For the fluorescence images the BX51 microscope system and F-View II CCD camera (Olympus, Hamburg, Germany) were used.

#### Blocking buffer

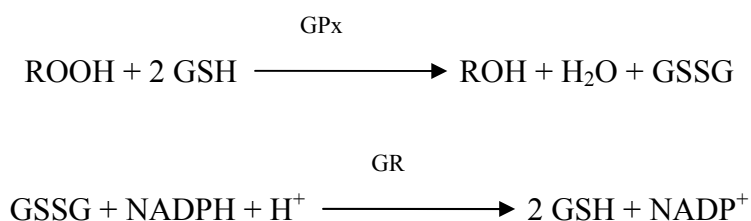
10% (w/v) BSA

10% (v/v) goat serum (Biozol, Eching, Germany)

in PBS buffer

### **3.2.2.10 Glutathione peroxidase activity assay**

The glutathione peroxidase activity was measured by means of a GPx-assay based on the oxidation of glutathione (GSH) to oxidized glutathione (GSSG) catalyzed by GPx. This is then coupled to the recycling of GSSG back to GSH utilizing glutathione reductase (GR) and NADPH ( $\beta$ -nicotinamide adenine dinucleotide phosphate, reduced). The decrease in NADPH absorbance at 340 nm is a measure for the GPx activity, since GPx is the rate-limiting factor of this coupled reaction:



The concentrations in the assay were: 50  $\mu\text{g}$  protein (determined by Bradford assay) diluted with tris-HCl buffer to a total volume of 500  $\mu\text{l}$ , 100  $\mu\text{l}$  GSH (3.07  $\text{mg ml}^{-1}$ ) and 200  $\mu\text{l}$  GR (2 u  $\text{ml}^{-1}$ ). The solution was incubated for 30 minutes at 37°C to ensure complete reduction of endogenous glutathione in the samples. Before measurement of the absorbance, 100  $\mu\text{l}$  NADPH (2.08  $\text{mg ml}^{-1}$ ) and 100  $\mu\text{l}$  tert.-butyl hydroperoxide (10  $\text{mmol l}^{-1}$ ) were added to start the reaction. For analysis the slope in absorbance was determined and sample GPx amount was calculated from a standard curve obtained by the measurement of purified GPx with a known enzymatic activity [68].

### **3.2.2.11 ABTS assay**

The total antioxidant status in cytosolic fractions of skeletal muscle, lung and spleen was measured in a test system involving the reduction of the green/blue radical cation of 2,2'-Azino-di-(3-ethylbenzthiazoline sulphonate) (ABTS<sup>•+</sup>) to the achromatic uncharged form by antioxidants.

As described above, tissues were homogenized but phosphate buffered saline (PBS, pH=7.4) was used instead of tris, which is known to interfere with the ABTS method. No proteases had been used, because of possible unknown effects on the determination of the total antioxidant status. ABTS<sup>•+</sup> was generated by mixing a 14 mM ABTS stock solution 1:1 with a 4.9 mM ammonium persulfate solution. The mixture was stored in the dark at room temperature for 24 h and finally diluted 1:200 with water. Protected from light and stored at 4°C, the radical was stable for several weeks.

For the assay to 50 µl of sample, ascorbic acid (as standard, final concentration 3 - 21 nM), distilled water (as blank) or control serum (Randox) in a microtiter plate, 200 µl radical solution were added. The absorbance at 736 nm was monitored for 30 minutes and plotted against the measurement time. The area under this curve was chosen as a measure for the antioxidative capacity of the sample [69].

## **3.2.3 Paraoxonase Purification**

### **3.2.3.1 Plasma pre-treatment**

Paraoxonase 1 (PON1) was purified from human blood plasma. The blood was obtained from a healthy, 30 year old female volunteer and was centrifuged after the extraction at 5000 x g and 4°C for 10 min. After this, the clear supernatant was pooled and incubated with Triton X-100 (1% v/v) with stirring at 4°C over night and then centrifuged at 5000 x g for 10 min again, to separate enzyme from HDL and remove any undissolved particles. Centrifugal devices with a 3 kDa cut-off (Millipore) were used to reduce plasma volume. PON1 was purified from the so concentrated plasma in a method modified from Golmanesh *et al* [70]. The main difference to the previously published

protocol is the omitting of a third chromatography step because a sufficiently pure enzyme was observed after the first two steps and each purification step could increase the risk of a loss or exchange of protein bound metals.

### **3.2.3.2 DEAE-Sephadex A-50 column chromatography**

The concentrated plasma from the previous steps was loaded onto a DEAE-Sephadex column, which had been equilibrated with buffer A. The column was washed with 10 volumes of buffer A and then eluted with a linear gradient of 0–700 mM NaCl in buffer A (see section 2.2.3.3). The collected fractions were assayed for enzyme activity. Peak fractions were pooled and pooled fractions were concentrated and desalted using ultrafiltration through a 3 kDa cut-off membrane.

### **3.2.3.3 Sephadex G 200 gel filtration chromatography**

PON-activity containing fractions after the first chromatographic step were further purified by gel filtration. The pooled fractions were loaded to a Sephadex G 200 column equilibrated with buffer A and eluted by an isocratic flow of the same buffer. The collected fractions were assayed for enzyme activity, peak fractions were pooled, dialyzed and stored at -40°C until used.

#### Buffer A

20 mM tris HCl, pH 8.0

0.1% (v/v) triton X-100

1 mM CaCl<sub>2</sub>

2% (v/v) glycerol

### **3.2.3.4 Paraoxonase activity**

Paraoxonase activity was determined using paraoxon (*O,O*-diethyl *O*-(4-nitrophenyl) phosphate) as the substrate. Enzyme activity was measured in 50 mM tris-HCl buffer at pH 8.0. Paraoxon with a final concentration of 1 mM was added to start the reaction, and the increase in absorbance at 412 nm was recorded [71]. Stock solution of paraoxon was prepared in water daily fresh.

## **3.2.4 Analytical method**

### **3.2.4.1 Neutron activation analysis**

In this study the instrumental neutron activation analysis (INAA) was used for the quantitative multi-element analysis of trace elements present in the skeletal muscle, lung and spleen and their subcellular fractions. For the analysis of the trace elements in the subcellular fraction the samples was prepared as described in 3.2.1. The samples were pipetted to quartz ampoules, weighted and sealed in them. The ampoules with samples were irradiated with neutrons in the nuclear reactor BER II of the Helmholtz Zentrum Berlin. At the reactor, the ampoules were variably placed, either in the core or near the core and irradiated for a suitable period of time. After irradiation and decay the gamma spectra of the samples were measured using a high purity germanium detector. For qualitative analysis the energy of the photons were used and the amount of an element in the sample was determined by the amount of radiation at a given energy, which is directly proportional to the amount of the element (72). The relation between the radioactivity of the irradiated isotope and its amount in the samples can be described by following equation:

$$A = n N_A \Phi \delta f (1 - e^{-\lambda t_A}) e^{-\lambda t_E}$$

A - activity of isotope in sample (Bq)

n - amount of isotope  ${}^A Z$  in sample (mol)

$N_A$  - Avogadro number

$\Phi$  - neutron flux density (neutrons  $\times$   $\text{cm}^2 \times \text{sec}^{-1}$ )

$\delta$  - neutron capture cross section ( $\text{cm}^2$ ) for isotope  ${}^A Z$

f - relative isotopic abundance

$\lambda$  - decay time of the isotope (s)

$t_A$  - irradiation time (s)

$t_E$  - decay time (s) of this isotope

As some of these variables can not be determined easily a multi-element solution (Merck, Darmstadt, Germany) was irradiated with the samples and used as a standard. Additionally, for quality control the trace element concentrations in bovine liver reference material (NIST, Gaithersburg, USA) was also investigated and compared with the certified values.

The reason for choosing neutron activation analysis was its sufficiently low detection limits. For other methods such as atom absorption spectrometry or inductively coupled plasma mass spectrometry the samples had to be dissolved or digested, which always increases the risk of contamination.

Element	Nuclide	Half-life	$E_\gamma$ [keV]
As	As-76	26.3 h	559
Cs	Cs-134	2.06 y	796
Cr	Cr-51	27.7 d	320
Co	Co-60	5.3 y	1173.2, 1332.5
Fe	Fe-59	44.5 d	1099.3; 1291.6
La	La-140	1.68 d	1596, 487
Rb	Rb-86	18.7 d	1077
Se	Se-75	120.6 d	136.0
Zn	Zn-65	244.1 d	1116

Table 3.2 Radionuclides used in the analysis of the elemental concentrations

### 3.2.4.2 Speciation Analysis

#### 3.2.4.2.1 Inductively coupled plasma mass spectrometry

Inductively coupled plasma mass spectrometry (ICP-MS) is a very sensitive analytical technique which affords determination of multiple elements at trace or ultra trace levels. The ICP-MS employs a plasma as the ionization source and a mass spectrometer usually a quadrupole mass filter to separate the produced ions.

Plasma is defined as a gas consisting of ions, electrons and neutral particles. In ICP-MS, the plasma which dries, atomizes and ionizes the elements in a sample is formed from argon. The liquid samples are introduced by a pump to the nebulizer where an aerosol consisting of the liquid sample and plasma gas is formed. A double-pass spray chamber ensures that a consistent aerosol is introduced to the plasma. Argon is introduced through a quartz torch, which is located in the center of the RF coil. A radio frequency current applied on this coil ionizes the argon and free electrons and positively charged argon and analyte ions are formed through a series of inelastic collisions between charged particles and remaining neutral argon atoms. At equilibrium a stable, high temperature plasma is generated. The sample aerosol is instantaneously decomposed in the plasma forming charged analyte particles. The ions are extracted from the plasma through a sampling cone and then are focused by a series of lenses into the mass analyzer region.

The quadrupole mass analyzer consists of two pairs of cylindrically metal rods placed in a high vacuum (in the order of  $10^{-9}$  bar). To filter a certain mass, an alternating current (AC) overlaid by a direct current (DC) is applied pairwise on the rods. This results in unstable flight paths for all mass-to-charge ratios ( $m/z$ ) except those within a small window. By combining different AC/DC-values multiple points around approximate  $m/z$  of the interesting analytes can be scanned in less than a second.

Finally the filtered ions are detected by a secondary electron multiplier and a spectrum (ion count over  $m/z$ ) for each scanning cycle is generated by the electronics and stored in the data file. Assuming the parallel measurement of a standard solution the concentration of an element in the sample can easily be calculated from the peak intensities then.

In this work the ICP-MS 7500c from Agilent Technologies (Waldbronn, Germany), equipped with a micro-concentric PFA-nebulizer in a Scott-spraying chamber was



employed. The sample was introduced as "flow-through" from the chromatographic system without any additional pumps.

Nebulizer:	
Carrier-Gas:	0.82 l·min <sup>-1</sup> Ar
Make-up-Gas:	0.27 l·min <sup>-1</sup> Ar
RF power	1300 W
Isotopes	Fe-59, Zn-66, Cu-63, Mn-55, Mo-95, Ni-60, Cd-111, Co-55, La-139, As-75, Se-82, V-51, Hg-202

Table 3.3 Instrumental set up of the ICP-MS system

#### 3.2.4.2.2 Size exclusion chromatography

ICP-MS can be used for the determination of element concentrations in a sample but also for a semi-quantitative or qualitative evaluation of different elemental species. This is done by using the ICP-MS as a detector subsequent to the separation of this species, e.g. by size-exclusion-chromatography of proteins.

In general the size-exclusion chromatography enables the separation of molecules in solution by their hydrodynamic size. The principle of this method is that proteins of different size will elute through a porous stationary phase made from cross linked agarose and dextran at different retention times. This means that larger particles will elute earlier with no or only few interactions, while smaller particles will enter more pores in the packing material and hence elute later.

In this work trace element binding proteins from the cytosolic protein mixtures of skeletal muscle, lung and spleen and the metals bound to purified human paraoxonase 1 have been investigated by this method. The HPLC system HP 1100 (Hewlett Packard/Agilent Technologies, Waldbronn, Germany) equipped with a GFC 300 pre column and a Superdex 75 analytical column was coupled to the ICP-MS system described above. The column was calibrated using a gel filtration standard (Amersham Biosciences, Buckinghamshire, UK) containing Dextran blue (2000 kDa), Conalbumin (75 kDa), Ovalbumin (43 kDa), Chymotrypsinogen (25 kDa), Ribonuclease A (13.7 kDa) and Aprotinin (6.5 kDa) and Vitamin B<sub>12</sub> (1.3 kDa).

The samples were separated by the chromatographic system and the flow-through was measured on-line with the ICP-MS operated in a time-resolving chromatography mode. The chromatograms were prepared from exported csv.-files utilizing origin 8.0. The instrumental set up of the ICP-MS system is described in the Table 3-4.

Colum	Superdex 75 PC 3.2×300mm
Pre-colum	GFC 300 4×3mm
Eluent	20 mM tris pH 7.4
Flow rate eluent	100 $\mu\text{l min}^{-1}$
Pressure	10 bar
Sample volume	20 $\mu\text{l}$
Autosampler temperature	4°C

Table 3.4 Instrumental set up of the chromatographic system

## **4. Results**

### **4.1 Elemental analysis**

#### **4.1.1 Determination of trace element concentration by means of INAA**

In numbers of studies it was reported about the mechanism of redox-active proteins contra oxidative stress, in which a majority of involved enzymes in their actives centre have metal ions. Correctly level in the nutrition of these elements was correlated with the prevention and reduction of muscle disuses or lung cancer. On the other hand they have been conduced with translation metal ions as well as lead, regarding the production of free radicals. The first important step in the metalloproteome is therefore the determination of the concentration of the trace elements present in the tissues and their distribution among in the cellular compartments.

In the study, the elemental analytical method was combined with biochemical separation procedures. Subcellular fractionation into nuclear, mitochondrial, microsomal and cytosolic fractions was separated by differential ultracentrifugation from the rat tissues. Instrumental neutron activation analysis was used for the determination of several trace elements in skeletal muscle, lung, spleen, heart, liver and kidney.

The tissues were obtained from rats which had been fed with a normal diet. The elemental concentrations in the whole tissues and subcellular fractions were related to the dry weight of the samples. The concentrations of elements found in rats were calculated as mean  $\pm$  standard deviation.

#### 4.1.1.1 Determination of element concentrations in selected tissues of the rat

In this experiment INNA had been used to determine the concentrations of selenium, zinc, iron, arsenic, cobalt, rubidium, cesium, chromium and lanthanum in the heart, liver, lung, spleen, skeletal muscle and kidney.

Figures 4.1, 4.2, 4.3 and 4.4 show the data for the nine elements concentration found in eight rats.

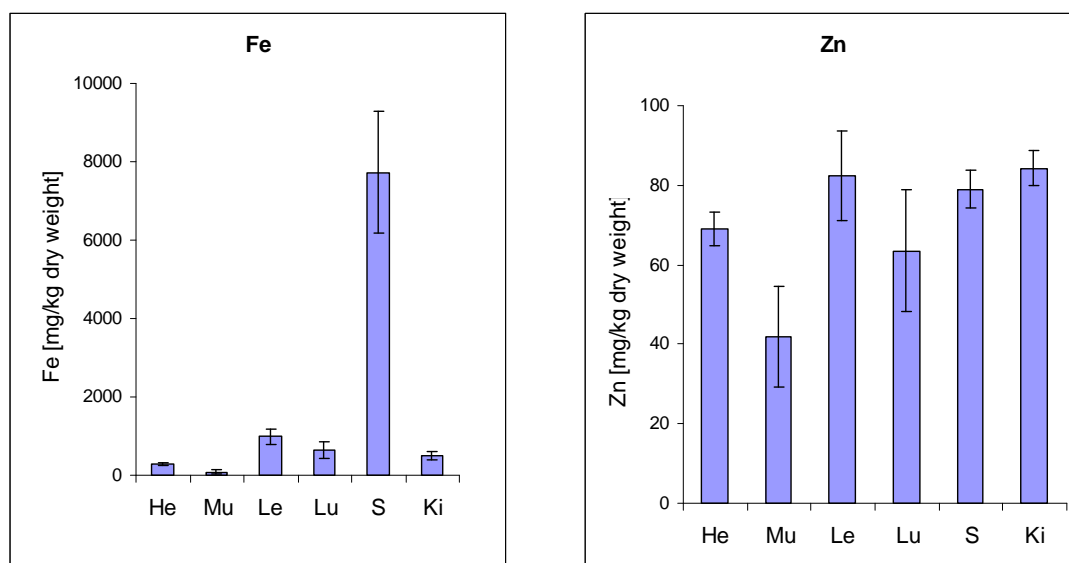


Figure 4.1 Concentration of iron (Fe) and zinc (Zn) in the heart (He), skeletal muscle (Mu), liver (Le), lung (Lu), spleen (S), kidney (Ki) of rats (mean  $\pm$  SD; n = 8)

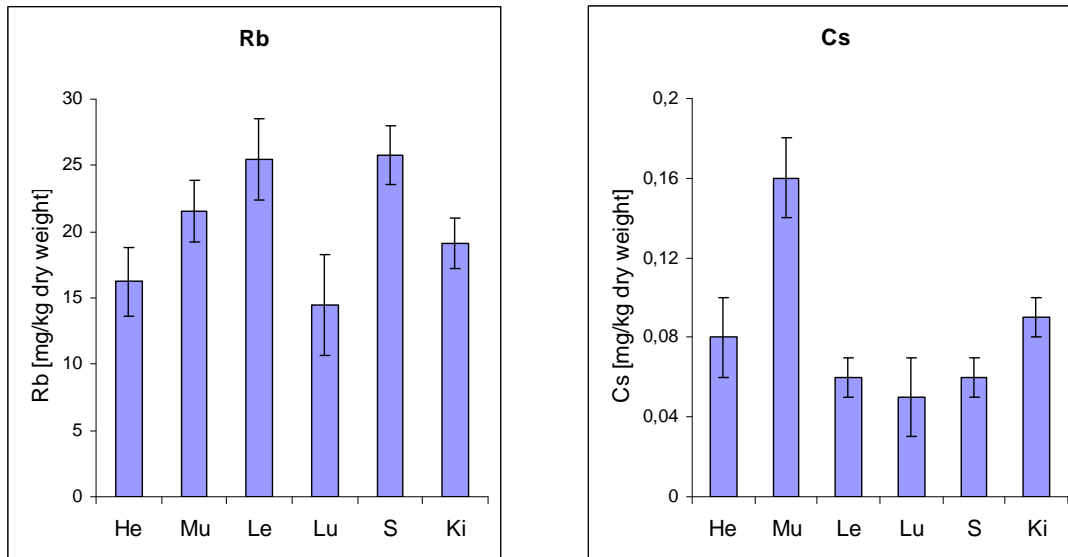


Figure 4.2 Concentration of rubidium (Rb) and cesium (Cs) in the heart (He), skeletal muscle (Mu), liver (Le), lung (Lu), spleen (S), kidney (Ki) of rats (mean  $\pm$  SD; n = 8)

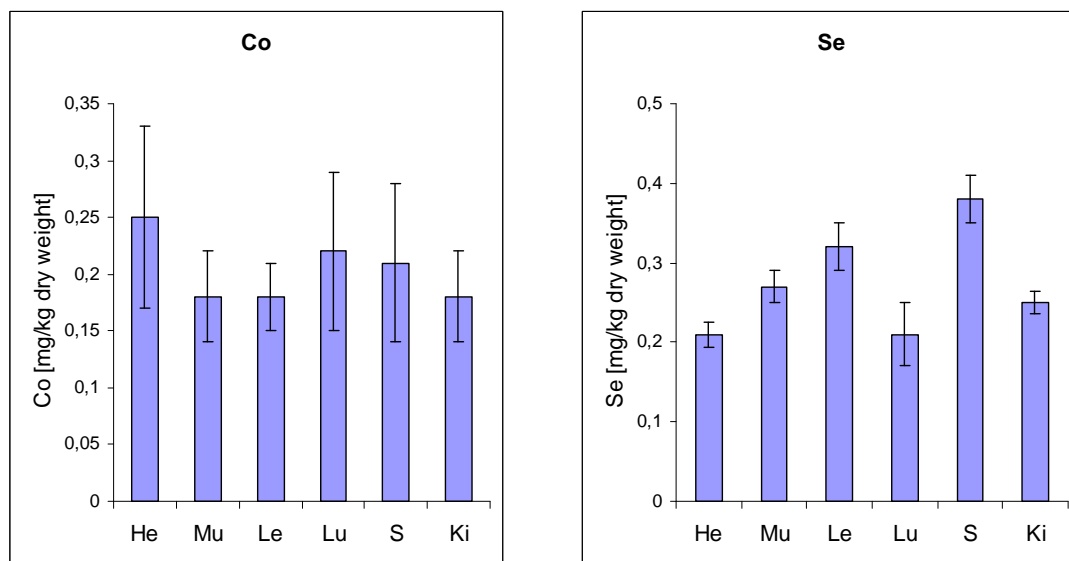


Figure 4.3 Concentration of cobalt (Co) and selenium (Se) in the heart (He), skeletal muscle (Mu), liver (Le), lung (Lu), spleen (S), kidney (Ki) of rats (mean  $\pm$  SD; n = 8)

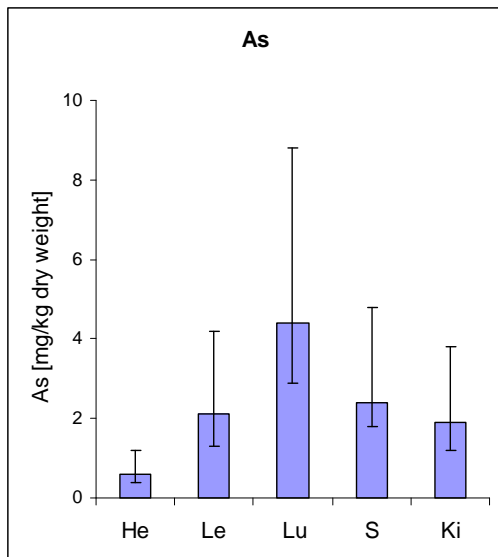


Figure 4.4 Concentration of arsenic (As) in the heart (He), liver (Le), lung (Lu), spleen (S), kidney (Ki) of rats (mean  $\pm$  SD; n = 8)

The explorative elements (on a large part) were distributed inhomogeneous in the body of the rat. The highest concentrations of iron and selenium were found in the spleen. The concentration of cesium in the skeletal muscle was higher compared to other organs. The concentration of arsenic in the skeletal muscle could not be detected, the highest concentration of this element was found in the lung. With the exception of zinc concentration in the skeletal muscle and rubidium concentration in the lung, which were lower, in other organs no significant differences had been observed.

#### 4.1.1.2 Distribution of trace element in the subcellular fractions of the skeletal muscle, lung and spleen

In further experiments, the concentrations of arsenic, cesium, chromium, cobalt, iron, lanthanum, rubidium, selenium and zinc in the skeletal muscle, lung and spleen and in their subcellular fraction of rat were determined to investigate the distribution of these elements in abovementioned tissues and their subcellular fraction. The distributions of these trace elements are shown in Table 4.1 – 4.3.

Elements	Nuclei	Mitochondria	Microsomes	Cytosol
As	-	< 12	< 3 - 7	< 3 - 5
Cs	< 0.003	0.07 ± 0.03	0.04 ± 0.01	0.14 ± 0.04
Cr	0.22 ± 0.15	< 0.9	< 0.7	< 0.1
Co	0.25 ± 0.06	0.66 ± 0.2	0.85 ± 0.08	0.17 ± 0.03
Fe	6.3 ± 1.7	102 ± 26	330 ± 113	48 ± 10
Rb	< 0.2	3.5 ± 1.4	< 3	12 ± 0.7
Se	0.22 ± 0.05	0.56 ± 0.02	0.45 ± 0.03	0.4 ± 0.01
Zn	14 ± 4	45 ± 16	38 ± 9	28 ± 10

Table 4.1 Concentration of arsenic, cesium, chromium, cobalt, iron, rubidium, selenium and zinc [mg/kg dry masse] in the nuclei, mitochondria, microsomes on cytosol of skeletal muscle of rat (mean ± SD; n = 6)

Elements	Nuclei	Mitochondria	Microsomes	Cytosol
As	< 0.5 - 1	< 2 - 4	< 4 - 7	0.59 ± 0.3
Cs	0.02 ± 0.01	< 0.008	< 0.02	0.032 ± 0.007
Cr	0.52 ± 0.22	< 0.8	1.1 ± 0.14	< 0.15
Co	0.22 ± 0.1	0.45 ± 0.3	0.57 ± 0.09	0.1 ± 0.05
Fe	24 ± 3	230 ± 30	1980 ± 577	534 ± 50
Rb	< 1.03	5 ± 0.8	< 7.2	7.6 ± 1.4
Se	0.38 ± 0.17	1.26 ± 0.1	2.34 ± 0.61	2.04 ± 0.16
Zn	22 ± 4	56 ± 9	102 ± 24	69 ± 31

Table 4.2 Concentration of arsenic, cesium, chromium, cobalt, iron, rubidium, selenium and zinc [mg/kg dry masse] in the nuclei, mitochondria, microsomes on cytosol of lung of rat (mean ± SD; n = 6)

Elements	Nuclei	Mitochondria	Microsomes	Cytosol
As	< 0.1	4.5 ± 0.52	2.2 ± 0.6	7.9 ± 0.85
Cs	< 0.012	< 0.008	< 0.02	0.05 ± 0.01
Cr	< 2	< 1	< 4	< 1
Co	0.3 ± 0.12	0.3 ± 0.12	0.3 ± 0.12	0.18 ± 0.08
Fe	1800 ± 300	1600 ± 300	18300 ± 1300	395 ± 66
Rb	< 10	< 12	< 25	27.8 ± 7.7
Se	0.14 ± 0.03	1.1 ± 0.14	1.21 ± 0.12	1.36 ± 0.3
Zn	69 ± 17	84 ± 10	129 ± 25	63 ± 7

Table 4.3 Concentration of arsenic, cesium, chromium, cobalt, iron, rubidium, selenium and zinc [mg/kg dry masse] in the nuclei, mitochondria, microsomes on cytosol of spleen of rat (mean ± SD; n = 6)

Between the tissues and their subcellular fractions no significant differences were observed. The investigated trace elements in all organs and their cellular components were distributed inhomogeneous. The concentration of arsenic was not detected in all subcellular fractions of the skeletal muscle and in lung except cytosol. In the spleen, the highest concentration of arsenic was found in cytosol. The concentration of this element in the subcellular fractions of spleen was between 2.2 and 7.9 mg/kg dry mass. Cesium was not detected in all cell fractions of the investigator organs. The highest concentration of this element was present in cytosol of skeletal muscle with concentration of 0.14 mg/kg dry mass. In the lung, cesium was found in the nuclei and cytosol. The concentration was between 0.02 and 0.032 mg/kg dry mass. In the cell fractions of spleen, cesium was detected in cytosol with concentration of 0.05 mg/kg dry mass. Chromium was only detected in the nuclei of skeletal muscle with concentration of 0.22 mg/kg dry mass. In the lung, this element was found in the nuclei and microsomes with highest concentration of 1.1 mg/kg dry mass in the microsomes. The concentration of chromium was not detected in all subcellular fractions of spleen. Cobalt was detected in all fractions of the examination organs. The highest concentration was found in the microsomes of skeletal muscle with concentration of 0.85 mg/kg dry mass. The highest concentration of rubidium was found in the cytosolic fraction of spleen with concentration of 27.8 mg/kg dry mass. This element was found also in mitochondria and cytosol of lung and skeletal muscle. The microsomes of lung and spleen contained the largest concentration of zinc and selenium. For both elements the largest concentration was observed in the mitochondria of skeletal muscle. The concentration of zinc in the subcellular fraction of skeletal muscle was between 14 and 45 mg/kg dry mass. In the subcellular fraction of lung it was between 22 and 102 mg/kg dry mass and in the spleen organelles it was between 63 and 129 mg/kg dry mass. The selenium concentration in the subcellular fraction of skeletal muscle was between 0.22 and 0.56 mg/kg dry mass, in the lung organelles it was between 0.38 and 2.34 mg/kg dry mass, and in the fractions of spleen the concentration was between 0.14 and 1.36 mg/kg dry mass. Of interest is the very high concentration of iron in the subcellular fraction mainly in the microsomes of all tissues. Iron is one of the main elements present in the blood. A possible explanation for this could be an enrichment of iron-containing enzymes such as catalase. The microsomal fractions contain catalase, one of the iron-binding enzymes.



## 4.1.2 Summary

INAA was used for determination of selected elements, as a sensitive multi-element analytical technique. This allowed the quantitative determination of a large number of trace elements in small amounts of biological material by irradiating the samples repeatedly at different irradiation environment. In this way the distribution of arsenic, cesium, chromium, cobalt, iron, rubidium, selenium and zinc in the organs and their subcellular fraction was studied. The elements were distributed inhomogeneous in the tissues and their compartments. The highest concentration of arsenic was found in the lung. The largest concentration of arsenic in the subcellular fractions was found in the cytosol of spleen, with concentration of 7.9 mg/kg and lung, with concentration of 5.64 mg/kg dry mass. The skeletal muscle presented the highest concentration of cesium. With regard to the distribution of cesium in the subcellular fractions, the highest concentration of 0.14 mg/kg dry mass was found in the cytosol of skeletal muscle. In the investigation organs, the highest concentration of cobalt was found in the lung and spleen, but in the cells compartments the highest concentration was found in the cytosol of skeletal muscle with a concentration of 0.14 mg/kg dry mass. The highest concentration of rubidium was found in the cytosolic fraction of spleen with a concentration of 27.8 mg/kg dry mass. This element was found also in mitochondria and cytosol of lung and skeletal muscle. The largest concentration of chromium with a concentration of 1.1 mg/kg dry mass was found in the microsomes of lung. The highest concentration of iron was found in the spleen, which could be explained with the function of this organ. The spleen, in the vertebrate animal, is responsible for the degradation of erythrocytes which contain this element in the hemoglobin and in this tissue the iron excess in the form of ferritin is accumulated. The highest Fe concentration of 18300 mg/kg dry mass was found in the microsomes of spleen. The microsomes of lung and spleen contained the largest concentration of zinc with concentration of 102 mg/kg and 129 mg/kg dry mass and selenium – 2.34 mg/kg and 1.21 mg/kg dry mass, but in the skeletal muscle the largest concentration of these elements in the mitochondrial fraction was observed. Various investigators have proposed that a biochemical function of zinc is the preservation of membrane structure and function. Bray et al reported that the dietary zinc deficiency can stimulate the production of carbon-centered free radicals in lung microsomes [73].

## 4.2 Trace experiments with <sup>75</sup>Se in the cultured cells

Reactive oxygen species (ROS) are known for their negative effect on multiple disease and aging processes. The amount of ROS production and their effect in the skeletal muscle are dependent on their difficult heterogeneous and complex nature. The tissues consist of different muscle fiber types with individual metabolic properties, nerves, endothelial and blood cells, and extracellular matrix that increase the possibility of ROS production. Therefore, muscle myoblasts cells are fortified with high intracellular and extra-cellular levels of antioxidants [74]. The lung epithelium is also concerned from reactive oxygen species, permanent exposure of this organ to high concentration of oxygen and oxidants conduce of this formation. Inflammation, air pollutants or cigarette smoke can increase generation massive amounts of ROS, consequently the oxidant – antioxidant balance is destroyed, they overall claim expenditure induce the tissue disorder [75]. These cells have developed effective antioxidant defenses, in which selenium may play an important role.

Twenty-five selenoproteins have been identified by eukaryotic, but more than thirty selenoproteins are expected to exist in mammals. The function of one part of them is poorly defined or still unknown. The selenoproteins with established function play an important role in biological processes and several of them are participating in antioxidant defense. [76].

This part of the study was concerned with the identification of selenium-containing proteins in cultured cells of the skeletal muscle and lung. For this experiment the muscle myoblasts cells line C2C12 (mouse) and the lung epithelial cells line A549 (human) were chosen. The cells were cultured as described in the section 3.1.2. The cells were labeled *in vitro* with 20kBq <sup>75</sup>Se, applied to the medium to 24 hours after cell subcultures. For 48 or 72 hours the cells were incubated with <sup>75</sup>Se and after this time the cells were abraded and homogenized. The nuclear, mitochondrial, microsomal and cytosolic fractions were separated by differential centrifugation after homogenization. For each sample the protein concentration was determined. The fractions with equal protein concentration were separated by means of SDS-PAGE or 2D-SDS-PAGE. After staining and drying of the gels, selenium-containing proteins were identified by autoradiography. The selenoproteins present in the subcellular compartments in cultured

cells of the skeletal muscle and lung were then characterized via their molecular mass and pI value.

#### 4.2.1 Selenium – containing proteins in the cell lines C2C12 with SDS-PAGE

The proteins of the homogenates and subcellular fractions of the muscle myoblasts cells line C2C12 were separated by using SDS-PAGE and the selenium present in the proteins was identified by autoradiography. The autoradiogram is show in Figure 4.5.

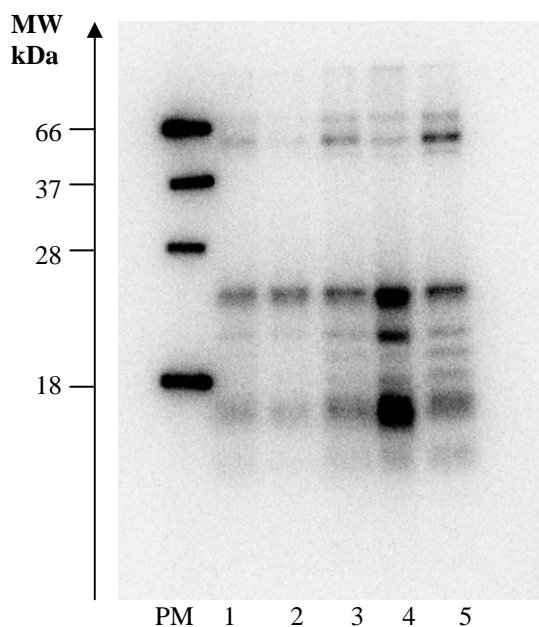


Figure 4.5 Autoradiogram of the Se-labeled proteins in the homogenate (1), nuclear (2), mitochondrial (3), microsomal (4) and cytosolic (5) fraction of the C2C12 cells after SDS-PAGE, PM - protein molecular weight marker

In the subcellular fractions of the cells line C2C12 9 selenium– containing proteins were found. Their relative molecular masses are: 70-65 kDa, 55 kDa, 53 kDa, 25 kDa, 23 kDa, in the range between 20 – 18 kDa, 18 kDa, 14 kDa, 10 kDa. The autoradiogram shows that the distribution of bands in the fractions was similar, but the selenoproteins between the fractions were differently labeled. The predominantly labeled protein in all fractions of the C2C12 cells line was at 25 kDa. In the microsomal fraction, the

selenoproteins at 25 kDa, 20 kDa and 14 kDa and in the cytosolic fraction protein at 55 kDa were strongly labeled.

## 4.2.2 Selenium – containing proteins in the cell lines A549 with SDS-PAGE

The selenium-containing proteins found in the homogenate and subcellular fractions of lung epithelia cells line A549 are shown in Figure 4.6.

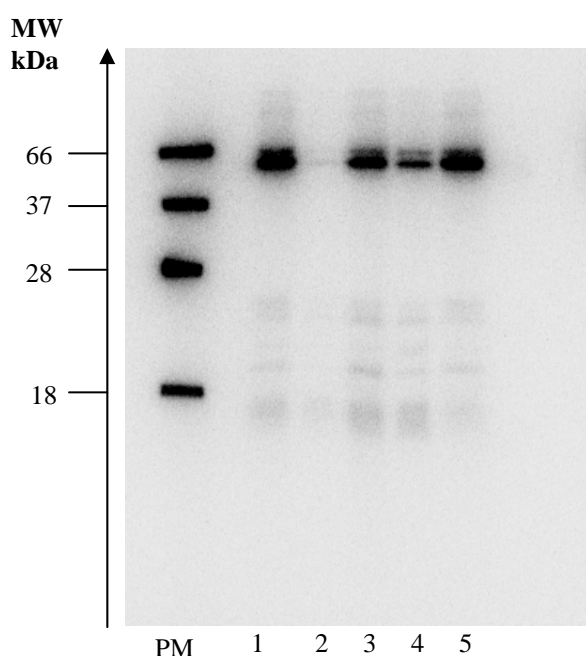


Figure 4.6 Autoradiogram of the Se-labeled proteins in the homogenate (1), nuclear (2), mitochondrial (3), microsomal (4) and cytosolic (5) fraction of the A549 cells after SDS-PAGE, PM - protein molecular weight marker

In this cell line meaningful differences of selenoproteins between these fractions were not observed. Eight proteins were found in all fractions. <sup>75</sup>Se-containing bands were detected at 75 kDa, 65 kDa, 55 kDa, 25 kDa, 23 kDa, one band between 23 and 20 kDa, 20 kDa and 15 kDa. In the epithelia cells a strong labeled band at about 55 kDa was observed in the homogenate, mitochondria, microsomes and cytosols, but in the nuclei it was weakly detected. A band between 23 and 20 kDa was found in the homogenate, mitochondria and mikrosomes. All proteins present in the nuclei were very weakly

labeled.

### **4.2.3 Characterization and identification of selenium containing proteins in the cell lines C2C12 and A549 with SDS-PAGE**

In further experiments the selenium-containing proteins in the muscle myoblasts cells C2C12 and in the lung epithelia cells line A549 were investigated more closely. For this study a homogenate and cytosolic fraction of this cell lines was used. In this way it was possible to characterize and compare the Se-containing proteins distribution among the homogenate and cytosol. The two autoradiograms in the Figure 4.7 show the <sup>75</sup>Se – containing proteins in both cell lines. The results of the evaluation of these data are listed in Table 4.4.

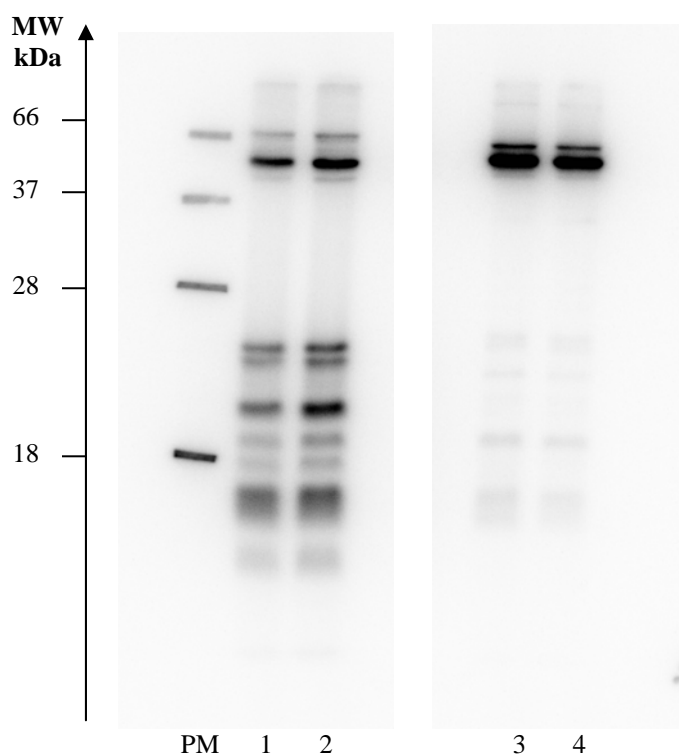


Figure 4.7 Autoradiogram of the Se-labeled proteins in the C2C12 cells line (left): 1-homogenate, 2-cytosolic fraction and in the A549 cells (right): 3-Homogenate, 4-cytosolic fraction after SDS-PAGE, PM - protein molecular weight marker

<sup>75</sup> Se-labeled bands [kDa]	C2C12		A549		Se-proteins
	Hom	Cyt	Hom	Cyt	
75			✓	✓	Sel O
70-65	✓	✓			Sel N
55	✓	✓	✓	✓	TRxR1
53	✓	✓	✓	✓	TRxR 3
50			✓	✓	?
40-37			✓	✓	Sel P
25	✓	✓	✓	✓	Gpx 3
23	✓	✓	✓	✓	Gpx 1
20	✓	✓	✓	✓	Gpx (?)
20-18	✓	✓			Sel T
18	✓	✓	✓	✓	18 kDa
15	✓	✓	✓	✓	15 kDa
10-7	✓	✓			Sel W

Table 4.4 Classification of the <sup>75</sup>Se-containing proteins found in the C2C12 and A549 cell line

The same proteins between homogenate and cytosol in the C2C12 and A549 cell lines were detected. In both cell lines the band at about 55 and 53 kDa was detected. This protein could be classified to the Thioredoxin reductases (TRxR). The autoradiogram shows three bands in the range from 25 to 20 kDa. These proteins could represent the family of Glutathion peroxidasis (Gpx). Two proteins in C2C12 and A549 cells were found at about 18 and 15 kDa. In the lung epithelia cells line a protein with a molecular weight of 75 kDa could be identified as selenoprotein O (Sel O). One protein at about 50 kDa could not be assigned to known Se-proteins. The bands between 70-65, 20-18 and 10-7 kDa were detected only in the mouse myoblasts cells, which could be classified to selenoprotein N (Sel N), selenoprotein T (Sel T) and selenoprotein W (Sel W).

#### **4.2.4 Distribution of the selenium-containing proteins in the subcellular fractions of the cell lines C2C12 by two - dimensional gel electrophoresis**

For the next part of this study of the selenoproteins present in the homogenates and subcellular fractions of the muscle myoblasts cells line C2C12 two-dimensional electrophoresis (IEF/SDS-PAGE) was applied. The electrophoresis technique has a better resolution, as the proteins are first separated via their pI and then via their molecular masses. The localization of the proteins was obtained after autoradiography. The following autoradiograms show the distribution of the selenium-containing proteins in the homogenate, nuclear, mitochondrial, microsomal and cytosolic fractions.

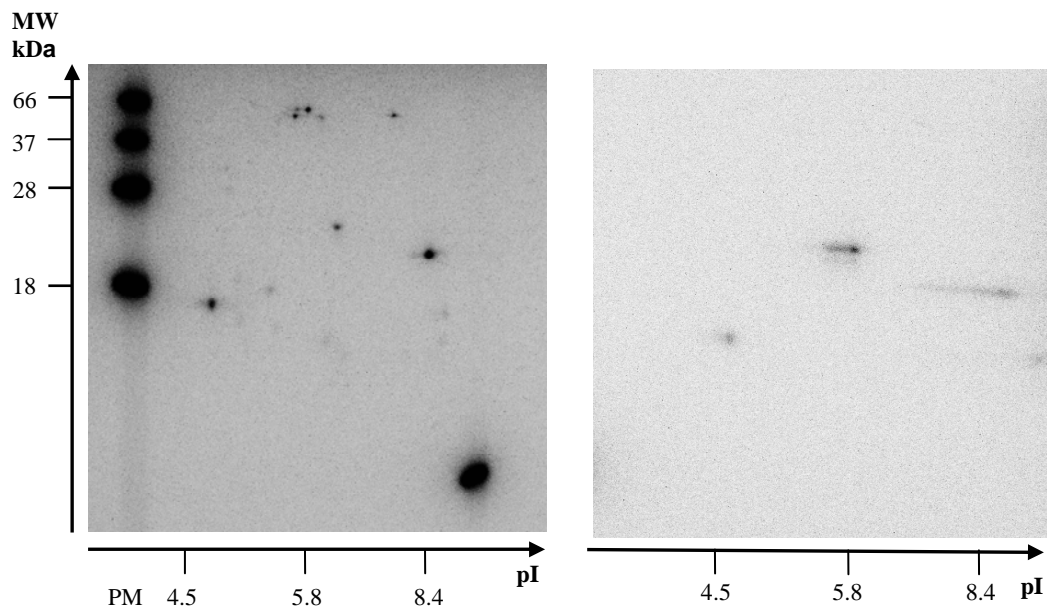


Figure 4.8 Autoradiogram of the Se-labeled proteins in the homogenate (left) and in the nucleus (right) of the C2C12 cells after 2D electrophoresis, PM - protein molecular weight marker

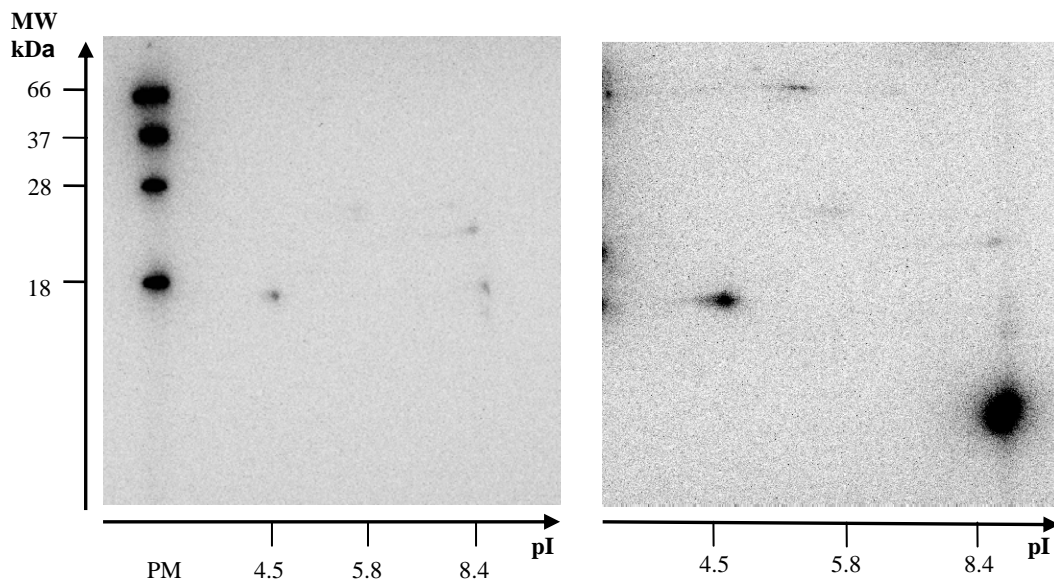


Figure 4.9 Autoradiogram of the Se-labeled proteins in the mitochondrial fraction (left) and in the microsomes (right) of the C2C12 cells after 2D electrophoresis, PM - protein molecular weight marker



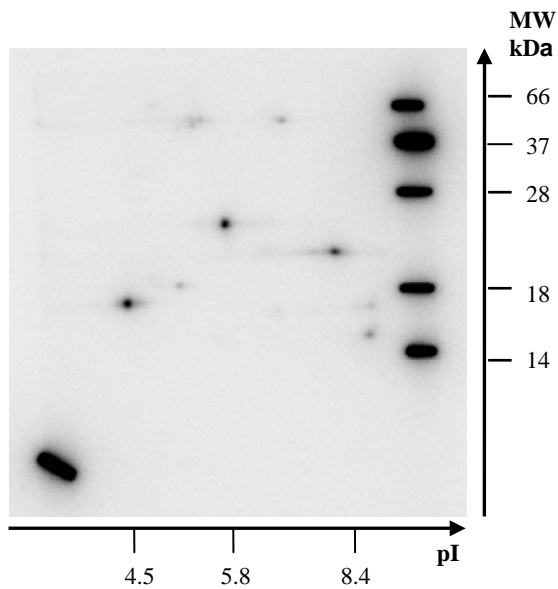


Figure 4.10 Autoradiogram of the Se-labeled proteins in the cytosolic fraction of the C2C12 cells after 2D electrophoresis

The distribution of the selenium-containing proteins in the homogenates of the muscle myoblasts cells line after separation with 2D electrophoresis can be seen in Figure 4.8. The autoradiogram shows more than 20  $^{75}\text{Se}$ -containing proteins with molecular masses between 74 – 10 kDa and with pI values between 3.0 and 10. One spot with molecular masses between 74 and 65 kDa and pI value between 5.0 and 5.5 was found. Two spots at 55 – 50 kDa and pI value of 5.2 and 6.0 were detected. These molecular masses and pI value are characteristic for the Thioredoxin reductases. One spot with molecular masses between 60 and 55 kDa and pI value of 8.0 was observed. In the range of molecular masses between 28 – 10 kDa and pI value 4.8 – 8.0 several spots were found. The Se-proteins with molecular masses 25, 23 and below 18 kDa were labeled very strongly. The distribution of the selenoproteins in the subcellular fraction of cells line C2C12 is relatively similar, but the spots are labeled differently between these fractions. In all fractions the proteins 25 kDa, 20 kDa and 15 kDa were observed. The 15 kDa protein was labeled very strongly in the microsomes and cytosolic fraction. The 25 kDa spot was labeled strongly in the cytosolic and nuclei fractions. In the microsomes, at 55 kDa two proteins with pI between 5.0 and 6.0 were labeled strongly.

#### 4.2.5 Distribution of the selenium-containing proteins in the subcellular fractions of the cell lines A549 by two - dimensional gel electrophoresis

For the study of the selenoproteins present in the homogenates and subcellular fractions of the lung epithelia cells line A549, two-dimensional electrophoresis (IEF/SDS-PAGE) was applied. The localization of the proteins was obtained after autoradiography. The following autoradiograms show the distribution of the selenium-containing proteins in the homogenate, nuclear, mitochondrial, microsomal and cytosolic fractions.

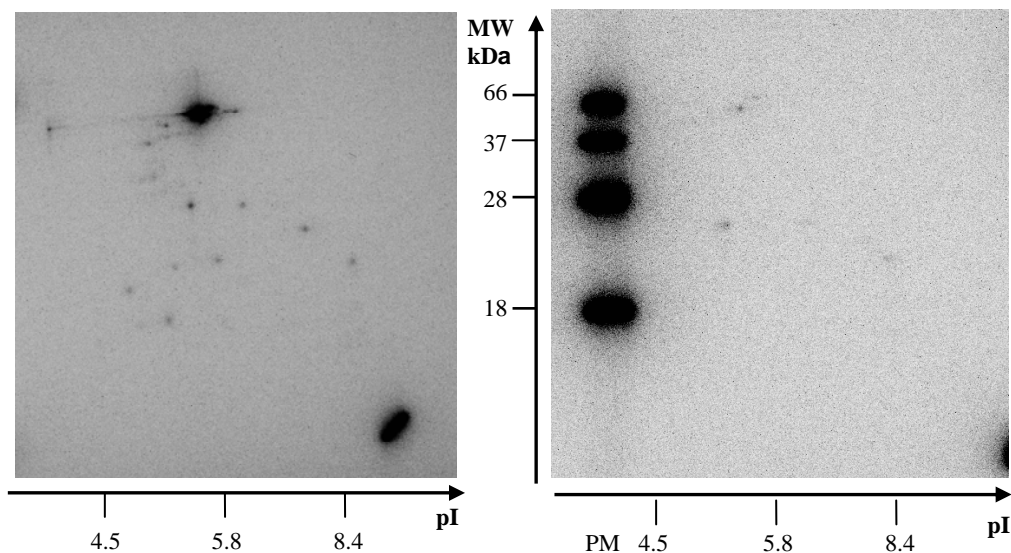


Figure 4.11 Autoradiogram of the Se-labeled proteins in the homogenate (left) and nuclei (right) of the A549 cells after 2D electrophoresis, PM - protein molecular weight marker

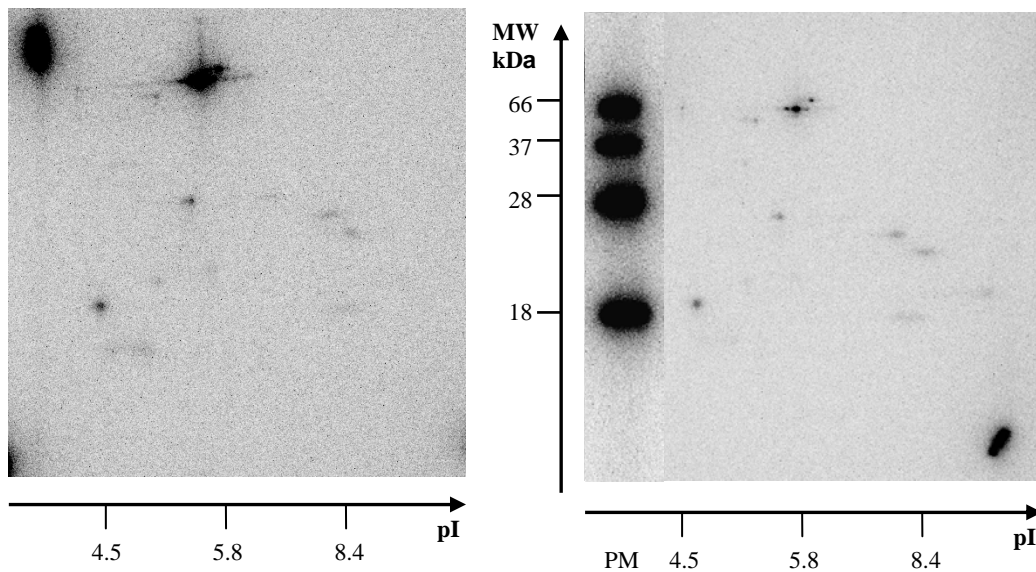


Figure 4.12 Autoradiogram of the Se-labeled proteins in the mitochondrial fraction (left) and microsomes (right) of the A549 cells after 2D electrophoresis, PM - protein molecular weight marker

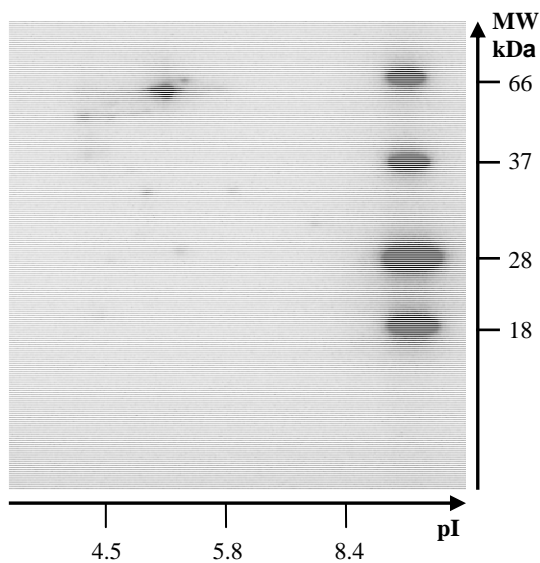


Figure 4.13 Autoradiogram of the Se-labeled proteins in the cytosol of the A549 cells after 2D electrophoresis

In the homogenate of the A549 cells line, more than 20 <sup>75</sup>Se -containing proteins were detected. In the range of molecular masses between 75 and 50 kDa eight proteins were found. Several of them were labeled very strong. Numerous of low labeling spots were found in the range of molecular masses between 40 and 30 kDa with pI value between 5 and 6. Four proteins with molecular masses between 20 and 10 kDa and pI between 4.5 – 6.0 and two with pI 8.0 – 8.4 were established. The autoradiogram shows that the

selenium-containing proteins in the nuclei of epithelia cells were labeled very weakly. In this fraction, five proteins at 65 kDa, 55 kDa with pI between 5.4 and 5.8, 25 kDa with pI values of 5.0 and 6.0 and 20 kDa with pI in the range 8.4 were detected. In the mitochondria, microsomes and cytosol the distribution of selenoproteins were relatively similar, but the spots were labeled differently. A strongly labeled protein at about 55 kDa with pI between 5.5 and 5.8 was observed in the mitochondria and cytosol. In the cytosol, 25 kDa protein with pI 6 and two proteins in the mitochondria and microsomes in the range between 23 and 20kDa and pI between 7.5 and 8.4 were observed. The 25 kDa <sup>75</sup>Se -containing protein was detected in all fraction of the A549 cell line.

#### **4.2.6 Study on the selenium-containing proteins in the cell lines C2C12 and A549 by two-dimensional gel electrophoresis**

This part of the study was concerned with the identification and characterization of the selenium-containing proteins in cultured cells of the skeletal muscle and lung. For this purpose the muscle myoblasts cells line C2C12 (mouse) and lung epithelia cell line A549 (human) were chosen. The homogenate and cytosolic fraction with equal protein concentration were separated by means of 2D-SDS-PAGE. After staining and drying of the gels, selenium-containing proteins were identified by autoradiography. The selenoproteins present in cultured cells of the skeletal muscle and lung were then characterized via their molecular mass and pI value. The Figures 4.14 – 4.15 show the distribution of the selenium-containing proteins in the homogenate and cytosol of the C2C12 and A549 cells after separation by 2D electrophoresis.

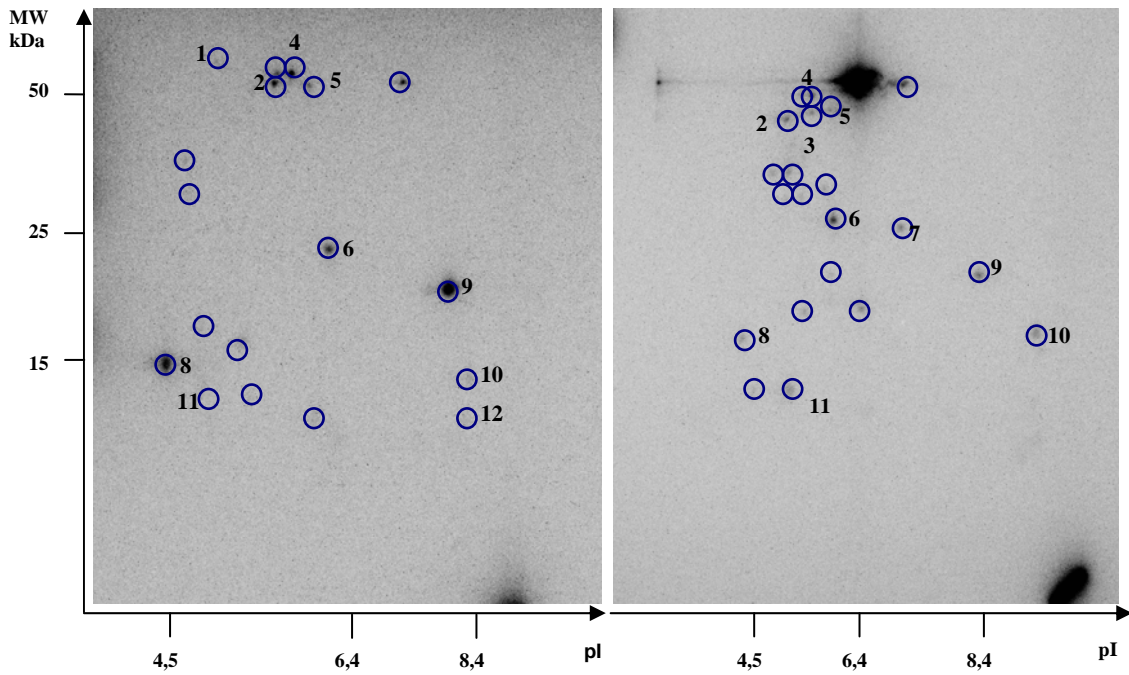


Figure 4.14 Autoradiogram of  $^{75}\text{Se}$ -labeled proteins found after IEF/SDS-PAGE in the homogenate of the C2C12 (left) and A549 (right) cell lines

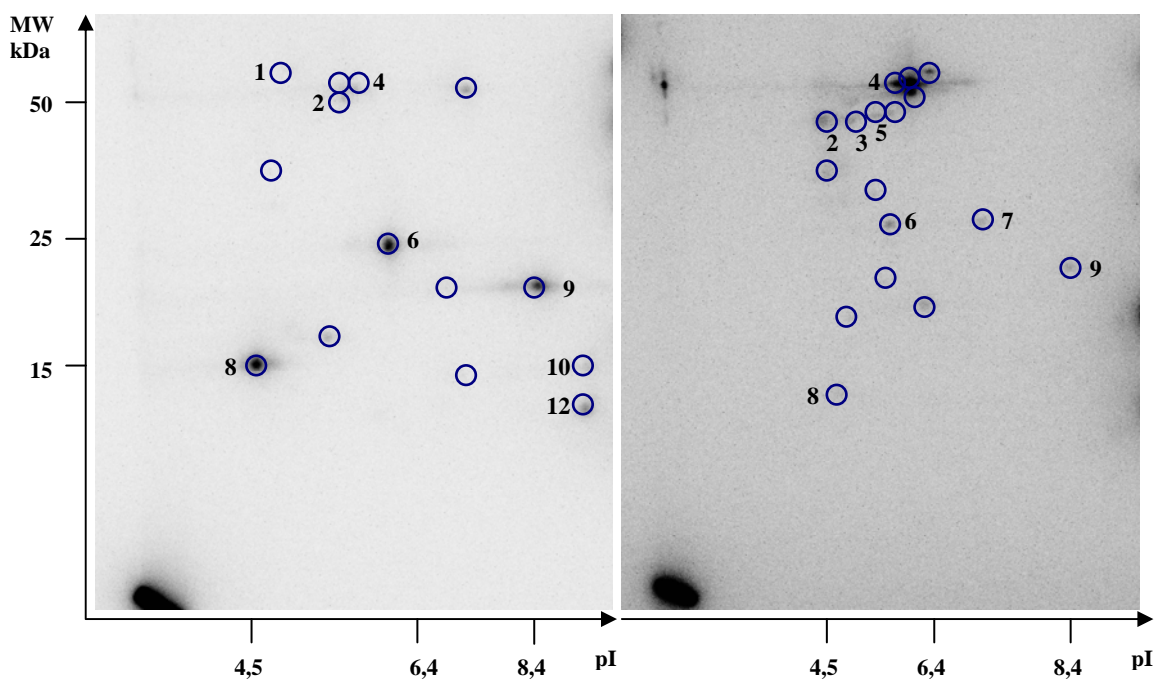


Figure 4.15 Autoradiogram of  $^{75}\text{Se}$ -labeled proteins found after IEF/SDS-PAGE in the cytosol of the C2C12 (left) and A549 (right) cell lines

Number	Selenoprotein
1	Sel O
2	TRx 1-TRx 2
3	TRx 1-TRx 2
4	TRx 1 or 3
5	Sel P
6	Gpx 1
7	Gpx 3
8	15 kDa
9	Gpx 4
10	Gpx ?
11	12 kDa
12	Sel W

Table 4.5 Classification of the  $^{75}\text{Se}$  containing-proteins found in the C2C12 and A549 cell lines

Some of the selenium-containing proteins found in both cell lines could be identified as it is shown in Table 4.5. The protein spot about 70 kDa with the pI 4.8 - 5.0 is most likely the Selenoprotein O [77]. This protein is only seen in the homogenate and cytosol of C2C12 cells. In the area between 55 – 70 kDa with pI 5.2 - 6.0 in the homogenate as well as cytosol were found five proteins, four of them could belong to the Thioredoxin reductases family [44, 78]. In the homogenate of A549 cell line was found a very strong labelled protein with molecular mass at 70 – 75 kDa and a pI of 6.5. In the cytosol, in the same area, the autoradiogram shows more than one protein. The 25 kDa and 23 kDa spots with the pI value at 6.2 – 6.8 likely belong to Gpx 1 and Gpx 3 [79, 80]. One protein of 20 kDa with pI 7.5 – 8.0 in both cell lines was detected, which corresponds to the Gpx 4 [81].

In all presented autoradiograms one protein was seen at 15 kDa and pI values between 4.5 – 4.8 which can be the 15 kDa Selenoprotein [82]. The 12 kDa selenoprotein with pI at 4.8 – 5.3 was found only in the homogenate of C2C12 and A549 cells. The Sel 12 kDa is also known as SelR [51]. In the mouse myoblasts cells, one protein of 10 kDa with pI 8.5 – 8.8 is found, which possibly could belong to Sel W [49, 83].

More than ten selenium-containing proteins can not be allocated to known selenoproteins.

## 4.2.8 Summary

In the current study more than 10 Se-containing proteins were detected in the muscle myoblasts C2C12 and the lung epithelial A549 cells lines. Their relative molecular masses were: 75 kDa, 70-65 kDa, 55 kDa, 53 kDa, 50 kDa, 40 – 37 kDa, 25 kDa, 23 kDa, in the range between 20 – 18 kDa, 18 kDa, 14 kDa, 10 kDa. The autoradiogram shows that the distribution of bands in the cells compartments in both cell lines was similar, but the selenoproteins between the fractions were labeled differently. The predominantly labeled proteins in all fractions of the C2C12 and A549 cells line were at 55 and 25 kDa. In the microsomal fraction of C2C12, the selenoproteins at 25 kDa, 20 kDa and 14 kDa and in the cytosolic fraction protein at 55 kDa were labeled most strongly. In the A549 cell lines a protein at about 53 kDa was labeled especially strong. More than 20 selenium-containing proteins in the muscle myoblasts and lung epithelia cells lines were detected after separation with 2D electrophoresis. The autoradiogram in either cells lines have shown strong labeled proteins between 55 – 50 kDa with pI at 5.2 – 6.0. The molecular masses and pI value are characteristic for the Thioredoxin reductases. Two proteins at 25 kDa with pI 5.5 and 20 kDa with pI of about 8.4 were found in both investigated cells lines.

Some of the selenium-containing proteins found in the both cell lines could be identified. One protein spot about 70 kDa with the pI 4.8 - 5.0 is most likely the Selenoprotein O. In the area between 55 – 70 kDa with pI 5.2 - 6.0 in the homogenate as well as cytosol were found five proteins, four for them could belong to the Thioredoxin reductases family. The 25 kDa and 23 kDa spots with the pI value at 6.2 – 6.8 likely belong to Gpx 1 and Gpx 3. One protein of 20 kDa with pI 7.5 – 8.0 in both cell lines was detected, which corresponds to the Gpx 4. In all presented autoradiograms one protein was seen at 15 kDa and pI values between 4.5 – 4.8 which can be the 15 kDa Selenoprotein. The 12 kDa selenoprotein was found only in the homogenate of C2C12 and A549 cells. In the mouse myoblasts cells, one protein of 10 kDa with pI 8.5 – 8.8 was found, which possibly could be belong to Sel W.

More than ten selenium-containing proteins can not be allocated to known selenoproteins.

## 4.3 Antioxidant activity

Generation of reactive oxygen species (ROS) is a normal process in the aerobic life. Under normal physiological conditions, these harmful species are degraded by the cellular antioxidant defense system. All normal functioning cells contain different mechanisms for protection against the oxidants. The mechanisms are based on the antioxidant activity as antioxidant enzymes, antioxidant vitamins and protein and non-protein thiols [84, 85]. It was reported that the trace element selenium is necessary for the antioxidant defense system [3, 86, 87]. Therefore, it is very important to understand the Se regulation function not only as antioxidant but also for the whole antioxidant status.

In this study the effect of selenium for the whole antioxidative activity was examined. For these experiments the skeletal muscle, the lung and the spleen of rats were used. The rats were fed with a selenium deficient diet and a selenium sufficient diet.

### 4.3.1 The total antioxidant status in cytosolic fraction

ABTS assay was used for the screening of the total antioxidant status in cytosolic fractions of skeletal muscle, lung and spleen of rat fed with a selenium deficient diet and a selenium sufficient diet. The method described gives a measure of the lipophilic and hydrophilic antioxidant including flavonoids, carotenoids, hydroxycinnamates and plasma antioxidants.

The total standard deviation  $s_T$  was calculated as follows:

$s_T^2 = s_G^2 + s_{IG}^2$ , where  $s_G^2$  and  $s_{IG}^2$  were used for intra- and inter-group variance correspondingly.

The values of  $s_G^2$  and  $s_{IG}^2$  were calculated as follows:

$$s_G^2 = \frac{\sum_i n_i s_i^2}{n}, \quad n = \sum_i n_i$$

$$s_{IG}^2 = \frac{\sum_i (\bar{x}_i - \bar{x})^2}{n-1}$$



where  $\bar{x}_i$  is used for  $i$ -th group average and  $\bar{x}$  - for total average,  $n$  is the total number of measurements,  $n_i$  is the number of parallel measurements for  $i$ -th group.

Organ	Se	Cytosol [nmol/ml]	Average
Skeletal muscle 1	-	390 ± 7	<b>415 ± 21</b>
Skeletal muscle 2	-	433 ± 4	
Skeletal muscle 3	-	414 ± 8	
Skeletal muscle 4	-	424 ± 14	
Skeletal muscle 5	+	378 ± 8	
Skeletal muscle 6	+	414 ± 6	
Skeletal muscle 7	+	333 ± 11	
Skeletal muscle 8	+	348 ± 8	
Lung 1	-	338 ± 9	<b>334 ± 14</b>
Lung 2	-	329 ± 7	
Lung 3	-	320 ± 9	
Lung 4	-	348 ± 3	
Lung 5	+	322 ± 5	
Lung 6	+	341 ± 5	
Lung 7	+	312 ± 7	
Lung 8	+	303 ± 10	
Spleen 1	-	250 ± 6	<b>267 ± 25</b>
Spleen 2	-	298 ± 8	
Spleen 3	-	275 ± 3	
Spleen 4	-	245 ± 4	
Spleen 5	+	212 ± 11	
Spleen 6	+	251 ± 3	
Spleen 7	+	207 ± 9	
Spleen 8	+	269 ± 7	
			<b>235 ± 31</b>

Table 4.6 Antioxidants in cytosol from rat skeletal muscle, lung and spleen, expressed as equivalents to 1 nmol·ml<sup>-1</sup> ascorbic acid (mean ± SD; n = 4)

The total antioxidative status, which is presented in Table 4.6 did not decrease in the cytosol of the skeletal muscle, lung and spleen in the group with selenium deficient diet compared to the group with selenium sufficient diet. The reason for this could be that the protective function of selenium is possibly taken over by other antioxidants. The measured integral antioxidative capacity in the skeletal muscle was similar to the lung.

In the spleen, the measured integral antioxidative capacity was considerable lower in comparison to skeletal muscle and lung.

### **4.3.2 AOS-scavenging enzymes**

In this part of the study the occurrence of important antioxidant enzymes in the skeletal muscle, lung and spleen of rat and the effect of selenium on these enzymes were examined.

#### **4.3.2.1 GPx 1 activity in the cytosol**

Glutathione peroxidase (GPX; EC 1.11.1.9) catalyses the reduction of hydrogen peroxide using reduced glutathione to water. In this way the cells are protected against oxidative damage. This enzyme exists as a tetramer with four identical subunits. Each subunit contains a selenocysteine in the active site which participates directly in the two electron reduction of the peroxide substrate. The enzyme uses glutathione as the ultimate electron donor to regenerate the reduced form of the selenocysteine [88].

The activity of the glutathione peroxidase – GPx1 in the cytosol of the skeletal muscle, lung and spleen of rats fed with a selenium deficient diet and a selenium sufficient diet was measured. The results are presented in the Figure 4.18 – 4.20.

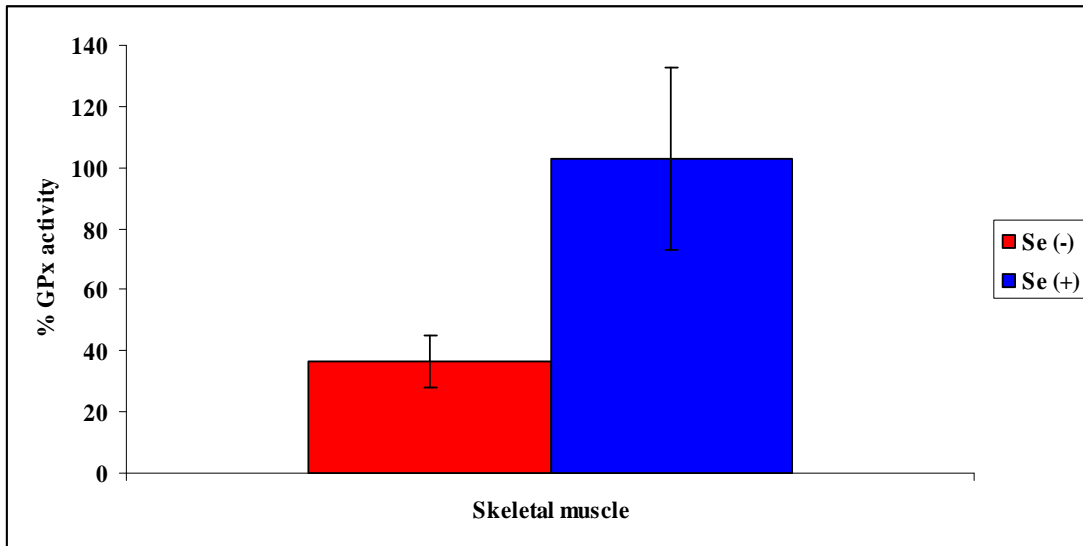


Figure 4.18 GPx activity (% of control) in the cytosolic fraction of the skeletal muscle of selenium deficient [Se (-)] and selenium sufficient animals [Se (+)]

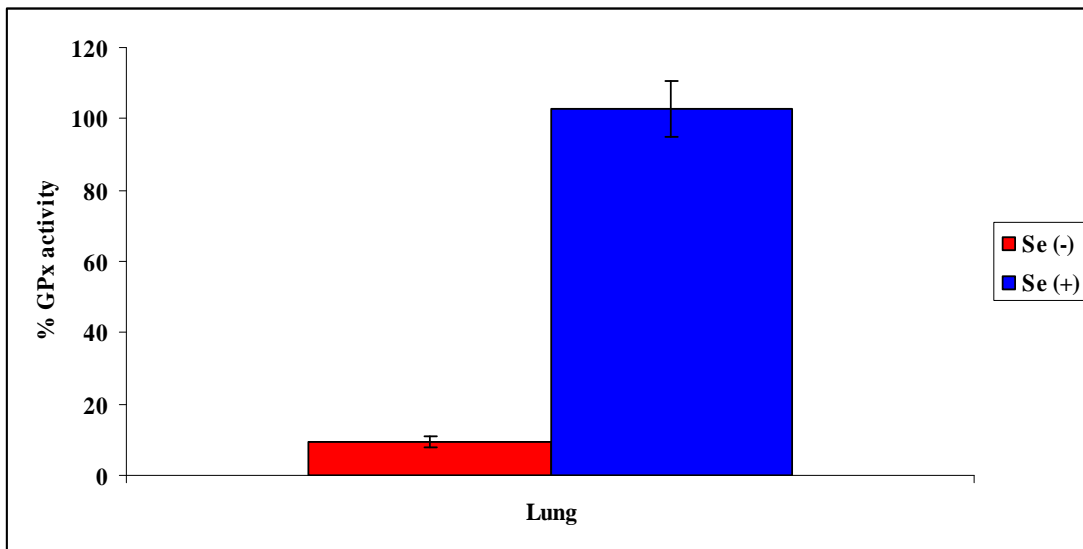


Figure 4.19 GPx activity (% of control) in the cytosolic fraction of the lung of selenium deficient [Se (-)] and selenium sufficient animals [Se (+)]

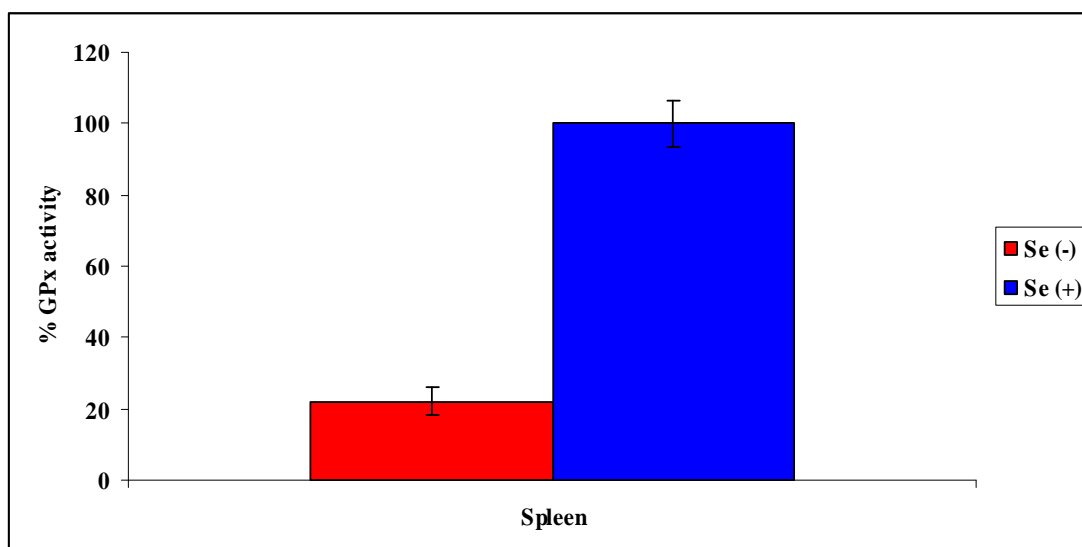


Figure 4.20 GPx activity (% of control) in the cytosolic fraction of the spleen of selenium deficient [Se (-)] and selenium sufficient animals [Se (+)]

The graphics show decreases in GPx 1 activity in the cytosol in presented tissues in the deficient rats compared with selenium sufficient animals. The activity in the Se (-) lung was ten times lower than in the Se (+) lung. In the spleen, the activity was five times lower. In the skeletal muscle of the deficient animals, the GPx activity was determined at approximately 40%.

#### 4.3.2.2 Detection and localization of antioxidants proteins

The immunoassay is the fastest and most specific method for the detection and localization of proteins, when a suitable antibody is available. As most of the antioxidants proteins are not completely characterized and identified, it was only possible to obtain antibodies for the recognition of the TrxR 1, Gpx 1, Selenoprotein 15 kDa, Cu/Zn SOD, catalase and Pon 1. For the study of these proteins the immunoassays were used. The results are shown below.

#### 4.3.2.2.1 TrxR1

The selenoenzyme family of thioredoxin reductases (TrxRs) has a function of degrading hydroperoxides. The mammalian TrxRs family belongs to three members which contain an essential selenocysteine residue in their C-terminus [3, 89]. Human TrxRs reduce thioredoxin and several other substrates in a complex reaction cascade, requiring electron transfer from NADPH via FAD to a disulfide in the N-terminal redox center of one subunit and from there to the selenenylsulfide in the C-terminal of the other subunit [90].

These enzymes are involved in protection against reactive oxygen species during control of redox state of thioredoxin. Thioredoxin was primarily considered to be an intracellular protein located in cytosol and mitochondria, but it is secreted as well [91].

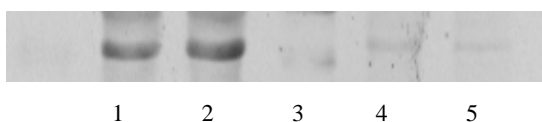


Figure 4.21 Immunological detection of TrxR1 in the subcellular fractions of skeletal muscle: homogenate (1), cytosolic (2), nuclei (3), mitochondrial (4) and microsomes fractions

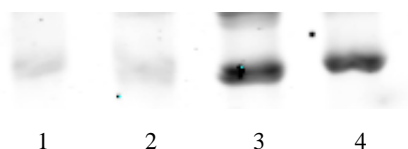


Figure 4.22 Immunological detection of TrxR1 in the homogenate and cytosolic fraction of the skeletal muscle: 1- homogenate Se (-), 2- cytosolic Se (-), 3- homogenate Se (+), 4- cytosolic Se (+)

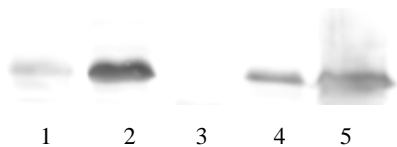


Figure 4.23 Immunological detection of TrxR1 in the subcellular fractions of lung: homogenate (1), cytosolic (2), nuclei (3), mitochondrial (4) and microsomes fractions (5)



Figure 4.24 Immunological detection of TrxR1 in the homogenate and cytosolic fraction of the lung: 1- homogenate Se (-), 2- cytosolic Se (-), 3- homogenate Se (+), 4- cytosolic Se (+)



Figure 4.25 Immunological detection of TrxR1 in the subcellular fractions of spleen: homogenate (1), nuclei (2), mitochondrial (3), cytosolic (4) and microsomes fractions (5)

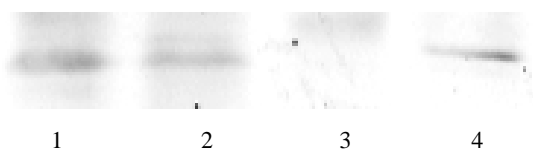


Figure 4.26 Immunological detection of TrxR1 in the homogenate and cytosolic fraction of the spleen: 1- homogenate Se (+), 2- cytosolic Se (+), 3- homogenate Se (-), 4- cytosolic Se (-)

In the skeletal muscle in homogenate and cytosol TrxR 1 was identified. The signaling of this enzyme was strongly marked in the group with selenium sufficient diet. In the lung the enzymes were observed in the homogenate, cytosolic, mitochondrial and microsomes fraction. The signaling of TrxR1 was seen in the homogenate and cytosol

of lung in the Se (+) animal group. The immunoassay of spleen showed TrxR 1 signal in homogenate, cytosol, mitochondrial and microsomes fraction.

#### 4.3.2.2.2 GPx1

In addition to redoxin reductase, the family of glutathione peroxidases (Gpxs) is also capable of reducing of hydrogen peroxide and lipid hydroperoxide.

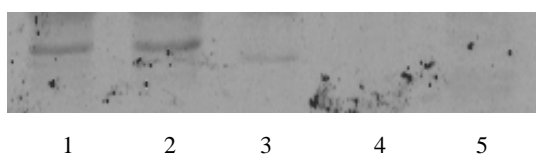


Figure 4.27 Immunological detection of GPx1 in the homogenate (1), cytosolic (2), nuclear (3), mitochondrial (4), and microsomal (5) fraction of the skeletal muscle of rat

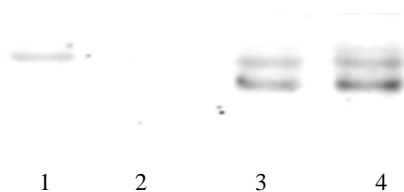


Figure 4.28 Immunological detection of GPx1 in the homogenate and cytosolic fraction of the skeletal muscle: 1-homogenate Se (-), 2- cytosolic Se (-), 3-homogenate Se (+), 4- cytosolic Se (+)

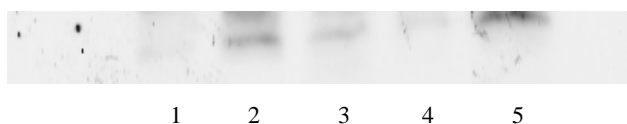


Figure 4.29 Immunological detection of GPx1 in the homogenate (1), cytosolic (2), nuclear (3), mitochondrial (4), and microsomal (5) fraction of the lung of rat

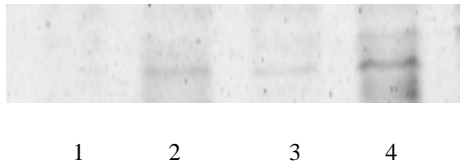


Figure 4.30 Immunological detection of GPx1 in the homogenate: 1-Se (-), 2-Se (+) and cytosol 3-Se (-), 4-Se (+) of the lung of rat



Figure 4.31 Immunological detection of GPx1 in the homogenate (1), cytosolic (2), nuclear (3), mitochondrial (4), and microsomal (5) fraction of the spleen of rat

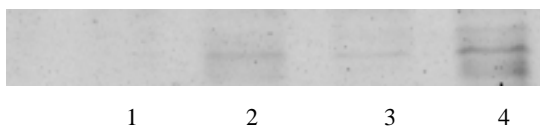


Figure 4.32 Immunological detection of GPx1 in the homogenate: 1-Se (-), 2-Se (+) and cytosol: 3-Se (-), 4-Se (+) of the spleen of rat

The previous study has shown a low signaling of Gpx 1 in the homogenate and cytosol of the skeletal muscle. This enzyme was identified only in the homogenate and cytosol of the Se (+) group. The immunoblot of lung shows a signaling of Gpx 1 in the homogenate and cytosol of the selenium sufficient group. In the other group only in the cytosol a low signal of this enzyme could be seen. In the spleen in homogenate and in cytosol Gpx 1 was detected. In the selenium sufficient group in both fractions the Gpx 1 was demonstrated and in the cytosol of Se (-) group a low signaling of this protein was observed.

#### 4.3.2.2.3 Selenoprotein 15 kDa

The 15 kDa selenoprotein (Sel 15) was identified in mammals for several years, but its specific function and biological roles are still unknown. The expression of Sel 15 is regulated by dietary selenium. Many studies reported that this protein is localized in the



endoplasmic reticulum and a different part of this protein takes part in the calnexin-calreticulin glycoprotein folding cycle [92] It was suggested that the 15 kDa protein has a role in cancer prevention [93, 94].

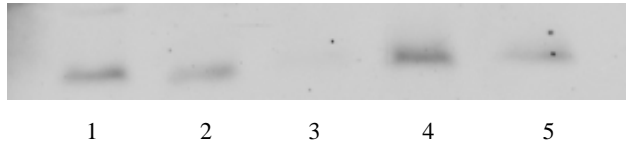


Figure 4.33 Immunological detection of 15 kDa protein in the homogenate (1), cytosolic (2), nuclear (3), mitochondrial (4), and microsomal (5) fraction of the skeletal muscle of rat

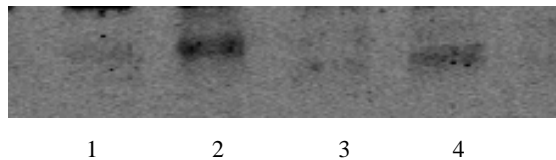


Figure 4.34 Immunological detection of 15 kDa protein in the homogenate: 1-Se (-), 2-Se (+) and cytosol: 3-Se (-), 4 Se (+) of the skeletal muscle of rat

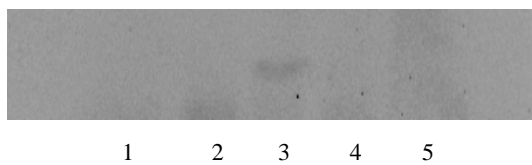


Figure 4.35 Immunological detection of 15 kDa protein in the homogenate (1), nuclear (2), cytosolic (3), mitochondrial (4), and microsomal (5) fraction of the lung of rat

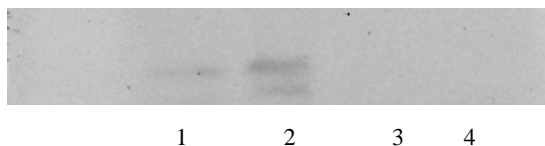


Figure 4.36 Immunological detection of 15 kDa protein in the homogenate: 1-Se (+), 3-Se (-) and cytosol: 2-Se (+), 4 Se (-) of the lung of rat

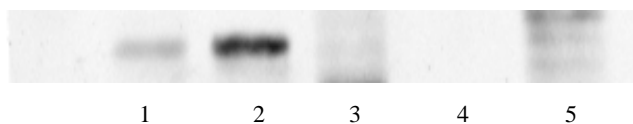


Figure 4.37 Immunological detection of 15 kDa protein in the homogenate (1), nuclear (2), cytosolic (3), mitochondrial (4), and microsomal (5) fraction of the spleen of rat

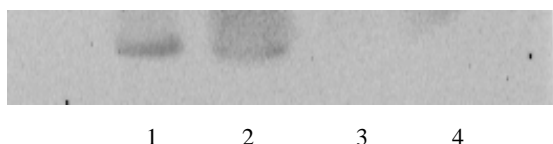


Figure 4.38 Immunodetection of 15 kDa protein in the homogenate: 1-Se (+), 2-Se (-) and cytosol: 3-Se (+), 4 Se (-) of the spleen of rat

In the homogenate, cytosol, mitochondria and microsomes, the 15 kDa protein was detected. In the animal with selenium sufficient diet the signalling was strongly detected compared to the Se (-) group. In the lung, the enzyme was only seen in the cytosol but in the Se (+) group it was present in the homogenate und cytosol. The 15 kDa protein was identified in the homogenate and cytosolic fraction of spleen.

#### 4.3.2.2.4 Cu/Zn SOD

Early studies reported that SOD is an important enzyme which controls cellular ROS level and may have potential to be used as therapeutic agents in oxidative stress-related diseases [95]. The protection function is rested on neutralization of oxygen – free radical to molecular oxygen and hydrogen peroxide. The SODs proteins group contains three isoforms, which were identified in mammals. Two of them have copper or zinc in their catalytic center and one mitochondrial enzyme posses Mn atom [96, 97].

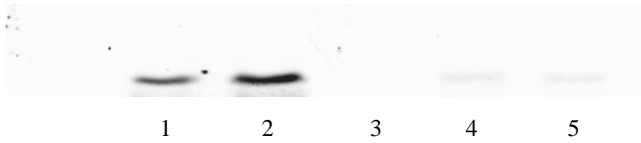


Figure 4.39 Immunological detection of Cu/Zn SOD in the homogenate (1), cytosolic (2), nuclear (3), mitochondrial (4), and microsomal (5) fraction of the skeletal muscle of rat

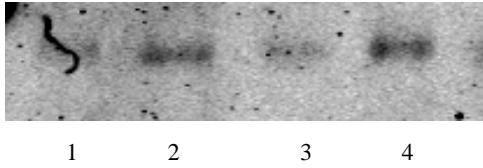


Figure 4.40 Immunological detection of Cu/Zn SOD in the homogenate: 1-Se (-), 2-Se (+) and cytosol: 3-Se (-), 4 Se (+) of the skeletal muscle of rat

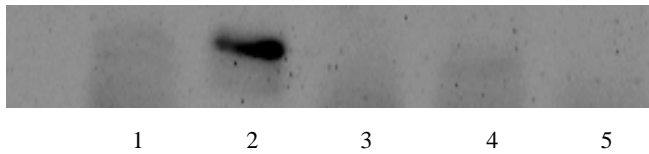


Figure 4.41 Immunological detection of Cu/Zn SOD in the homogenate (1), cytosolic (2), nuclear (3), mitochondrial (4), and microsomal (5) fraction of the lung of rat

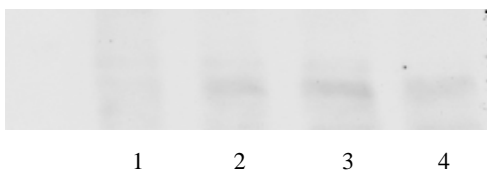


Figure 4.42 Immunological detection of Cu/Zn SOD in the homogenate: 1-Se (+), 2-Se (-) and cytosol: 3-Se (+), 4 Se (-) of the lung of rat

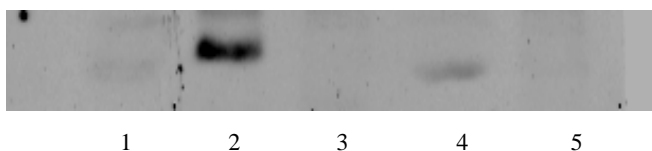


Figure 4.43 Immunological detection of Cu/Zn SOD in the homogenate (1), cytosolic (2), nuclear (3), mitochondrial (4), and microsomal (5) fraction of the spleen of rat

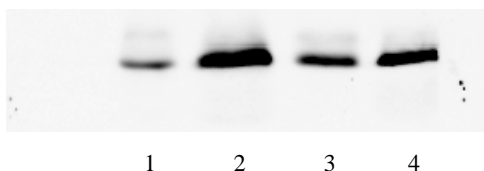


Figure 4.44 Immunological detection of Cu/Zn SOD in the homogenate: 1-Se (+), 2-Se (-) and cytosol: 3-Se (+), 4 Se (-) of the spleen of rat

The immunoblot of skeletal muscle shows signals of Cu/Zn SOD in the homogenate and cytosol. In the Se (+) and Se (-) group homogenate and cytosol this enzyme was detected. In the lung the superoxide dismutase was identified in the cytosol and in both animals group in the homogenate and also in the cytosol. The same result presents the immunoblot of spleen. The enzyme was observed only in the cytosol. In the Se (+) and Se (-) group the enzyme was detected in cytosol and homogenate.

#### 4.3.2.2.5 Catalase

Tissues peroxide levels are largely regulated by the activity of hydroperoxidases. The catalase belongs to this enzymes group. Catalase catalysed reaction, which lead to dissolution of hydrogen peroxide to water and oxygen [98].

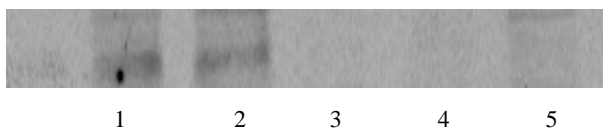


Figure 4.45 Immunological detection of Catalase in the homogenate (1), cytosolic (2), nuclear (3) mitochondrial (4), and microsomal (5) fraction of the skeletal muscle of rat

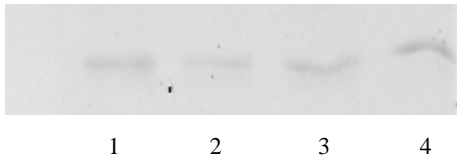


Figure 4.46 Immunological detection of Catalase in the homogenate: 1-Se (+), 2-Se (-) and cytosol: 2-Se (+), 4 Se (-) of the skeletal muscle of rat

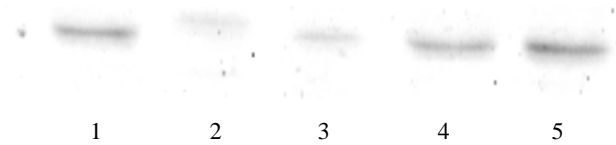


Figure 4.47 Immunological detection of Catalase in the homogenate (1), nuclear (2), mitochondrial (3) cytosolic (4), and microsomal (5) fraction of the lung of rat

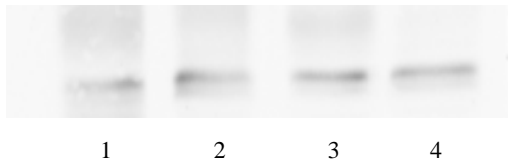


Figure 4.48 Immunological detection of Catalase in the homogenate: 1-Se (+), 2-Se (-) and cytosol: 2-Se (+), 4 Se (-) of the lung of rat

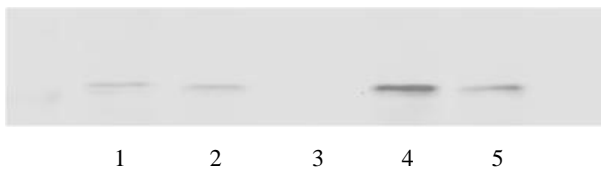


Figure 4.49 Immunodetection of Catalase in the homogenate (1), cytosolic (2), nuclear (3) mitochondrial (4), and microsomal (5) fraction of the spleen of rat

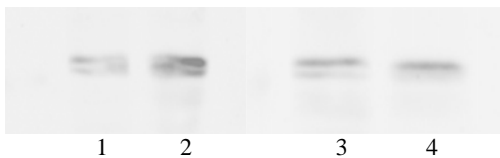


Figure 4.50 Immunological detection of catalase in the homogenate: 1-Se (-), 3-Se (+) and cytosol: 2-Se (-), 4 Se (+) of the spleen of rat

In the skeletal muscle in homogenate and cytosol the catalase was identified. In the selenium groups the signalling of this enzyme was similar to each other. In the lung and spleen the 59 kDa protein was detected in homogenate and cytosol as well as in the mitochondrial and microsomes fraction. The catalases signalling was similar in the homogenate and cytosol of the Se (+) and Se (-) group.

#### 4.3.2.2.6 PON 1

The paraoxonase (PON) family includes three members, PON 1, PON 2 and PON 3. The physiological functions of these enzymes are still unexplained. PON 1 has paraoxonase, arylesterase and lactonase activated [99, 100] and plays a role in the protection against xenobiotic intoxication [101]. All the PONs are capable to delay the oxidation of LDL. Many studies showed that expressing human PON 1, 2 or 3 inhibits or reverses the development of atherosclerosis which can be involved in the mechanism of reduction of oxidative stress and the normalisation of vascular endothelium function [102 – 104].

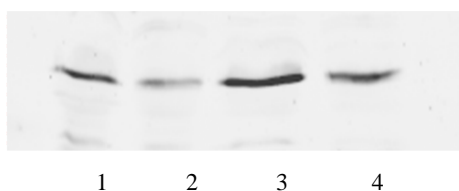


Figure 4.51 Immunological detection of Paraoxonase 1 in the homogenate: 1-Se (+), 2-Se (-) and cytosol: 2-Se (+), 4 Se (-) of the skeletal muscle of rat



Figure 4.52 Immunological detection of Paraoxonase 1 in the homogenate (1), nuclear (2), cytosolic (3) mitochondrial (4), and microsomal (5) fraction of the skeletal muscle of rat

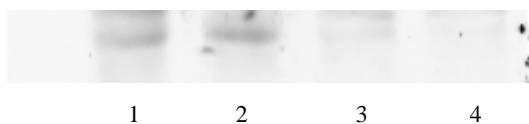


Figure 4.53 Immunological detection of Paraoxonase in the homogenate: 1-Se (+), 2-Se (-) and cytosol: 2-Se (+), 4 Se (-) of the lung of rat

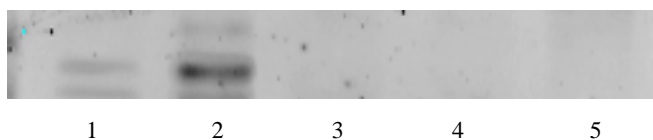


Figure 4.54 Immunological detection of Paraoxonase 1 in the homogenate (1), cytosolic (2), nuclear (3) mitochondrial (4), and microsomal (5) fraction of the lung of rat

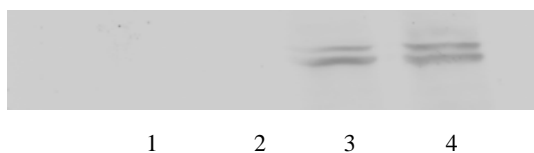


Figure 4.55 Immunological detection of Paraoxonase in the homogenate: 1-Se (+), 2-Se (-) and cytosol: 2-Se (+), 4 Se (-) of the spleen of rat

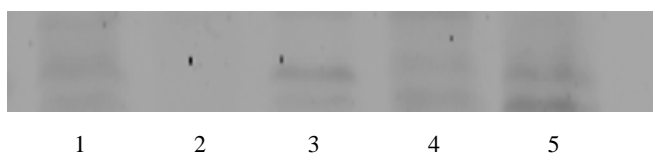


Figure 4.56 Immunological detection of Paraoxonase 1 in the homogenate (1), nuclear (2), cytosolic (3), mitochondrial (4), and microsomal (5) fraction of the spleen of rat

The study presents the first information of the immunochemical localisation of PON 1 in the examined rat species.

In the skeletal muscle in homogenate and cytosol the paraoxonase was identified. In the selenium groups the signalling of this enzyme was similar to each other. In the lung and spleen in homogenate and cytosol the Pon 1 was detected. The enzyme signalling was similar in the homogenate and cytosol of the Se (+) and Se (-) group.

#### 4.3.2.2.7 Effect of the selenium status on the distribution of antioxidants proteins in the tissues of the skeletal muscle, lung and spleen

In the Table 4.7, the detected antioxidative active proteins in the homogenate and cytosol of skeletal muscle, lung and spleen of the selenium-sufficient and –deficient animals groups are presented. The reviewed enzymes were separated by means of SDS PAGE and then identified by immunoassays.

Species	TrxR1	Gpx 1	Sel 15	Cu/Zn SOD	Catalase	PON 1
Mu Hom Se(+)	■	■	■	■	■	■
Mu Hom Se(-)	■	■	■	■	■	■
Mu Cyt Se(+)	■	■	■	■	■	■
Mu Cyt Se(-)	■	■	■	■	■	■
Lu Hom Se(+)	■	■	■	■	■	■
Lu Hom Se(-)	■	■	■	■	■	■
Lu Cyt Se(+)	■	■	■	■	■	■
Lu Cyt Se(-)	■	■	■	■	■	■
Sp Hom Se(+)	■	■	■	■	■	■
Sp Hom Se(-)	■	■	■	■	■	■
Sp Cyt Se(+)	■	■	■	■	■	■
Sp Cyt Se(-)	■	■	■	■	■	■

Table 4.7 Antioxidants proteins present in the homogenate and cytosol of the skeletal muscle, lung and spleen of the selenium-deficient Se (-) and selenium-sufficient Se (+) rats; ■ - strong signal, ■ - weak signal



The results confirm the previous hypothesis that the activity of selenium binding enzymes is strongly dependent on the selenium status. In the group of selenium-sufficient animals selenoproteins were detected in all tissues. In the second group the signalling of these proteins was meaningfully lower. Many studies reported that selenium protects mammals from ROS, oxidative stress and free radicals [3, 105, 106]. Adequate dietary selenium supply has been proposed to be useful for the prevention and reduction of several muscle diseases, cardiovascular and neurological disorder or lung cancer [107 - 109], but the possible participation of the Se-proteins in those mechanisms has not been explained. The selenoproteins level in the organism can be strongly affected by the nutritional selenium consumption. Most of the considerations in this area have been focussed to glutathione peroxidase and thioredoxin reductase. On the other hand, the role of selenium in these enzymes could explain numerous, but not all the effect of selenium deficiency. About one third of the selenium present in the organism is bound with glutathione peroxidase. This suggests that there may be further biologically active forms of selenium [110]. The fact that with insufficient selenium intake the element is mainly used for restoring the level of other selenoproteins is an indication for their biological significance. The chemopreventive effect of selenium is probably mediated through its role in more than one metabolic process [111]. However, it is also important to determine how selenoproteins are related to action of such metabolites, because individuals differ substantially in their ability to increase selenoprotein activity in response to additional dietary Se [112].

To the most important intracellular antioxidants in human except Gpx belong also superoxide dismutase and catalase. In this study, the effect between selenium supplementation and non Se-antioxidants enzymes was not observed. In both group animals, these enzymes were detected. A number of hormones, growth factors and cytokines were shown in neutralization process of reactive oxygen species and free radicals.

### 4.3.3 Speciation analysis of the trace element-containing proteins

High performance liquid chromatography (HPLC) linked to inductive coupled plasma was used to obtain information on the trace elements bound biomolecules in the cytosolic fraction. This method is very useful for monitoring individual element species at ultra trace level.

For this study, the speciation analysis was used to examine the trace element-containing proteins in the cytosol fraction of the skeletal muscle, lung and spleen of rats fed with a selenium deficient diet and a selenium sufficient diet. The graphics below show the distribution profile of selected elements after chromatographic separation.

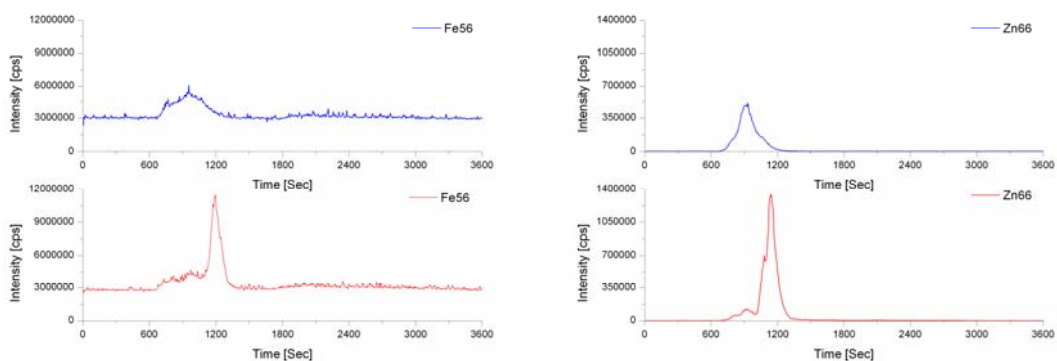


Figure 4.57 Distributions profile of iron (left) and zinc (right) in the cytosolic fraction of skeletal muscle fed either a selenium deficient diet (-) or selenium sufficient diet (-)

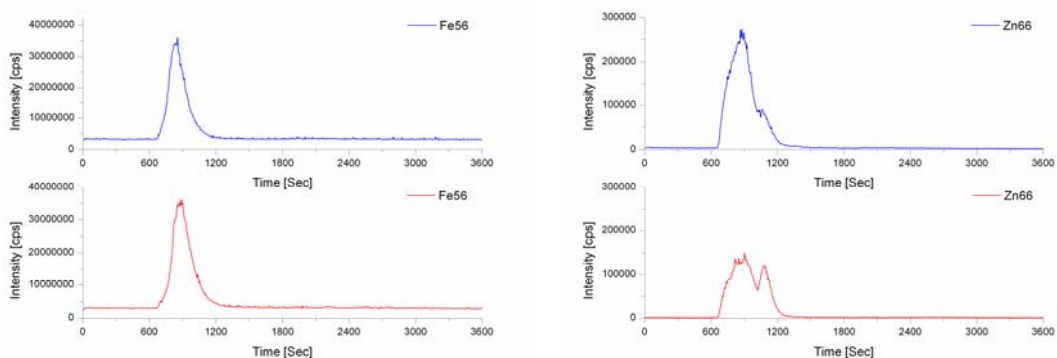


Figure 4.58 Distributions profile of iron (left) and zinc (right) in the cytosolic fraction of lung fed either a selenium deficient diet (-) or selenium sufficient diet (-)

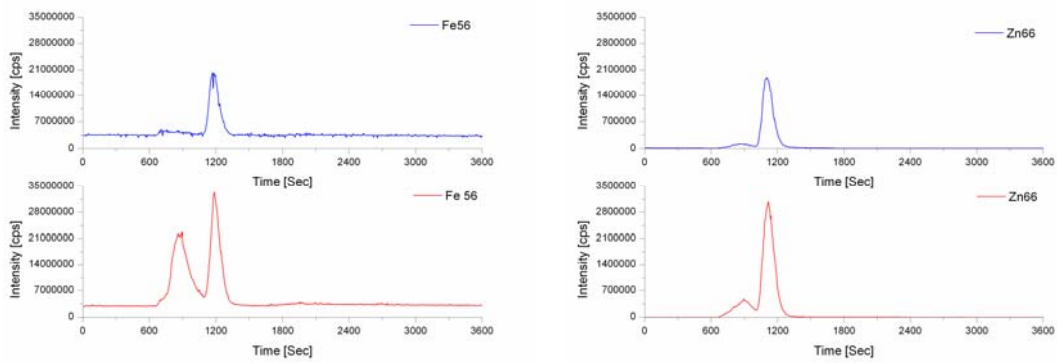


Figure 4.59 Distributions profile of iron (left) and zinc (right) in the cytosolic fraction of spleen fed either a selenium deficient diet (-) or selenium sufficient diet (+)

The distribution profile of iron in the cytosolic fraction of the skeletal muscle showed one peak in the retention time of 850 s, which corresponds the molecular mass of 32 kDa. The other peak is present only in the skeletal muscle of rat fed with a selenium deficient diet and had molecular mass of 7.5 kDa (retention time ~1225 s). In the cytosolic fraction of lung in both groups one peak is presented, which had molecular mass of about 32 kDa. In the cytosol fraction of spleen two peaks were presented in the Se (-) group, the retention time of 850 s and 1225 s which corresponds with 32 and 7.5 kDa. In the group with Se (+) diet there was one peak, which had molecular mass of 7.5 kDa.

The zinc profile shows two peaks in all species without skeletal muscle – Se (+) group. The first peak appeared after 900 s and the second was detected after 1140 s. Their molecular mass corresponded about 26.8 and 10.5 kDa. The peak with the high molecular masses have the highest intensity in the cytosol of lung. The peak found in the low molecular range has the highest intensity in the cytosol of spleen.

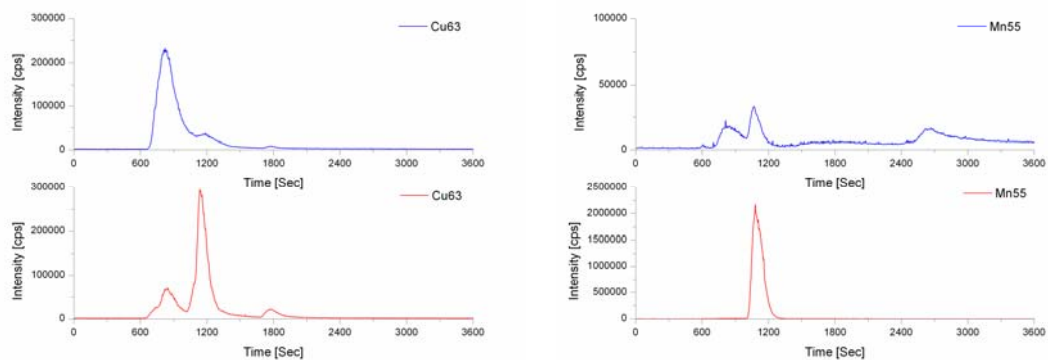


Figure 4.60 Distributions profile of copper (left) and manganese (right) in the cytosolic fraction of skeletal muscle of rat fed either a selenium deficient diet (-) or selenium sufficient diet (+)

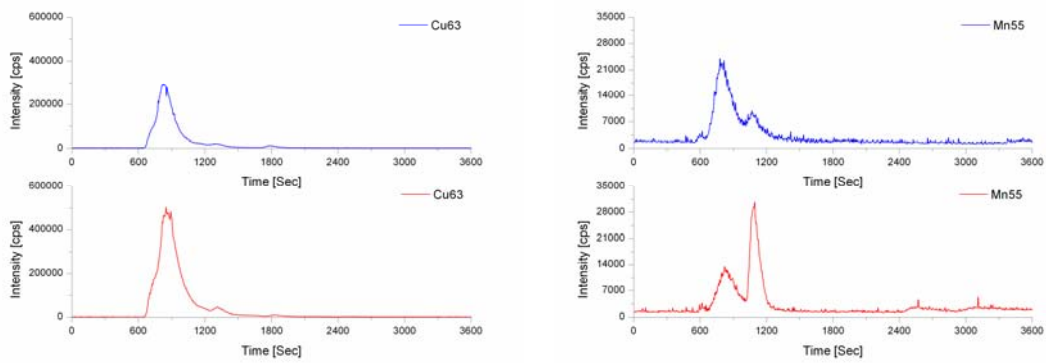


Figure 4.61 Distributions profile of copper (left) and manganese (right) in the cytosolic fraction of lung of rat fed either a selenium deficient diet (-) or selenium sufficient diet (+)

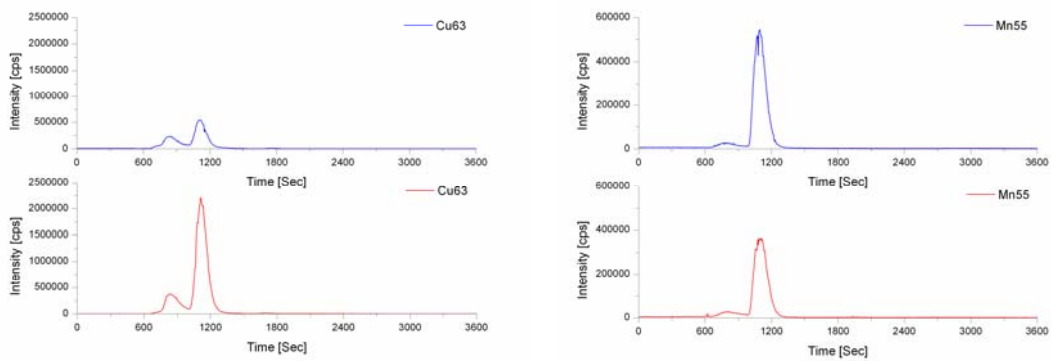


Figure 4.62 Distributions profile of copper (left) and manganese (right) in the cytosolic fraction of spleen of rat fed either a selenium deficient diet (-) or selenium sufficient diet (+)

The copper profile demonstrated two peaks in all fractions. The first peak was detected after 825 s and the second peak after 1175. Their molecular masses correspond 36 kDa and 9 kDa. In the cytosolic fraction of the skeletal muscle and spleen the intensity of these peaks were different between Se (+) and Se (-) groups.

In the chromatographic manganese profile of skeletal muscle in the Se (+) group and spleen in both groups two peaks were detected. The first peak appeared after 790 s and the second peak was detected after 1125 s. Their molecular masses correspond 40 and 11 kDa. In the skeletal muscle Se (-) group only one peak with molecular mass 11 kDa was observed. The intensity of this peak was higher compared to Se (-) group. In the lung three peaks were detected, which corresponded to molecular mass of 87 (retention time ~ 600 s), 40 and 11 kDa, The intensity of the first peak was similar in both groups,

the 40 kDa peak has the highest intensity in the cytosol of Se (+) group and the last peak has the highest intensity in the Se (-) group.

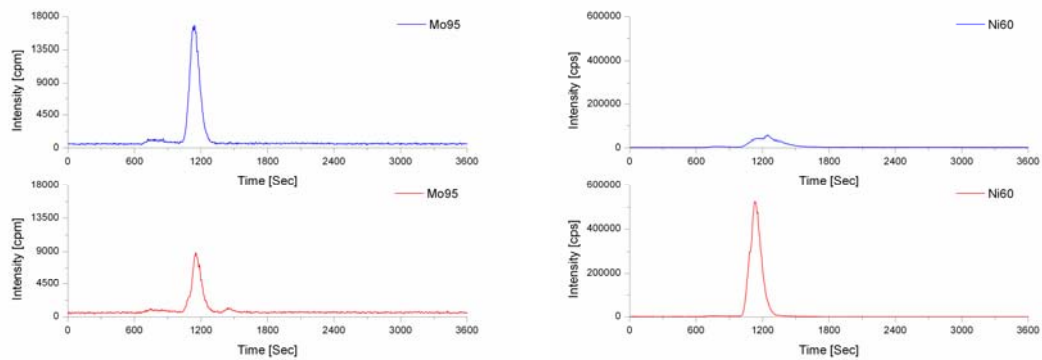


Figure 4.63 Distributions profile of molybdenum (left) and nickel (right) in the cytosolic fraction of skeletal muscle of rat fed either a selenium deficient diet (-) or selenium sufficient diet (+)

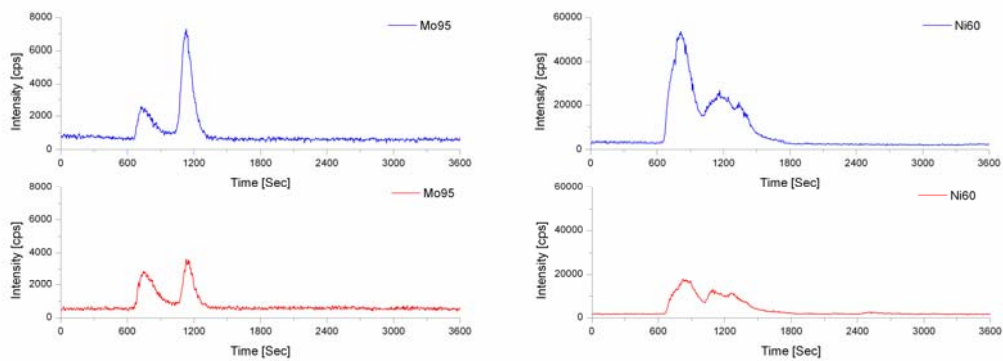


Figure 4.64 Distributions profile of molybdenum (left) and nickel (right) in the cytosolic fraction of lung of rat fed either a selenium deficient diet (-) or selenium sufficient diet (+)

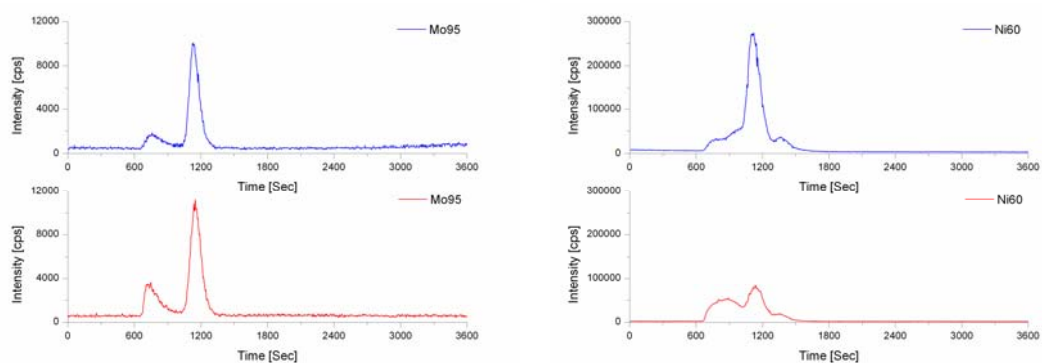


Figure 4.65 Distributions profile of molybdenum (left) and nickel (right) in the cytosolic fraction of spleen of rat fed either a selenium deficient diet (-) or selenium sufficient diet (+)

In the chromatographic molybdenum profile two peaks were detected. The first peak had a molecular mass of about 59 kDa (retention time ~ 700 s) and its intensity was similar in the cytosols of lung and spleen. In the skeletal muscle fraction the intensity of this peak was very small in both groups. The second peak was detected in all organs and its molecular mass was 10 kDa (retention time ~ 1150 s). The intensity of this peak was higher in the Se (+) group of skeletal muscle and lung. In the spleen of the Se (+) and Se (-) groups it was not observed.

The nickel profile in all groups showed one peak. The peak appeared after 1130 s, this corresponds molecular masses at 10 kDa, the intensity of which in the skeletal muscle in the selenium deficient group is higher. In other species this peak was higher in the group with selenium sufficient diet. In cytosol of lung and spleen presented another two peaks with molecular mass of about 32 (retention time ~ 850 s) and 4 kDa (retention time ~ 1375 s). The higher intensity level of both peaks was presented in the Se (+) group of lung. In the spleen differences were not observed.

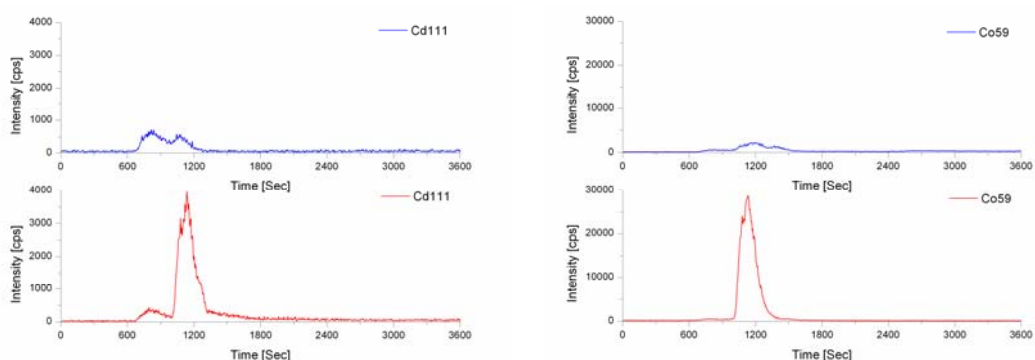


Figure 4.66 Distributions profile of cadmium (left) and cobalt (right) in the cytosolic fraction of skeletal muscle of rat fed either a selenium deficient diet (-) or selenium sufficient diet (+)

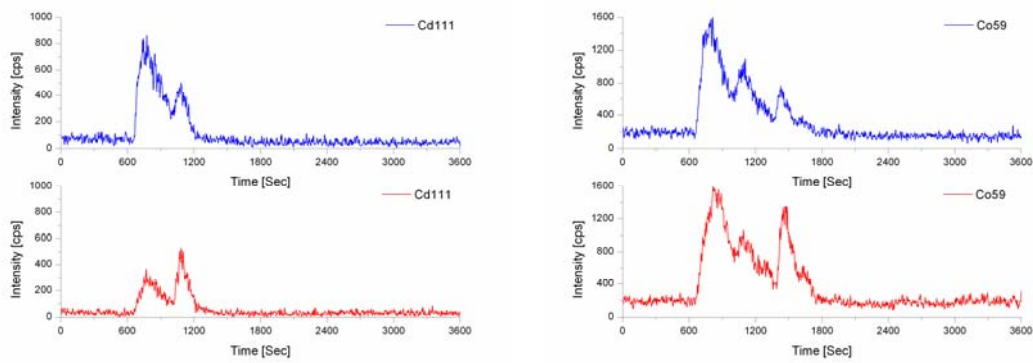


Figure 4.67 Distributions profile of cadmium (left) and cobalt (right) in the cytosolic fraction of lung of rat fed either a selenium deficient diet (-) or selenium sufficient diet (+)

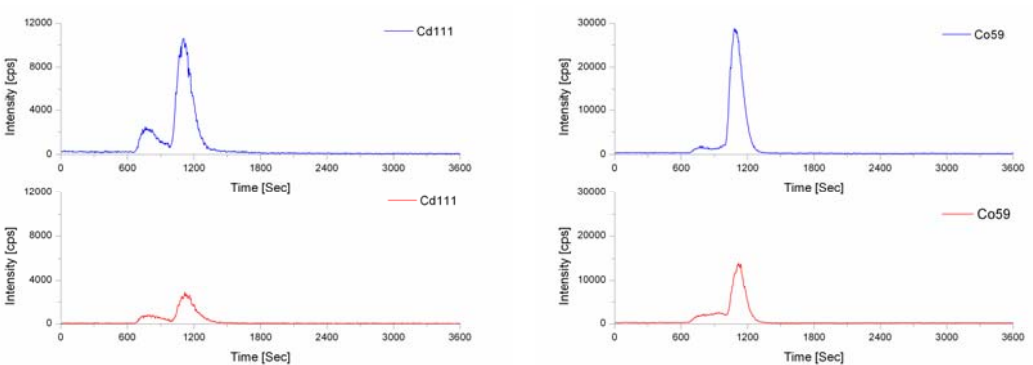


Figure 4.68 Distributions profile of cadmium (left) and cobalt (right) in the cytosolic fraction of spleen of rat fed either a selenium deficient diet (-) or selenium sufficient diet (+)

The cadmium distribution profile in all species showed two peaks. The first peak appeared after 775 s and the second peak was detected after 1140 s, which correspond to 43 and 10 kDa. In skeletal muscle and spleen the intensity of the second peak, 10 kDa, was different between Se (+) and Se (-) animals. In the selenium deficient group in skeletal muscle it was higher compared to the Se (-) group and in the spleen the peak was higher in the group with selenium sufficient diet.

The cobalt profile in the cytosol of skeletal muscle has shown one peak at 12 kDa (retention time 1095 s). In the lung and spleen two peaks were observed. The first peak was about 48 kDa (retention time 750 s) and the second ~12 kDa. Only the second peak in the spleen demonstrates differences between both animals groups.

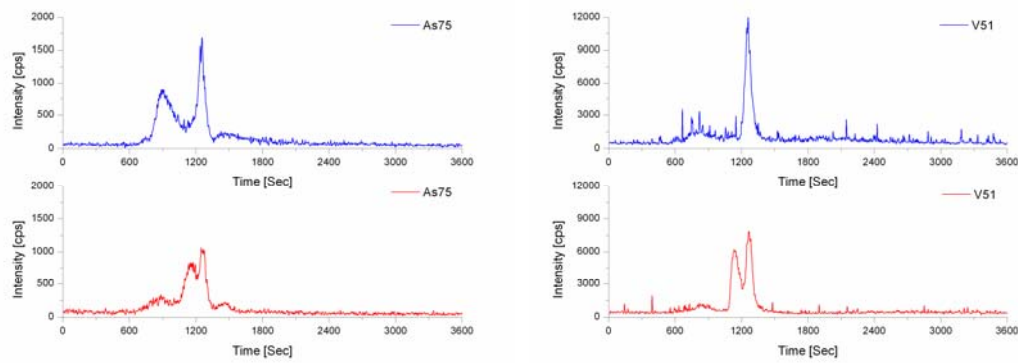


Figure 4.69 Distributions profile of arsenic (left) and vanadium (right) in the cytosolic fraction of skeletal muscle of rat fed either a selenium deficient diet (-) or selenium sufficient diet (+)

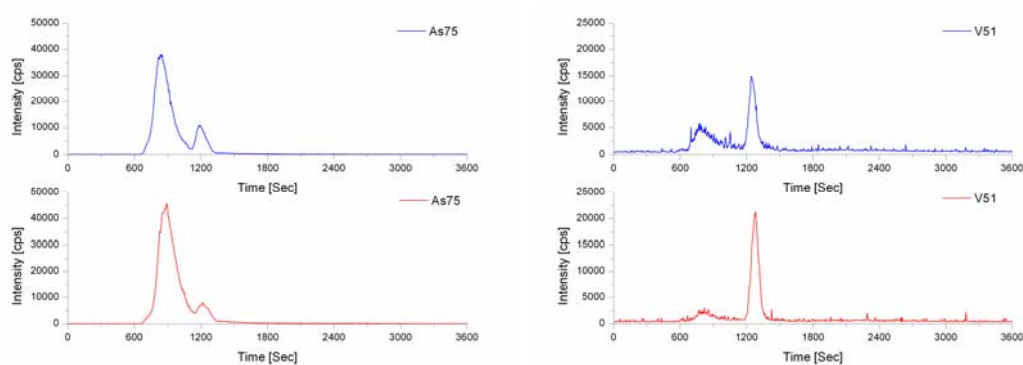


Figure 4.70 Distributions profile of arsenic (left) and vanadium (right) in the cytosolic fraction of lung of rat fed either a selenium deficient diet (-) or selenium sufficient diet (+)

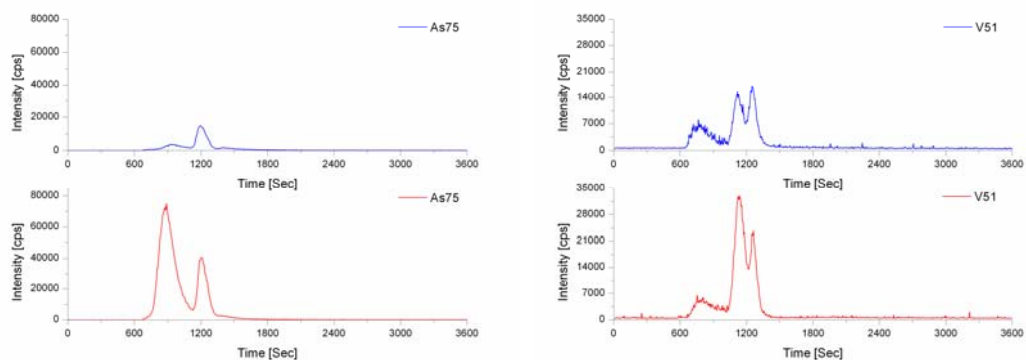


Figure 4.71 Distributions profile of arsenic (left) and vanadium (right) in the cytosolic fraction of spleen of rat fed either a selenium deficient diet (-) or selenium sufficient diet (+)

The arsenic profile shows in the cytosol of skeletal muscle two peaks in the Se (+) group and three peaks in the Se (-) group. Their molecular masses were 29 (retention time 875 s), 8 (retention time 1200) and under 7 kDa (retention time 1250). The



intensity of the first peak was higher in the group with Se (+). The last peak was related in both groups. In the cytosolic fraction of the lung and spleen two peaks approximately 29 and 7 kDa were observed. The intensity of the peak in the lung was similar in both groups. In the spleen both peaks were higher in the Se (-) group.

In the vanadium profile three peaks in the skeletal muscle and spleen with molecular mass at 41 (retention time ~ 790), 10 (retention time ~ 1150 s) and 6 kDa (retention time ~ 1270 s) were observed. The first peak was similar in both groups of skeletal muscle and spleen. The next peak was higher in the Se (-) group and the last peak was higher in the Se (+) group in the skeletal muscle. In the lung there were two peaks with about 41 and 6 kDa. The first peak in the selenium sufficient group was higher and the second peak was higher in the Se (-) group.

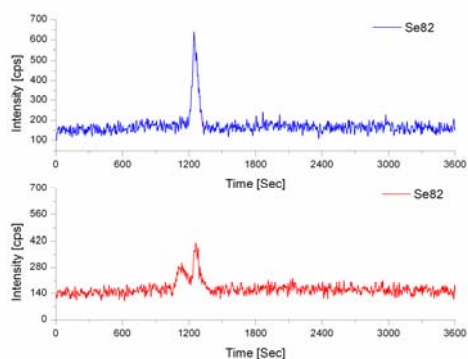


Figure 4.72 Distributions profile of selenium in the cytosolic fraction of skeletal muscle of rat fed either a selenium deficient diet (-) or selenium sufficient diet (+)

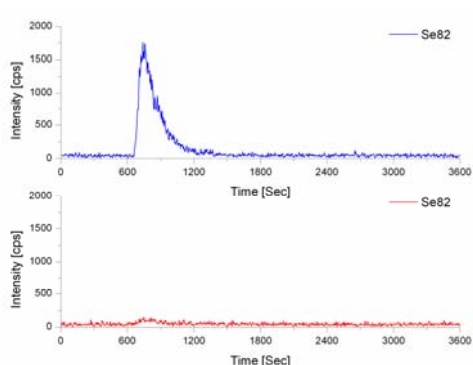


Figure 4.73 Distributions profile of selenium in the cytosolic fraction of lung of rat fed either a selenium deficient diet (-) or selenium sufficient diet (+)

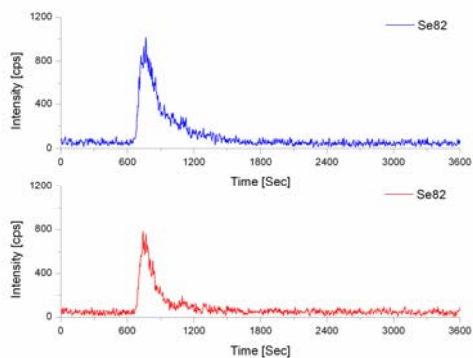


Figure 4.74 Distributions profile of selenium in the cytosolic fraction of spleen of rat fed either a selenium deficient diet (-) or selenium sufficient diet (+)

The selenium profile showed one peak with about 53 kDa (retention time ~725) in the lung and spleen. Their intensity was higher in the Se (+) group. In the skeletal muscle of both groups one peak with molecular mass > 5 kDa (retention time ~ 1300 s) and one peak in the Se (-) group of approximately 8.6 kDa (retention time ~ 1190 s) was observed.

#### 4.3.3.1 Column calibration

The base of the calibration of the column is a logarithmic correlation between retention time and molecular mass of the molecules. This allows the determination of the native molecular mass of protein.

The substances, which were used to column calibration, are listed in the Table 4.8. The calibration curve is shown in Figure 4.75.

Substance	Molecular mass [kDa]	Retention time [sec]	Log MM
Aprotinin	6.5	1269.0	3.81
Ribonuclease	13.7	1068.2	4.14
Chymotripsinogen	29	858.2	4.46
Ovalbumin	43	729.5	4.63
Conalbumin	75	696.5	4.88

Tabelle 4.8 Molecular masses and retention time of the substances used in the calibration of the Superdex 75 PC column

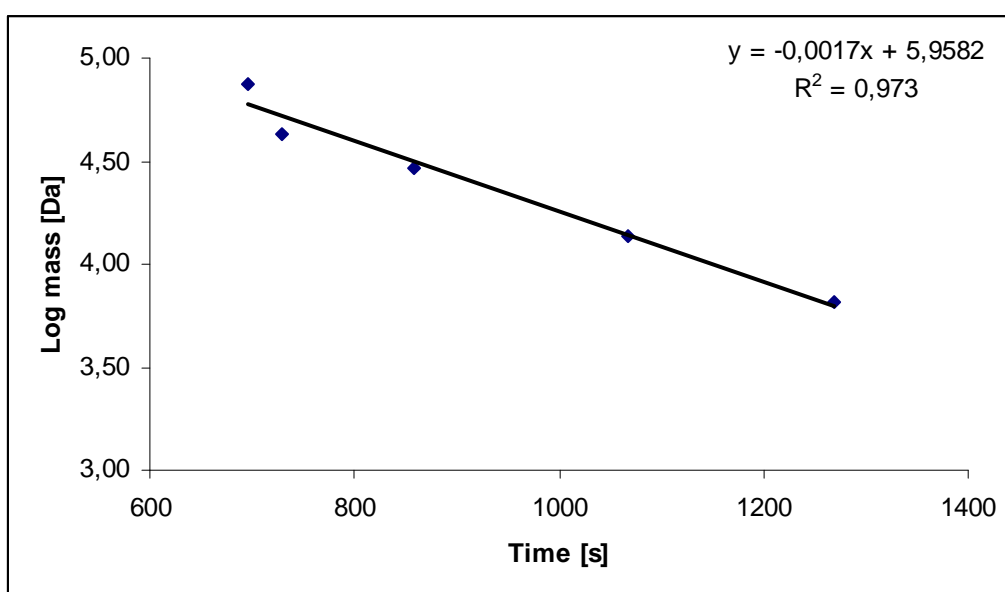


Figure 4.75 Correlation between retention time and molecular mass of several substances (see Table 4.8) separated on a Superdex 75 PC column

The linear separation range was located between 696.5 and 1269.0 sec. The regression line for this linear correlation was:

$$\log \text{molecular mass [g/mol]} = -0.0017 \cdot \text{retention time [s]} + 5.9582$$

### 4.3.3.2 Summary

The distribution profiles of iron, zinc, copper, manganese, molybdenum, nickel, cadmium, cobalt, arsenic, selenium and vanadium in the rat skeletal muscle, lung and

spleen cytosol was obtained by chromatographic separations of the cytosolic proteins. With this method it was possible to obtain the first information on cytosolic protein-bound forms of these elements and determined of the distribution of these elements among the separated proteins. In all samples the same element distributions profile in the separated proteins were observed.

The iron profile showed two proteins at 32 and 7.5 kDa, the 32 kDa protein could belong to a PHYDH1 (Phytanoyl-CoA dioxygenase domain-containing protein 1) [113]. The 26 kDa zinc – binding proteins can correspond to the superoxide dismutase 3 [114] or a zinc finger protein Zmynd19 (zinc finger MYND domain-containing protein 19) [115]. In the investigatory cytosol three manganese-containing proteins were found. The 41 kDa protein can attach to manganese or iron binding catalytic subunit of PP1 (Protein phosphatase 1-alpha catalytic subunit), which is essential for muscle contractility and protein synthesis and participates in the regulation of glycogen metabolism [116]. The nickel-containing proteins are a relatively new class of metalloenzymes. Currently only seven nickel enzymes are known: urease, hydrogenase, CO- dehydrogenase, Ni-SOD, methyl-coenzym M reductase, glyoxalase 1, and cis-trans isomerase [117]. In this study three nickel-containing protein were detected, but none of the known proteins correspond with them. The cadmium profile showed two proteins, the 43 kDa proteins could belong to the Cytochrome b [118]. From the literature a lot of arsenic-containing proteins are known, but most of them are not characterized. The 29 kDa As-protein could belong to the uncharacterized isoforms of RCG47444 (Uroporphyrinogen 3 synthase) [119,120]. The selenium profile showed three proteins, the 53 kDa could be the Thioredoxin reductase1 [121], the 8 kDa can correspond to the Sel W [122] and the last protein, about 5 kDa can not be identified as well as the cobalt, molybdenum and vanadium containing protein..

Iron, copper, zinc, manganese, and selenium are known to be essential constituents of redox-active enzymes, but there is the possibility that in the skeletal muscle these elements may also be contained in further proteins not yet being identified. Interestingly, vanadium and arsenic were also found to be protein-bound. So far nothing is known about interactions between these elements and skeletal muscle. Further studies are therefore carried out to investigate more closely the biological functions of these elements.

### 4.3.4 Effect of selenium status of the proteome of skeletal muscle, lung and spleen

In this part of the study, the proteome of the skeletal muscle, lung and spleen of rats was analyzed. The expression of proteins in the homogenate of this tissues of selenium deficient Se (-) and selenium adequate Se (+) animals was carried out by 2D- gel electrophoresis and Melanie 08 – software. Spots which show differences between Se (-) and Se (+) animals are marked with circle. The blue circles indicate increased expression of the protein and red circles indicate a less expression. The result is shown in figures 4.76 - 4.78.

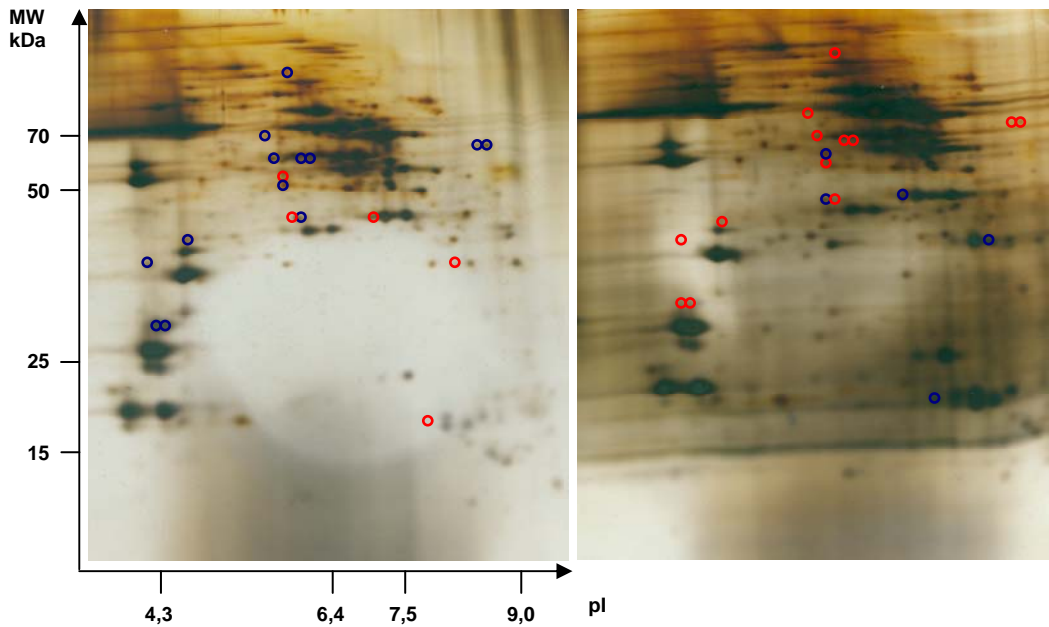


Figure 4.76 Distribution of proteins in the homogenate of skeletal muscle of the selenium deficient (left) and selenium sufficient (right) rats, the blue circles indicate increased expression of the protein and red circles indicate a less expression

In the skeletal muscle homogenate in the Se (+) and Se (-) group was above 800 spots detected. This proteins were accursed in area with molecular masses between 180 – 10 kDa and isoelectric point in range of 3-9. 18 proteins were differently expressed. In the Se (-) animals were found twelve spots which demonstrated increased expression and in the Se (+) animals eight spots were determined.

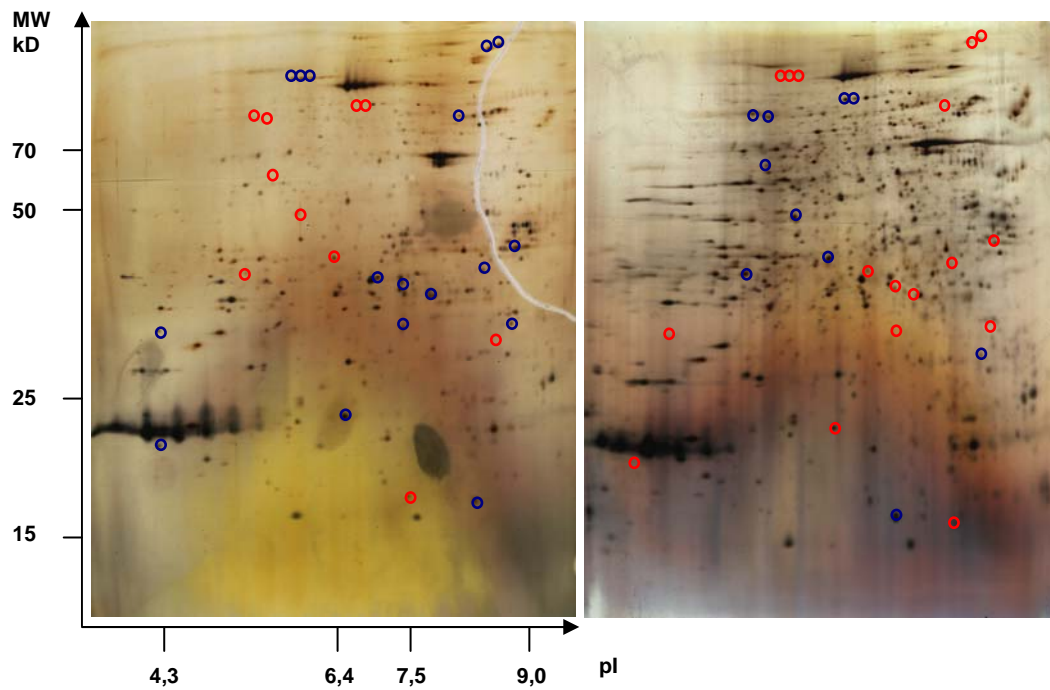


Figure 4.77 Distribution of proteins in the homogenate of lung of the selenium deficient (left) and selenium sufficient (right) rats, the blue circles indicate increased expression of the protein and red circles indicate a less expression

In the homogenate proteome of lung in each gel there were detected more than 900 proteins with a molecular mass between 180 – 10 kDa and isoelectric point in range of three to nine.

By proteins comparison between Se (-) and Se (+) homogenate, 27 proteins were differently expressed. In the Se (-) animals 17 spots were found with increased expression and in the Se (+) animals ten spots were determined.

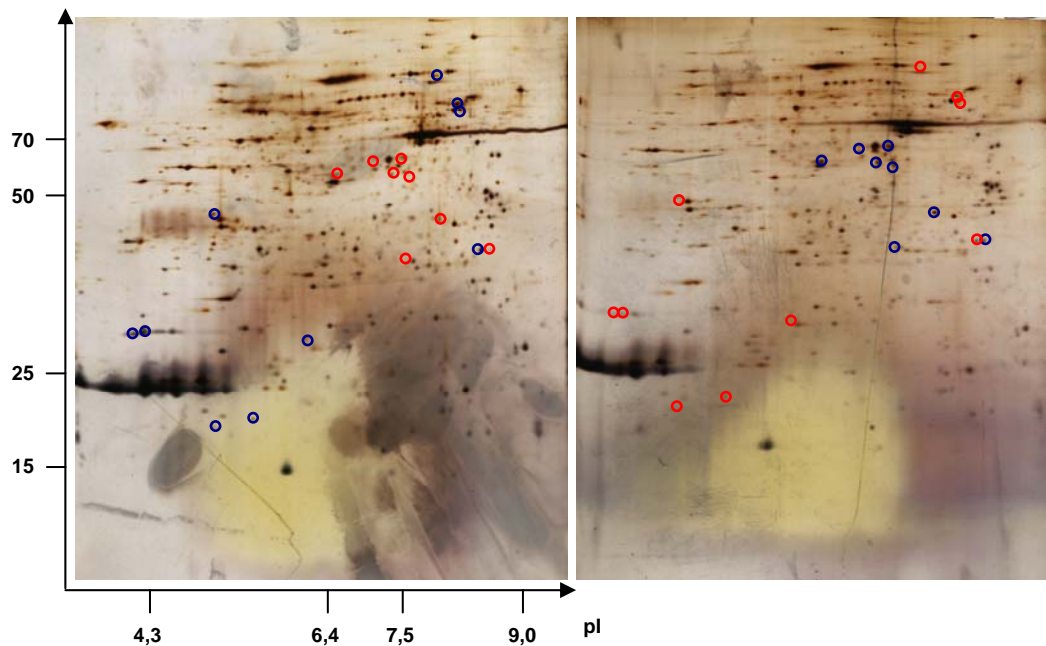


Figure 4.78 Distribution of proteins in the homogenate of spleen of the selenium deficient (left) and selenium sufficient (right) rats, the blue circles indicate increased expression of the protein and red circles indicate a less expression

In the homogenate of spleen were more than 800 proteins in each gel detected. 18 spots in the Se (-) animals and eight in the Se (+) animals have demonstrated increased expression.

### 4.3.5 Summary

The development of pro-oxidant in the living organism is a normal process in the cells metabolisms. In a correctly functional body, the generated oxidants are destroyed by antioxidants so that the very sensitive balance between oxidants and antioxidants are maintained. Imbalance of this system is a result of increased level of free radicals and reactive oxygen species (ROS) which impaired the antioxidant defence system against them. Therefore, it is very important to understand the mechanism of strategy of antioxidant defence system not only the function of individual enzymes but also of total antioxidant status.

It was reported that selenium containing proteins as one compound of the defence system protect the organism against reactive oxygen species and free radicals [123, 124]. It is interesting to gain knowledge about the distribution of antioxidants in tissues

and the alteration of whole antioxidativ activity, when activity of selenium status is decreased. Both questions are important to evaluate the results of studies, action with antioxidants and disease caused by oxidative stress, like cancer or neurological disorder. For proteomic science the determination of the protein related antioxidativ activity could help to understand the function of specific protein improved.

The study showed that the selenium status has no effect on the whole antioxidativ activity. In the cytosol of skeletal muscle, lung and spleen of rat between the selenium deficient and sufficient animals no differences in the total antioxidant status was observed. The reason for this could be, that the protective function of selenium probably is taken over by other antioxidant. Recently studies demonstrated that a number of metal- or metalloid-binding proteins play important roles in degradation of free radical or oxidative stress. Therefore, SEC-ICP-MS, as a largely preferential method for the investigation of metal-biomolecule complexes in biological sample, was used for the study of protein-bound trace elements in the cytosol of skeletal muscle, lung and spleen fractions from selenium deficient and selenium sufficient rats. Iron, zinc, cooper, manganese, molybdenum, nickel, cadmium, cobalt, lanthanum, arsenic, selenium and vanadium in the rat skeletal muscle, lung and spleen cytosol was found in protein-bound form. One of the most interesting results in this study is the protein-bound form with vanadium and arsenic in the studied organs.



## **4.4. Paraoxonase 1**

Serum paraoxonase 1 (PON1) is an important protein, which protects low-density lipoproteins (LDL) from oxidative modification. PON 1 is synthesized primarily in the liver and a portion is secreted into the plasma and is there associated with high-density lipoproteins (HDL). The 43 kDa protein is a calcium dependent esterase that hydrolyzes aromatic carboxylic acid ester and toxic organophosphate compounds. The localization, biological and physiological functions of this enzyme is not accurately established [125, 126].

### **4.4.1 Purification**

In this study, human Paraoxonase 1 was purified from human plasma. Human blood was transported in venous blood collection tubs (BD Vacutainer, SST II, BD, Heidelberg, Germany). After centrifuging at 1500xg in room temperature for five minutes, the plasma was collected and freezed at -40°C. For the protein purification the DEAE Sephadex anion exchanger and G-200 a gel filtration chromatographic media was used. The Purification procedure was performed as described previously (3.2.3). The strategy for the purification of the PON1 allows obtaining purity enzymes in a few short steps, which permit further characterization of PON 1.

#### **4.4.1.1 Activity**

After the chromatography the collected fraction was assayed for paraoxonase activity, which was determined using paraoxon (diethyl p-nitrophenyl phosphate). The peak fraction was pooled and used for the next steps of the purification. Figure 4.77 shows the elution profile of activity of human serum paraoxonase 1 from DEAE Sephadex A-50 anion exchanger and G-200 gel filtration chromatography.

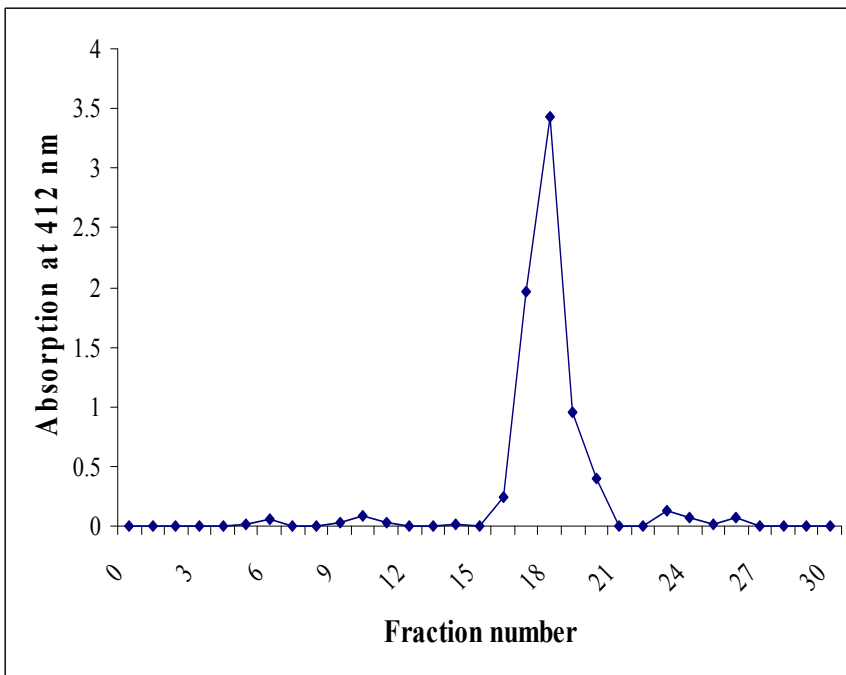
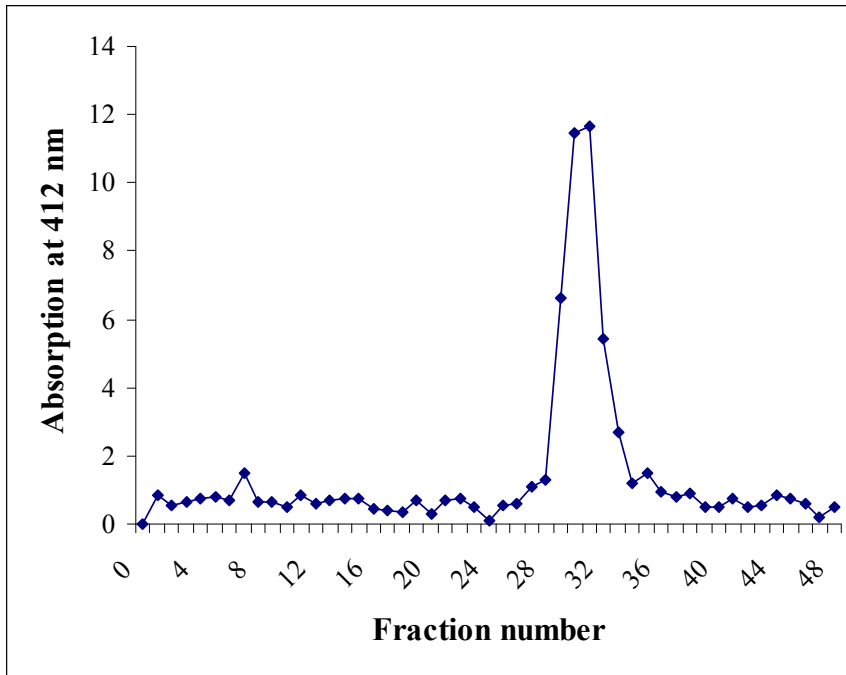


Figure 4.79 Elution profile of activity of serum Paraoxonase 1 from DEAE Sephadex A-50 anion exchanger (above) and G-200 gel filtration chromatography (below)

#### 4.4.1.2 Detection and localization of Paraoxonase 1 in the human plasma

In this part of the study the purity of paraoxonase 1 was analyzed. The enzyme-containing fraction from the last column was dialyzed and then stored at  $-40^{\circ}\text{C}$ . For the SDS-PAGE and 2D gel electrophoresis, 5 or  $10\mu\text{l}$  purified enzyme-containing approximately  $10\text{-}20\mu\text{g}$  protein was used. After protein separation PON 1 was identified by immunoassay.

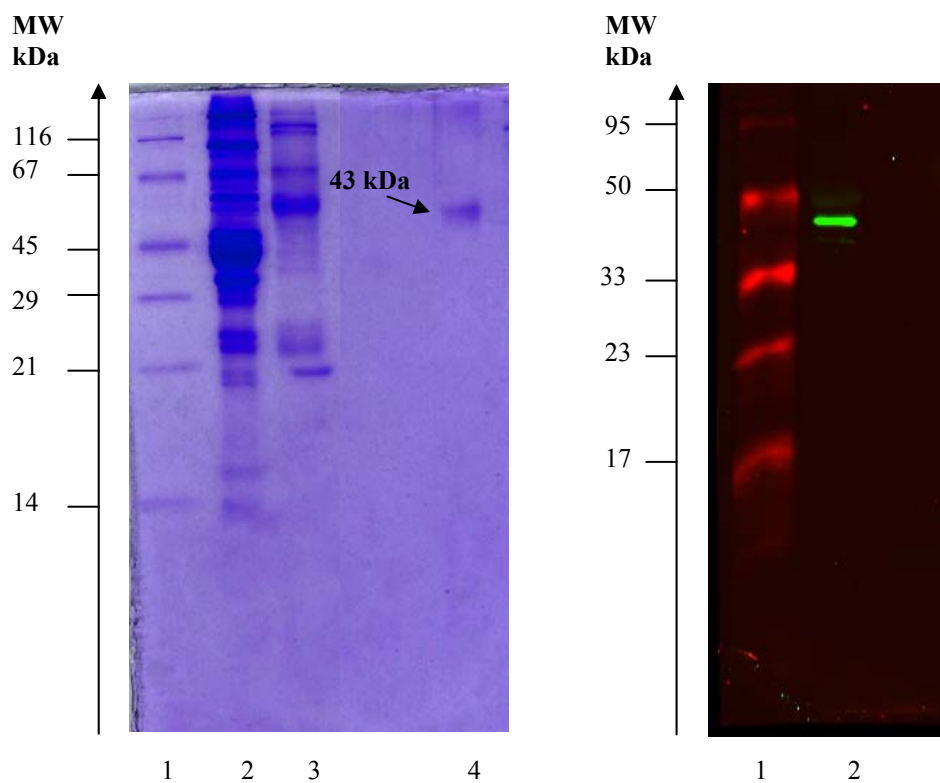


Figure 4.80 SDS-PAGE of purified human serum PON1, gel was stained with coomassie blue (left): 1- protein standards, 2- homogenate of skeletal muscle from rat, 3- enzyme eluted from first column, 4- purified serum PON1 from second column. Right – Immunodetection: 1- protein standards, 2 - purified serum PON1 from second column

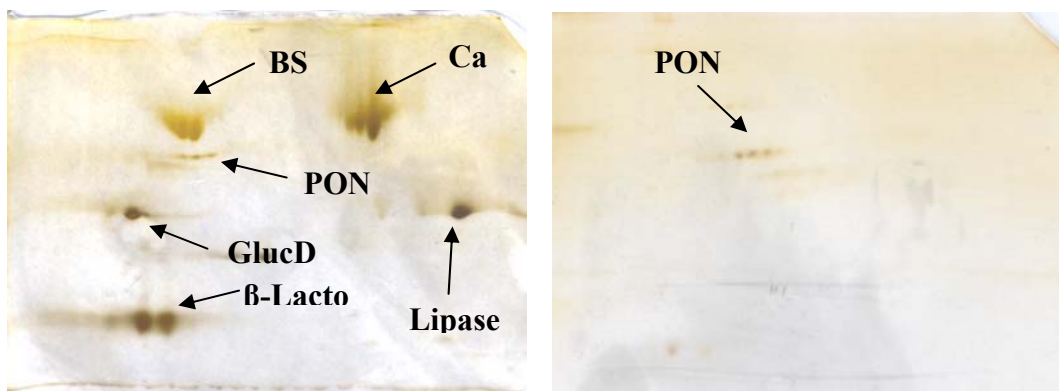


Figure 4.81 2DE of purified human serum PON1, gel was stained with silver according to the method of Rabilloud [127, 128]. Left: protein standards with PON1 from second column, right - purified serum PON1 from second column.

Protein	MW	pI
β-lactoglobulin	18	5.5
Glucose-1-Dehydrogenase	32	5.4
Lipase	33	7.2
Catalase	58	7.3
Albumin	67	6.3

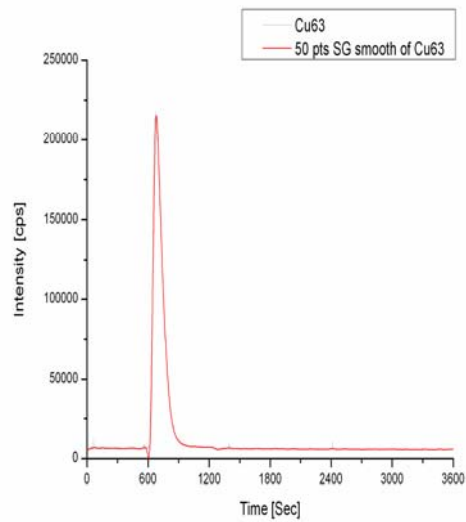
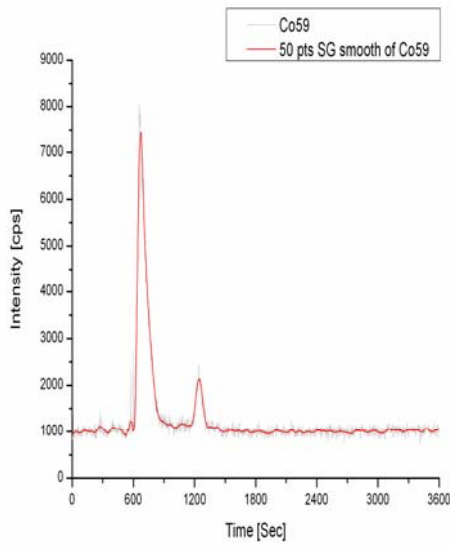
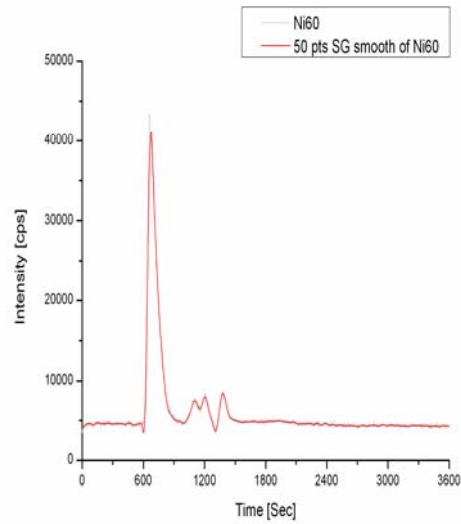
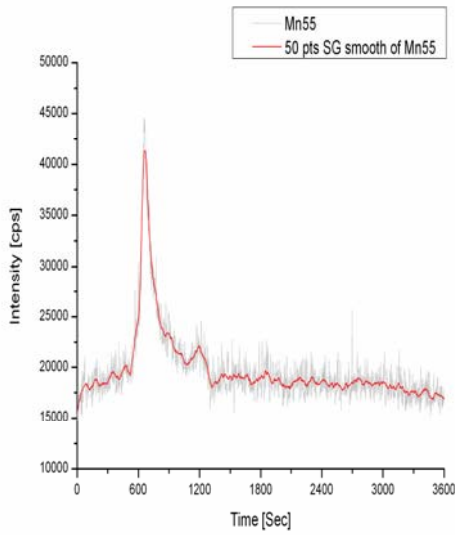
Table 4.9 Molecular weight protein marker from Serva (Germany)

After SDS-PAGE and staining with coomassie blue, the final purified enzyme showed a signal protein band of approximately 43 kDa corresponding to human PON 1. The selected and not complicated purification procedure which was used in this study, allows to obtain very pure enzyme. The 2D gel electrophoresis showed spots in a range between 58 and 32 kDa with pI of about 6.

#### 4.4.2 Speciation analysis of the paraoxonase 1

The purified enzyme - paraoxonase 1 was fractionated by size exclusion chromatography (SEC). Inductive coupled plasma mass spectrometry (ICP-MS) was employed to determine the trace elements-containing PON 1 on-line in the eluate of this protein. This

method allows the investigation of the native metal composition in this protein. The distribution (content) profiles of selected elements after chromatography of Paraoxonase 1 are shown in Figure 4.82.



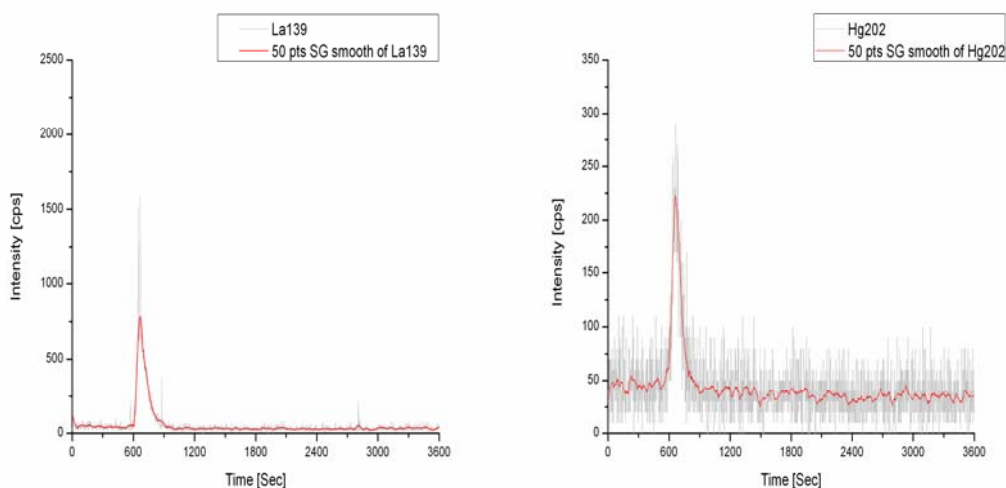


Figure 4.82 Distributions profile of manganese, cobalt, lanthanum (left) and nickel, cooper, mercury (right) in the Paraoxonase 1 solution

The distribution profiles of manganese, nickel, lanthanum, cobalt, cooper and mercury in the enzyme eluate was obtained by chromatographic separation. With this method, it was possible to present the first information on human plasma PON 1-bound forms of these elements. The elements copper and manganese are known for many redox processes which take part as active enzymes. Interestingly, lanthanum, nickel and mercury were also found to be protein-bound. So far nothing is known about interaction between this protein and these elements.

#### 4.4.3 PON 1 localization in the cell lines

The immunocytochemistry method permits localisation of proteins in intact cells by the use of primary antibodies as specific reagents through antigen – antibody interactions that are visualized by the use of secondary antibody such as fluorescent dye. In this part of the study the localization of the Paraoxonase 1 was investigated and the H<sub>2</sub>O<sub>2</sub> effect of this protein in cultured cells of the skeletal muscle, lung and liver was examined. For this experiment the muscle myoblasts cells line C2C12 (mouse), the lung epithelial cells line A549 (human) and hepatocellular carcinoma cell line HepG2 (human) were chosen. The cells were cultured as described in the section 3.1.2. After 24 hours the cell subcultures of the cells were incubated for five hours with 250 μM H<sub>2</sub>O<sub>2</sub>. The results are shown in Figure 4.83 – 4. 85.

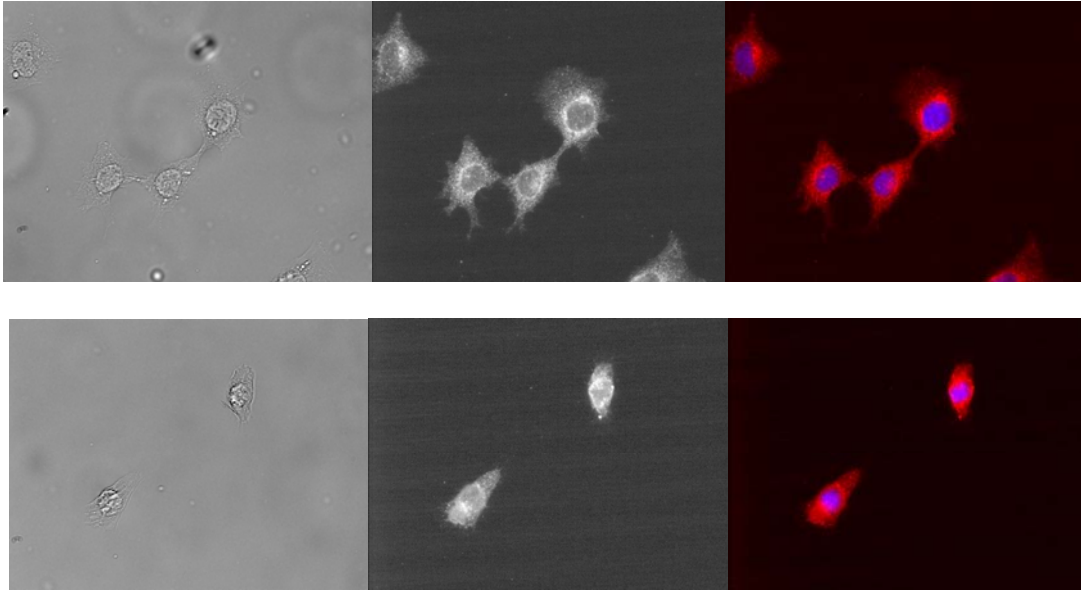


Figure 4.83 Immunocytochemistry labels PON1 (red), blue- nuclei (Hoechst stein) in the mouse myoblasts cells, above - control, below- treatment with 250 $\mu$ M H<sub>2</sub>O<sub>2</sub>. For the left side: investigated by light microscope and fluorecence microscope

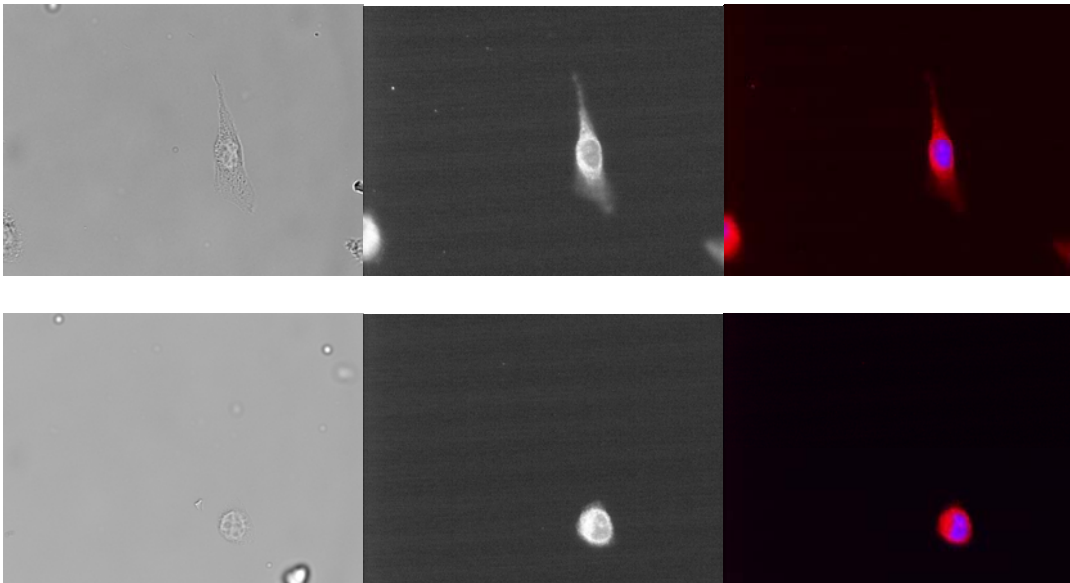


Figure 4.84 Immunocytochemistry labels PON1 (red), blue- nuclei (Hoechst stein) in the human lung epithelial cells, above - control, below- treatment with 250 $\mu$ M H<sub>2</sub>O<sub>2</sub>. For the left side: investigated by light microscope and fluorecence microscope

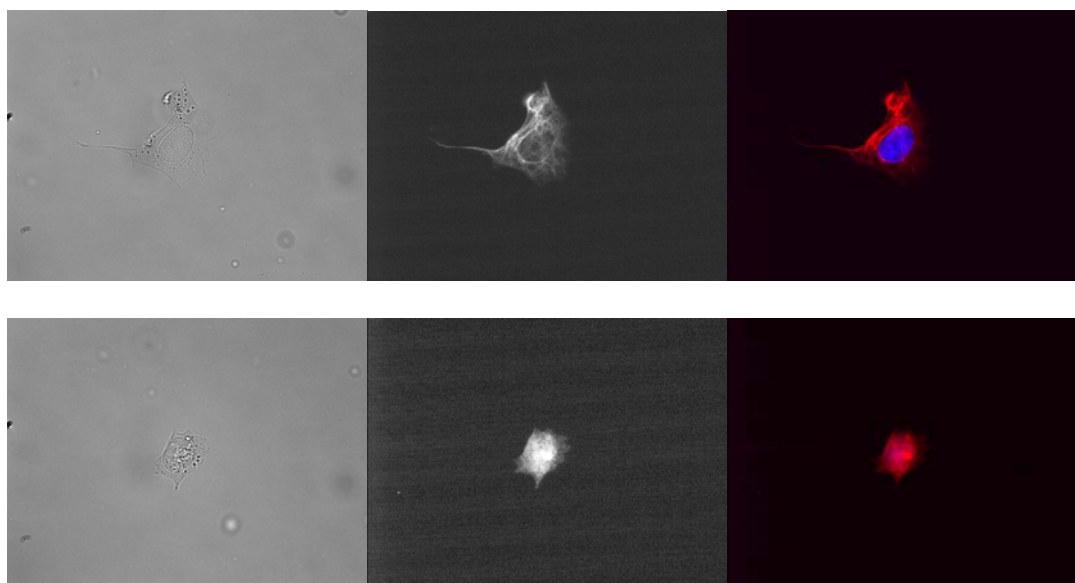


Figure 4.85 Immunocytochemistry labels PON1 (red), blue- nuclei (Hoechst stein) in the human hepatocellular carcinoma cells, above - control, below- treatment with 250 $\mu$ M H<sub>2</sub>O<sub>2</sub>. For the left side: investigated by light microscope and fluorescence microscope

In the three cell lines, PON 1 was clearly detected. In both groups, this enzyme showed intensive activity. In myoblasts and epithelia cell line, its concentration was highly near nuclei compared to other parts of cells. The cells treatment with H<sub>2</sub>O<sub>2</sub>, demonstrated meaningfully changes in the cell structure but the alteration in enzymes activity was not observed.

#### 4.4.4 Localization of lanthanum-binding proteins

This study was investigated to obtain information on lanthanum-containing proteins in the cytosol of skeletal muscle, lung and spleen of rat. The speciation analysis was used for the chromatographic separation and the inductive coupled plasma mass spectrometry (ICP-MS) was employed to determine the La-containing protein on-line in the cytosolic fraction of the investigatory species.

After the finding of lanthanum on human plasma PON 1-bound forms it was interesting to exanimate whether La-containing protein exists in the rat species.



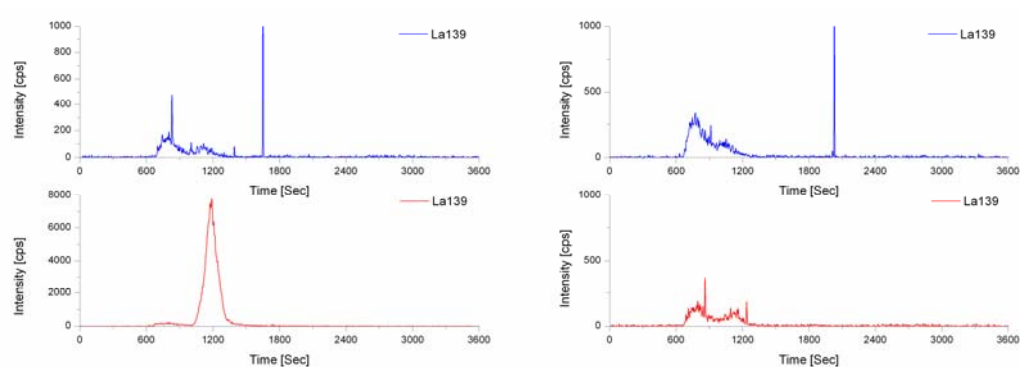


Figure 4.86 Distributions profile of lanthanum in the cytosolic fraction of skeletal muscle (left) and lung (right) of rat fed either a selenium deficient diet (-) or selenium sufficient diet (+)

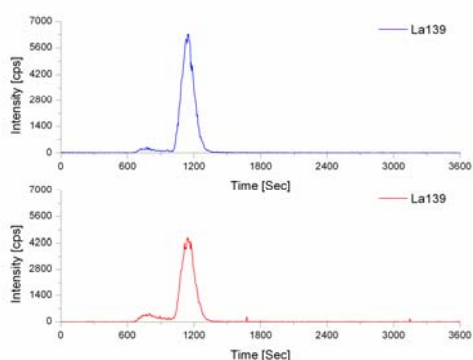


Figure 4.87 Distributions profile of lanthanum in the cytosolic fraction of spleen of rat fed either a selenium deficient diet (-) or selenium sufficient diet (+)

In the lanthanum profile two peaks were observed in all species. The first peak appeared after 775 s and the second peak was detected after 1175 s. Their molecular masses were approximately 43 and 9 kDa. The intensity of the first peak in the spleen of the Se (-) group was higher compared to Se (+) group but in the lung the peak was higher in the group with selenium sufficient diet. In the skeletal muscle no significant differences were observed. The second peak with about 9 kDa was higher in skeletal muscle of the Se (-) group. In other species of these groups no important differences were observed. The 43 kDa protein could belong to the serum PON 1. The 9 kDa protein could not be identified. In the available literature is some information about small molecules containing lanthanum [129], but they are not characterized. Further studies are needed to investigate more closely the biological function of lanthanum and especially its role in the organisms.

#### 4.4.5 Summary

Human serum Paraoxonase 1 (PON 1) is a member of PONs proteins that also includes PON 2 and PON 3. The PONs family demonstrates a wide range of physiologically important hydrolytic activities. In the plasma, after secretions from liver, this enzyme is associated with high-density lipoprotein (HDL). Earlier observation showed that PON1 inhibits the oxidation of lipids in low-density lipoprotein (LDL), in this way reducing the level of oxidizing lipids, which are involved in the initiation of atherosclerosis [130]. Possibly the protection mechanism of LDL from oxidation is the same mechanism which HDL protects against atherosclerosis [131]. The protein is also involved in hydrolysis and inactivation of various organophosphates and the nerve agent sarin and soman [132]. A number of metal- or metalloid- binding proteins have been identified as free radicals captors. The detection of the several elements in this protein, by using SECI-ICP-MS, can suggest that this enzyme has probably more than one function in the organism. The protein in this study was observed in plasma and in other tissues such as skeletal muscle, lung and in the cells. It was suggested that PON 1 acts as an *in vivo* bioscavenger. This can explain its presence in the lung and skeletal muscle, which are mostly exposed on pollution particles from environment and exposure of oxygen [133].

One of the most interesting results in this study is the PON 1- bound form with lanthanum and mercury. Manganese, nickel, cobalt and copper were also found to be protein-bound. Actually, about the metabolism and biological function of lanthanum and mercury in the live organism nothing is known. It was reported that the lanthanides probably cause granulomatous lesions or pneumoconiosis in the smelter's and photoengraver's lung [134]. Previous studies have demonstrated only the toxicity side of mercury. Elemental, inorganic and organic forms of mercury have an effect on lipid peroxidation and formation of reactive oxygen species [135]. In this case, PON 1 probably has a function as transport-protein or formed a complex within the body and in this way neutralized the toxicity of this element. The examples above illustrate how important it is to know the biological effect of these elements on the human health. Monitoring and toxicological studies of these element-bound proteins are needed to realize its meaning and their impact on medical treatment.

In this study, a short strategy for the purification of the PON 1 enzyme was developed. Human serum paraoxonase 1 was purified by two sequential steps. In the first step the DEAE Sephadex anion exchanger was used and in the second step G-200 gel filtration chromatographic media was applied. For the purification, the human plasma was treated over night with Triton X-100 which helps to separate the enzyme from lipoproteins. The purity of this protein was checked by SDS-PAGE and Western blot analysis. The final purified enzyme showed a signal protein band of approximately 43 kDa corresponding to human PON 1. This protocol allows purification of this enzyme on a large scale.

## 5. Discussion

Essential trace elements play an important role in many biological processes. A correct level of nourishment of trace elements correlates with the prevention and reduction of muscle or lung diseases. The first important step in the metalloproteome is therefore the determination of the trace element concentration in the tissues and their distribution in the cellular compartments.

In this study the skeletal muscle, lung and spleen of rat and their subcellular fractions were explored to analyze the concentration of trace elements to obtain information on their chemical forms and on their probable sites of activities within the different cell compartments. In addition some other tissues with important functions in the body like liver, heart and kidney were used for the performance of the current experiments. The tissues were obtained from rats which had been fed with a normal diet. Instrumental Neutron Activity Analysis (INAA), as a sensitive multi-element analytical technique, was used for the determination of selected elements.

The investigated elements iron, zinc, rubidium, cesium, cobalt, selenium, arsenic and chromium were found to be distributed inhomogeneous in the examined tissues of rat and subcellular compartments of the skeletal muscle, lung and spleen. The highest concentration of iron was found in the spleen, which is amongst other things an important organ for the immune system. The high concentration of iron in the spleen can be explained with the function of this organ. The spleen in the vertebrate is responsible for the degradation of erythrocytes. They contain iron in the hemoglobin and in the spleen the iron excess in form of ferritin is accumulated. The concentration of cesium in the skeletal muscle was higher compared to other organs. Beaugé et al. showed in their studies that cesium can promote the extrusion of sodium from muscle with high intracellular sodium concentration [136]. In the skeletal muscle, a lower concentration of zinc was observed compared to other tissues. The highest concentration of this element was present in the liver, spleen and kidney. Zinc is known for many roles in the body such as signal transduction, gene expression, metabolism of DNA and RNA and it also regulates apoptosis. Zinc in blood plasma is bound to and transported by albumin and transferrin [137]. These two proteins are synthesized in the liver and zinc is probably held in metallothionein

reserves in the liver of animals [138]. The rubidium concentration in the lung was lower and the highest concentration was observed in spleen and liver. The highest concentration of selenium was found in spleen and liver. The high concentration in liver could possibly explain that the liver is one of the main selenium pools [139]. The concentration of cobalt in the organs shows no significant differences.

The concentration of arsenic was not detected in all subcellular fractions of the skeletal muscle and the lung except cytosol in which the concentration of this element was very high. The highest concentration of rubidium was located in the cytosolic fraction of spleen. This element was also detected in mitochondria and cytosol of lung and skeletal muscle. The highest distribution of cesium in the subcellular fractions was found in the cytosol of skeletal muscle. The highest concentration of cobalt was found in the microsomes of skeletal muscle and the largest concentration of chromium was detected in the microsomes of lung. The microsomes of lung and spleen contained the largest concentration of zinc and selenium. For both elements the largest concentration was observed in the mitochondria of skeletal muscle. Of great interest is the very high concentration of iron in the subcellular fractions, mainly in the microsome of all tissues. Iron is one of the main elements present in blood. A possible explanation for this could be an enrichment of iron-containing enzymes. The microsomal fractions contain catalase, one of the iron-binding enzymes. From literature it is known that the iron in ferritin supports the lipid peroxidation in the microsomes [140].

In the second part of the study the effect of selenium as antioxidant was examined. In the first step selenium-containing proteins in cultured cells of the skeletal muscle and lung were identified. For this experiment the muscle myoblasts cell line C2C12 (mouse) and the lung epithelial cell line A549 (human) were chosen. The cells were labeled *in vitro* with 20kBq <sup>75</sup>Se, applied to the medium after 24 hours of cell subcultures. The proteins of the homogenates and subcellular fractions of the C2C12 and A549 cell lines were separated by using SDS-PAGE and the selenium present in the proteins was identified by autoradiography. In the subcellular fractions of the cell line C2C12 nine selenium-containing proteins were found. Their relative molecular masses were 70-65 kDa, 55 kDa, 53 kDa, 25 kDa, 23 kDa, in the range between 20 – 18 kDa, 18 kDa, 14 kDa and 10 kDa. The autoradiogram shows that the distribution of bands in the fractions was similar, but the selenoproteins in the fractions were differently labeled. The predominant labeled proteins in

all fractions of the C2C12 cell line was at 25 kDa. In the microsomal fraction, the selenoproteins at 25 kDa, 20 kDa and 14 kDa and in the cytosolic fraction protein at 55 kDa were most strongly labeled. In the A549 cell line a significant difference of selenoproteins between these fractions was observed. Eight proteins were found in all fractions. <sup>75</sup>Se – containing bands were detected at 75 kDa, 65 kDa, 55 kDa, 25 kDa, 23 kDa, one band between 23 and 20 kDa, 20 kDa and 15 kDa. In the epithelia cells a strongly labeled band at about 55 kDa was observed in the homogenate, mitochondria, microsomes and cytosols, but in the nuclei it was weakly detected. A band between 23 and 20 kDa was found in the homogenate, mitochondria and microsomes. All existing proteins in the nuclei were labeled very weakly.

For the precise characterization of <sup>75</sup>Se-containing proteins in both cell lines two-dimensional electrophoresis (IEF/SDS-PAGE), which is a very sensitive method for the characterization of proteins in protein mixtures, was applied. The electrophoresis technique has a better resolution, as the proteins are first separated via their pI and then via their molecular masses. The localization of the proteins was obtained after autoradiography.

After the separation of the homogenates of the muscle myoblasts cell line more than 18 <sup>75</sup>Se-containing proteins with a molecular mass between 74 – 10 kDa and with pI value 3.0 to 10 was detected. One spot with the molecular mass at 74 – 65 kDa and pI value between 5.0 and 5.5 can be seen. At 55 – 50 kDa and pI value of 5.2 and 6.0 two spots were detected. The molecular masses and pI value are characteristic for the Thioredoxin reductases. One spot with the molecular mass at 60 – 55 kDa and pI value of 8.0 was observed. In the range of molecular mass between 28 – 10 kDa and pI value 4.8 – 8.0 several spots were found. The Se-proteins with the molecular masses 25, 23 and below 18 kDa were labeled very strong. The distribution of the selenoproteins in the subcellular fractions of cell line C2C12 was relatively similar, but the spots were labeled differently within these fractions. In all fractions, the proteins at 25 kDa, 20 kDa and 15 kDa were observed. The 15 kDa protein was labeled very strong in the microsomes and cytosolic fraction. The 25 kDa spot could be seen very well in the cytosolic fraction and nuclei. In the microsomes, at 55 kDa two proteins with pI between 5.0 and 6.0 were labeled strongly. In the homogenate of the A549 cell line more than 20 <sup>75</sup>Se -containing proteins were detected. In the range of molecular mass between 75 and 50 kDa eight proteins were found. Several of them were labeled very strongly. Within 40 – 30 kDa with pI value between 5

and 6 numerous of weak labeling spots were demonstrated. Four proteins with molecular mass at 20 – 10 kDa and pI value between 4.5 and 6.0 and two with pI value 8.0 – 8.4 were established. The autoradiogram shows that the selenium-containing proteins in the nuclei of epithelia cells were labeled very weakly. In this fraction five proteins at 65 kDa, 55 kDa with pI between 5.4 and 5.8, 25 kDa with pI values of 5.0 and 6.0 and 20 kDa with pI value 8.4 were detected. In the mitochondrial fraction, microsomes and cytosol the distribution of selenoproteins were relatively similar, but the spots were labeled differently. A strong labeled protein at about 55 kDa with pI value between 5.5 and 5.8 was observed in the mitochondria and cytosol. A protein at 25 kDa and pI value 5.5 was detected in all fractions and at 20 kDa with pI value of about 4.5 was strongly labeled in the mitochondrial fraction and microsomes. In cytosol a 25 kDa protein with pI value 6 and two proteins in the mitochondrial fraction and microsomes in the range between 23 and 20 kDa and pI value between 7.5 and 8.4 were observed.

Some of the selenium-containing proteins found in both cell lines could be identified. The protein spot at about 70 kDa with pI value between 4.8 and 5.0 is probably the selenoprotein O [77]. This protein can be seen in the homogenate and cytosol of C2C12 cells only. In the area between 55 and 70 kDa with pI value between 5.2 and 6.0 in the homogenate as well as cytosol five proteins were found. Four of them could belong to the Thioredoxin reductases family [78, 140]. In the homogenate of A549 cell line a very strong labelled protein with molecular mass at 70 – 75 kDa and pI about 6.5 was located. In the same area, in the cytosol, the autoradiogram shows more than one protein. The 25 kDa and 23 kDa spots with the pI value at 6.2 – 6.8 most likely belong to GPx 1 and GPx 3 [141, 142]. In both cell lines one protein at about 20 kDa with pI 7.5 – 8.0 was detected that corresponds to the GPx 4.

In all autoradiograms one protein at 15 kDa and pI value between 4.5 and 4.8 was seen which can be assigned to the 15 kDa selenoprotein [143]. The 12 kDa selenoprotein was found in the homogenate of C2C12 and A549 cells only. In the mouse myoblast cells one protein under 10 kDa with pI 8.5 – 8.8 could belong to Sel W [144]. More than ten selenium-containing proteins can not be allocated to known selenoproteins.

The 15 kDa protein is expressed in numerous tissues and its expression is regulated in response to nutritional selenium [145]. The function of this protein is not known. Previous studies showed that the 15 kDa protein can play a role in regulation of apoptosis. In

malignant mesothelioma cells, selenite-induced apoptosis was shown to depend on the presence of Sel 15 [146]. The GPx 4 selenoprotein (PHGPx) was detected in cytosol, mitochondria and nuclei in different tissues. Its function is known as phospholipid- and cholesterol-hydroperoxides reduction, by using electrons from protein thiols [147]. The result of numerous studies suggests that the enzyme may have an essential role in redox regulation [148]. Lipid peroxidation in a disordered muscle was observed and associated with a decrease in glutathione peroxidase activity. On the other hand, it was also shown that with a low selenium diet, adequate in tocopherol and low in polyunsaturated fatty acids no myopathy in calves occurred [149]. The small 9.5 kDa Sel W is ubiquitously expressed in tissues. It is known that selenium deficiency causes reduction of this protein in skeletal muscle, heart, intestine and prostate but in the brain its expression level remains maintained during selenium deficiency. Earlier studies presented that the Sel W is missing in the selenium deficient sheep with a white muscle disease [150]. Involvement of this protein in muscle disease was proposed but its function is still unknown.

In the next step of this study the selenium effect for the whole antioxidative activity was examined. For these experiments, the skeletal muscle, the lung and the spleen of rats were used. The rats were fed with selenium deficient and a selenium sufficient diet. The antioxidant capacity needed is regulated during maintenance of adequate levels of antioxidant and the localization of antioxidant compounds and enzymes [85]. It was reported that the trace element selenium is necessary for the antioxidant defence system. Therefore it is very important to understand the Se regulation function not only as antioxidant but also for the whole antioxidant status. The results confirm the previous hypothesis that the activity of selenium binding enzymes strongly depend on the selenium status. In the group of selenium-sufficient animals investigatory selenoproteins were detected in all tissues. In the second group the signalling of these proteins was significantly lower. It was reported about the selenium defensive function against ROS, oxidative stress and free radicals [151]. Adequate dietary selenium supply has been proposed to be useful for the prevention and reduction of several muscle diseases, cardiovascular and neurological disorder or lung cancer [152], but the possible participation of the Se-proteins in those mechanisms is not explained yet. The nutritional selenium consumption can affect the selenoproteins level in the organism. Most of the action was described on glutathione peroxidase and thioredoxin reductase. However, the function of this element in the form of



these enzymes could explain several, but not every effect of selenium insufficiency. More than 80% of the selenium in the rat is present as selenocysteine. Half of this selenocysteine or approximately 40% of the selenium present in the body is bound on glutathione peroxidase and the rest of this element is present in other compounds [153]. It can be assumed that there may be further biologically active forms of selenium [110]. It is important to determine how selenoproteins are related to action of such metabolites, because individuals differ substantially in their ability to increase selenoprotein activity in response to additional dietary Se [112].

Superoxide dismutase and catalase belong to the most important intracellular antioxidants enzymes in the human body . In this study, the effect between selenium supplementation and non Se-antioxidants enzymes was not observed. In both animal groups these enzymes were detected. A number of hormones, growth factors and cytokines were shown in the destruction process of reactive oxygen species and free radicals. The development of pro-oxidant in the living organism is a normal process in the cell metabolisms. In a correct functional body, the generated oxidants are destroyed by antioxidants and the very sensitive balance between oxidants and antioxidants is maintained. Imbalance of this system is a result of an increased level of free radicals and reactive oxygen species (ROS), which impair the antioxidant defence system. Therefore it is very important to understand the mechanism of the strategy of the antioxidant defence system, not only the function of individual enzymes but also of the total antioxidant status. It is interesting to find out and to interpret the distribution of antioxidants in tissues and the alteration of the whole antioxidative activity, when the activity of the selenium status is decreased. Both questions are important to evaluate the results of studies, action with antioxidants and disease caused by oxidative stress, like cancer or neurological disorder. For proteomic science, the determination of the protein related antioxidative activity could improve to understand the function of specific proteins.

ABTS assay was used for the screening of the total antioxidant status in cytosolic fractions of skeletal muscle, lung and spleen of rats fed with a selenium deficient and a selenium sufficient diet. The method described gives a measure of the lipophilic and hydrophilic antioxidants including flavonoids, carotenoids, hydroxycinnamates and plasma antioxidants. The study shows that the selenium status has no effect on the whole antioxidative activity. In the cytosol of skeletal muscle, lung and spleen of rat no

differences between the selenium deficient and sufficient animals in the total antioxidant status were observed. The reason for this could be that the protective function of selenium is possibly taken over by other antioxidants.

Recent studies demonstrated that a number of metal- or metalloid-binding proteins play important roles in degradation of free radicals or oxidative stress. Therefore, SEC-ICP-MS, as a largely preferential method for the investigation of metal-biomolecule complexes in biological sample was used for the study of protein-bound trace elements in the cytosol of skeletal muscle, lung and spleen fractions from selenium deficient and selenium sufficient rats. Iron, zinc, copper, manganese, molybdenum, nickel, cadmium, cobalt, arsenic, selenium and vanadium in the rat skeletal muscle, lung and spleen cytosol was found in protein-bound form.

The iron profile shows two proteins at 32 and 7.5 kDa, the 32 kDa protein could belong to a PHYDH1 (Phytanoyl-CoA dioxygenase domain-containing protein 1) [113]. The 26 kDa zinc – binding proteins can correspond to the superoxide dismutase 3 [114] or a zinc finger protein Zmynd19 (zinc finger MYND domain-containing protein 19) [115]. In the investigatory cytosol three manganese-containing proteins were found. The 41 kDa protein can attach to manganese or iron binding catalytic subunit of PP1 (Protein phosphatase 1- $\alpha$  catalytic subunit), which is essential for muscle contractility and protein synthesis, and participates in the regulation of glycogen metabolism [116]. The nickel-containing proteins are a relatively new class of metalloenzymes. Currently only seven nickel enzymes are known: urease, hydrogenase, CO- dehydrogenase, Ni-SOD, methyl-coenzym M reductase, glyoxalase 1 and cis-trans isomerase [117]. In this study three nickel-containing protein were detected, but none of the known proteins correspond with them. The cadmium profile shows two proteins, the 43 kDa proteins could belong to the Cytochrome b [118]. From the literature is known a lot of arsenic-containing proteins, but most of them are not characterized. The 29 kDa As-protein could belong to the uncharacterized isoforms of RCG47444 (Uroporphyrinogen 3 synthase) [119,120]. The selenium profile shows tree proteins, the 53 kDa could be the Thioredoxin reductase1 [121], the 8 kDa can correspond to the Sel W [122] and the last protein, about 5 kDa can not be identified. The results shows that selenium in mammalian is present in the form of small proteins. A lot of small metal-containing proteins are known from their function as membrane transporter. Possibly the newly found small Se protein has also a function in the transport to those tissues. The

cobalt, molybdenum and vanadium containing protein can not be assigned to the known proteins.

Iron, copper, zinc, manganese and selenium are known to be essential constituents of redox – active enzymes, but there is the possibility that in the skeletal muscle, lung and spleen these elements may also be contained in further proteins not yet identified. Interestingly, vanadium and arsenic were also found to be protein-bound. So far nothing is known about interactions between these elements and skeletal muscle or lung. Therefore further studies are accomplished to investigate the biological functions of these elements more closely.

The finding of PON 1 in the skeletal muscle was conducted to interrogate whether this enzyme has more important functions in the organism. The next step in this work was to particularly recognize the function of PON1 in the body. In this study a short and very sensitive strategy for the purification of the PON 1 enzyme was developed. Human serum paraoxonase 1 was purified by two sequential steps. In the first step the DEAE Sephadex anion exchanger was used and in the next step G-200 gel filtration chromatographic media was applied. For the purification the human plasma was treated over night with detergent Triton X-100 which helps to separate the enzyme from lipoproteins. The purity of this protein was controlled by using SDS-PAGE and Western blot analysis. The final purified enzyme showed a signal protein band of approximately 43 kDa corresponding to human PON 1. This protocol allows purification of this enzyme on a large scale.

Human serum paraoxonase 1 (PON 1) is a member of PONs proteins group that also includes PON 2 and PON 3. The PONs family demonstrates a wide range of physiologically important hydrolytic activities. In the plasma, after secretions from the liver, this enzyme is associated with high-density lipoprotein (HDL). Earlier observations showed that PON1 inhibits the oxidation of lipids in low-density lipoprotein (LDL), reducing the level of oxidizing lipid forms, which are involved in the initiation of atherosclerosis [130]. Possibly the protection mechanism of LDL from oxidation is the same mechanism as HDL protects against atherosclerosis [131]. A number of metal- or metalloid- binding proteins have been identified as free radicals captor. The finding of the variable elements in this protein, by using SECI-ICP-MS, can indicate that this enzyme has probably more than one function in the organism. The protein in this study was observed in plasma and in other tissues like skeletal muscle, lung and in the cell lines. It was suggested

that PON 1 acts as an *in vivo* bioscavenger. This can explain its presence in the lung and skeletal muscle, which are mostly exposed to pollution particles from environment and exposure of oxygen [133].

After lanthanum had been found in human plasma as PON 1-bound forms it was interesting to examine whether La-containing proteins exist in the rat species. In the lanthanum profile two peaks were observed in the investigatory species. Their molecular masses were approximately 43 and 9 kDa. The 43 kDa protein could belong to the serum PON 1. The 9 kDa protein can not be assigned to the known proteins. In the available literature some information about small molecules containing lanthanum can be found [129], but there are not characterized.

One of the most interesting results in this study is the PON 1- bound form with lanthanum and mercury. Manganese, nickel, cobalt and copper were also found to be protein – bound. Actually, nothing is known about the metabolism and biological functions of lanthanum and mercury in the living organism. It was reported that the lanthanides probably cause granulomatous lesions or pneumoconiosis in the smelter's and photoengraver's lung [134]. In the medicine the lanthanum carbonate is known as phosphate binders which are used to reduce the absorption of high phosphate level (hyperphosphatemia) of patients with chronic renal failure (CRF). The control of serum phosphate is important for the normal function of bone and the correct regulation of serum calcium by the parathyroid hormone (PTH). Phosphate binders react with phosphate and form an insoluble component [154]. The protein is also involved in hydrolysis and inactivation of various organophosphates [132]. Probably in this way, the lanthanum assists this enzyme by phosphates deactivation. Previous studies have only demonstrated the toxicity side of mercury. Elemental, inorganic and organic forms of mercury have an effect on lipid peroxidation and formation of reactive oxygen species [135]. In this case, PON 1 probably has a function as transport – protein or forms a complex within the body and in this way neutralizes the toxicity of this element that decrease formation of oxidants. The given examples illustrate how important it is to know the biological effect of these elements on human health. Monitoring and toxicological studies of this element-bound protein are needed to realize its meaning and their impact on medical treatment.

## 6. Summary

In this study element analytical methods have been combined with biochemical separated method to achieve information about concentration and distribution of trace elements in the skeletal muscle, lung and spleen of rat and their subcellular fractionations in nuclear, mitochondrial, microsomal and cytosolic fractions. The subcellular compartments were separated by differential ultracentrifugation. Instrumental neutron activation analysis was used to determine the concentration of iron, zinc, rubidium, cesium, cobalt, selenium, arsenic and chromium. The analyzed elements were found to be distributed inhomogeneous in the examined tissues of rat and their subcellular compartments. The mitochondrial and microsomal fractions in all species present the highest concentrations of the investigatory elements. The highest concentration of iron, zinc, rubidium and selenium was detected in the spleen, cesium in the skeletal muscle and arsenic in the lung.

In order to gain more information about the effect of selenium as antioxidants and also on selenium-containing proteins and on their possible function in the body, radiotracer technique had been combined with biochemical separation methods. The mouse muscle myoblasts cells line C2C12 and human lung epithelial cells line A549 were used for this study. The cells were labelled *in vitro* with 20 kBq  $^{75}\text{Se}$ . By applying the SDS-PAGE method, the proteins of the homogenates and subcellular fractions of the two cell lines were separated and the selenium-containing proteins were identified by autoradiography. Nine selenium-containing proteins in the subcellular fractions of the cells line C2C12 and eight in the A549 cells line were found. Their relative molecular masses were: 75 kDa, 70-65 kDa, 55 kDa, 53 kDa, 25 kDa, 23 kDa, one band between 23 and 20 kDa, one protein in the range between 20 – 18 kDa, 18 kDa, 14 kDa, 10 kDa. The distribution of bands in the C2C12 fractions were similar but the selenoproteins between the fractions were labelled differently. Except the nuclei in the A549 cell line no meaningful differences of selenoproteins between these fractions were observed. Two-dimensional electrophoresis (IEF/SDS-PAGE) was applied for the precise characterization of  $^{75}\text{Se}$  proteins in both cell lines. After separation in the homogenates of the muscle myoblasts cells line more than 18  $^{75}\text{Se}$ -containing proteins were proven. In the homogenate of the A549 cells line more than 20  $^{75}\text{Se}$ -containing proteins were detected. The measured molecular mass was between 74 – 10 kDa, that is the molecular range of the newly selenium proteins, with pI value between 3.0 and 10 in both cases.

The selenium effect on the whole antioxidative activity shows that the activity of selenium binding enzymes strongly depends on the selenium status. In the group of selenium – sufficient animals selenoproteins were positive detected in every tissue. In the second group the signalling of these proteins was meaningfully lower. No effect between selenium supplementation and non Se – antioxidants enzymes was observed. In both animal groups these enzymes were detected.

The total antioxidant status in cytosolic fractions of skeletal muscle, lung and spleen of rats fed with a selenium deficient diet and a selenium sufficient diet was measured with the ABTS assay. The method described gives an analysis of the lipophilic and hydrophilic antioxidants including flavonoids, carotenoids, hydroxycinnamates and plasma antioxidants. The study showed that the selenium status has no effect on the whole antioxidative activity. In the cytosol of skeletal muscle, lung and spleen of the rat no differences between the selenium deficient and sufficient animals were observed regarding the total antioxidant status. The reason for this could be that the protective functions of selenium are fulfilled by other antioxidants.

A number of studies indicated that an amount of metal- or metalloid-binding proteins play important roles in the degradation of free radicals or in oxidative stress. To analyse the protein-bound trace elements in the cytosol of skeletal muscle, lung and spleen fractions of selenium deficient and selenium sufficient rats High-Pressure-Liquid-Chromatograph (HPLC) in combination with ICP-MS was used.

Iron, zinc, copper, manganese, molybdenum, nickel, cadmium, cobalt, lanthanum, arsenic, selenium and vanadium were found in the rat skeletal muscle, lung and spleen cytosol in protein-bound form. One interesting and new result in this investigation was that lanthanum was found in protein-bound form. Nothing is known about interactions between lanthanum and skeletal muscle, lung or spleen. The lanthanum profile shows two peaks with molecular masses of 43 and 7 kDa. Both peaks were detected in all species but the intensity was different.

The discovery of PON 1 in the skeletal muscle raises the question if this enzyme has further important functions in the organism. A fast and appropriate purification procedure for PON 1 enzyme was developed and allowed a closer characterization. The finding of variable elements in this protein by applying SECI-ICP-MS suggests that this enzyme has probably more than one function in the organism. The protein was observed in plasma and in other tissues such as skeletal muscle, lung and in the cell lines. One of

the most interesting result in this study is the PON 1- bound form with lanthanum. Manganese, nickel, cobalt, copper and mercury were also found to be protein – bound.

## 7. Zusammenfassung

In dieser Arbeit wurden analytische Methoden mit biochemischen Verfahren kombiniert, um Informationen über die Konzentration und Verteilung von Spurenelementen in Skelettmuskel, Lunge und Milz von Ratten und deren subzellulären Fraktionen (Zellkerne, Mitochondrien, Mikrosomen und Zytosol) zu erhalten. Die subzellulären Komponenten wurden mit differentieller Ultrazentrifugation gewonnen. Instrumentelle Neutronenaktivierungsanalyse (INAA) wurde eingesetzt, um die Konzentrationen der Spurenelemente Eisen, Zink, Rubidium, Cäsium, Kobalt, Selen, Arsen und Chrom zu bestimmen. Die untersuchten Elemente waren in den Geweben und subzellulären Fraktionen inhomogen verteilt. Die höchsten Elementkonzentrationen wurden in Mitochondrien und Mikrosomen nachgewiesen. Die höchsten Eisen-, Zink-, Rubidium- und Selenkonzentrationen wurde in der Milz gefunden. Die höchste Konzentration von Cäsium war im Skelettmuskel zu sehen und die Lunge hat die höchste Konzentration von Arsen gezeigt.

Weitere Untersuchungen wurden durchgeführt, um den Einfluss von Selen als Antioxidant und weitere Informationen zu Metabolismus und Funktion in den untersuchten Geweben und Zell Linien zu erhalten. Die Radiotracer-Methode wurde mit gelelektrophoretischen Methoden kombiniert und mit Hilfe von Autoradiogrammen wurden die Proteine visualisiert. Für diese Experimente wurden die Myoblasten der Maus-Zelllinie C2C12 und der humanen Lungen-Epithelia Zelllinie A549 *in vitro* mit 20kBq <sup>75</sup>Se markiert. In der C2C12 Zelllinie wurden neun und in der A549 Zelllinie acht selenhaltige Proteine gefunden. Ihre jeweiligen molekularen Massen waren: 75 kDa, 70-65 kDa, 55 kDa, 53 kDa, 25 kDa, 23 kDa, eine Bande zwischen 23 und 20 kDa, ein Protein zwischen 20 – 18 kDa, 18 kDa, 14 kDa und 10 kDa. In den subzellulären Fraktionen der C2C12 Zelllinie waren die Selenoproteine ähnlich verteilt, aber zwischen den Fraktionen waren die Selenoproteine unterschiedlich markiert. Außer in den Zellkernen konnte in den Fraktionen der A549 Zelllinie kein signifikanter Unterschied bei der Verteilung von Se-Proteinen nachgewiesen werden. Die präzise Charakterisierung von <sup>75</sup>Se-haltigen Proteinen erfolgte mit Hilfe der zweidimensionalen Elektrophorese. 18 Se-Proteine in der C2C12 Zelllinie und mehr als 20 Se-Proteine in der A549 Zelllinie wurden mit molekularen Massen zwischen 74 und 10 kDa und pI-Werten von 3-10 detektiert.



Der Seleneinfluss auf die antioxidativ wirkenden Proteine zeigt, dass die selenbindenden Enzyme stark vom Selenstatus abhängig sind. In der Gruppe von Tieren, die ausreichend mit Selen ernährt wurden, wurden alle untersuchten Selenoproteine detektiert. In der Gruppe mit mangelernährten Tieren waren die Protein-Signale bedeutend niedriger. Es wurde kein Einfluss des Selen-Status auf andere nicht-selenhaltige Proteine nachgewiesen.

In dieser Arbeit wurde gezeigt, dass der Selenstatus auf die gesamte antioxidative Aktivität keinen Einfluss hat. In Zytosol von Skelettmuskel, Lunge und Milz von selenadäquat- und -mangelernährten Tieren wurden keine Unterschiede im gesamten antioxidativen Status nachgewiesen. Eine Erklärung dafür kann sein, dass Funktionen des Selens von anderen Antioxidantien im Zytosol übernommen wurden.

In letzter Zeit haben viele Studien gezeigt, dass eine große Anzahl von metall- oder metalloiddbindenden Proteinen eine wichtige Rolle beim Abbau von freien Radikalen oder bei oxidativem Stress spielen. Zur Untersuchung von metallhaltigen Proteinen in Zytosol von Skelettmuskel, Lunge und Milz von selenadäquat- und -mangelernährten Ratten wurde ein Hochleistungsflüssigkeitschromatograph (HPLC) mit Kopplung an die ICP-MS eingesetzt. Eisen, Zink, Kupfer, Mangan, Molybdän, Nickel, Kadmium, Kobalt, Lanthan, Arsen, Selen und Vanadium wurden in proteingebundener Form gefunden. Ein wichtiges und sehr interessantes Arbeitsergebnis ist, dass Lanthan in proteingebundener Form im Gewebe vorkommt. Zurzeit ist wenig bekannt über die Interaktion zwischen diesem Element und den untersuchten Organen. Im Lanthan Profil sind zwei Peaks mit molekularen Massen von 43 und 7 kDa zu sehen. Die beiden Peaks wurden in allen untersuchten Spezies nachgewiesen, sie zeigen aber unterschiedliche Intensitäten.

Der Fund von Paraoxonase 1 (PON 1) im Skelettmuskel wirft die Frage auf, ob das Protein weitere wichtige Funktionen im Körper hat. Für diesen Zweck wurde ein schnelles und geeignetes Aufreinigungsverfahren etabliert, welches eine weitere Charakterisierung von PON 1 erlaubte. Mit Hilfe von SECI-ICP-MS wurde nachgewiesen, dass verschiedene Elemente in proteingebundener Form vorliegen. Das kann darauf hinweisen, dass das Protein im Körper vermutlich mehr Funktionen hat. In dieser Studie wurde das Protein in Human Plasma und auch in Skelettmuskel, Lunge, Milz von Ratten und in Zelllinien nachgewiesen. In dieser Arbeit wurde nachgewiesen, dass PON 1 mit Lanthan in gebundener Form vorliegt. Für Mangan, Nickel, Kobalt,

Kupfer und Quecksilber wurde nachgewiesen, dass das Protein mit den Elementen in gebundener Form vorliegt.

## 8 References

1. Sies H. Oxidative stress: oxidants and antioxidants. *Experimental Physiology*, 82: 291-295. 1997.
2. Prasad A.S. Zinc: role in immunity, oxidative stress and chronic inflammation. *Curr Opin Clin Nutr Metab Car.* 12 (6): 646-652. 2009.
3. Steinbrenner H., Sies H. Protection against reactive oxygen species by selenoproteins. *Biochim Biophys Acta* 1790 (11): 1478 – 1485. 2009.
4. Halliwell, B., Gutteridge, J.M.C. The antioxidants of human extracellular fluids. *Arch Biochem Biophys* 280:1-8. 1990.
5. Sies, H. Strategies of antioxidants defense. *Eur. J. Biochem.* 215: 213-219. 1993.
6. Valko M., Izakovic M., Mazur M., Rhodes C.J., Telser J. Role of oxygen radicals in DNA damage and cancer incidence. *Molecular and Cellular Biochemistry* 266: 37-56. 2004.
7. Halliwell B., Gutteridge, J.M.C., Cross C.E. Free-radicals, antioxidants, and human-disease-Where are we now? *J Lab Clin Med* 119:598-620. 1992.
8. Ames N.B., Shigenaga M. K., Hagen T.M. Oxidants, antioxidants, and the degenerative diseases of aging. *Proc Natl Acad Sci USA* 90:7915-7922. 1993.
9. McCord J. M., Fridovich I. superoxide dismutase: an enzymic function for erythrocytes. *J Biol Chem* 244, 6049-6055. 1969.
10. Grankvist K., Marklund S.L., Täljedal I.B. CuZn-superoxide dismutase, Mn-superoxide dismutase, catalase and glutathione peroxidase in pancreatic islets and other tissues in the mouse. *Biochem J.* 199(2): 393–398. 1981.
11. Nishikawa M., Hashida M., Takakura Y. Catalase delivery for inhibiting ROS-mediated tissue injury and tumor metastasis. *Adv Drug Deliv Rev* 61 (4): 319-326. 2009.
12. Perry J.J.P., Shin D.S., Getzoff E.D., Taine J.A. The structural biochemistry of the superoxide dismutases. *Biochimica et Biophysica Acta* 1804: 245-262. 2010.
13. Marklund S.L., Holme E., Helner L. Superoxide dismutase in extracellular fluids. *Clinica Chimica Acta* 128: 41-51. 1982.
14. Nozik-Grayck, E., Suliman, H.B., Piantadosi C.A. Extracellular superoxide dismutase. *Int J Biochem Cell Biol* 37(12): 2466-2471. 2005.

15. Herbette, S., Roecket-Drevet P., Drevet J. Seleno-independent glutathione peroxidases. More than simple antioxidant scavengers. *FEBS Journal* 274:2163-2180. 2007.
16. Toppo S., Flohe L., Ursini F., Vanin S., Maiorino M. Catalytic mechanisms and specificities of glutathione peroxidases: variations of a basic scheme. *Biochemical and Biophysical Acta* 1790:1486-1500. 2009.
17. Heck D. E., Shakarjan, M., Kim, D.H., Laskin, J.D., Vetrano A.M. Mechanisms of oxidant generation by catalase. *Ann. N.Y. Acad. Sci.* 1203:120-125. 2010.
18. Wagner J.R., Hu C.C., Ames B.N. Endogenous oxidative damage of deoxycytidine in DNA. *Proc Natl Acad Sci.* 89: 3380-3384. 1992.
19. Rigoulet M., Yoboue E. D., Devin A. Mitochondrial ROS generation and its regulation: mechanisms involved in H<sub>2</sub>O<sub>2</sub> signaling. *Antioxid Redox Signal.* 14: 456-468. 2011.
20. Brand M.D. The sites and topology of mitochondrial superoxide production. *Exp Gerontol.* 45: 466-472. 2010.
21. Stamler J.S., Singel D.J., Loscalzo J. Biochemistry of nitric oxide and its redox-activated forms. *Science.* 258: 1898-1901. 1992.
22. Terlecky S.R., Koepke J.I., Walton P.A. Peroxisomes and Aging. *Biochim Biophys Acta.* 1763 (12): 1749-54. 2006.
23. Banerjee A.K., Mandal A., Chanda D., Chakraborti S. Oxidant, antioxidant and physical exercise. *Molecular and Cellular Biochemistry* 253: 307-312. 2003.
24. Machlin L.J., Bendich A. Free radical tissue damage: protective role of antioxidants nutrients. *FASEB Journal.* 1: 441-445. 1987.
25. Manda G., Nechifor M.T., Neagu T.M. Reactive Oxygen Species, Cancer and Anti-Cancer Therapie. *Current Chemical Biology* 3: 342-366. 2009.
26. Sen CK. Oxidant and antioxidant in exercise. *J. Appl. Physiol.* 79: 675-686. 1995.
27. Urso M.L., Clarkson P.M. Oxidative stress, exercise and antioxidant supplementation. *Toxicology.* 189: 41-54. 2003.
28. Markesbery W.R., Lovell M.A. Damage to lipids, proteins, DNA and RNA in mild cognitive impairment. *Arch Neurol.* 64: 954-956. 2007.
29. Ansari M.A., Scheff S.W. Oxidative stress in the progression of Alzheimer disease in the frontal cortex. *J Neuropathol Exp Neurol.* 69 (2):155-167. 2010.

30. Nordberg G.F. Biomarkers of exposure, effects and susceptibility in humans and their application in studies of interactions among metals in China. *Toxicol Lett* 192 (1): 45-49. 2010.
31. Flora S.J., Mittal M., Mehta M. Heavy metal induced oxidative stress & its possible reversal by chelation therapy. *Indian J Med Res* 128 (4): 501-523. 2008.
32. Schwarz K., Foltz C.M. Selenium as an integral part of factor 3 against dietary necrotic liver degeneration. *J Am Chem Soc* 19: 3292-3293. 1957.
33. Ellis D.R., Salt D.E. Plants, selenium and human health. *Curr Opin Plant Biol* 6: 273-79. 2003.
34. Foster L.H., Sumar S. Selenium in health and disease: a review. *Crit Rev Food Sci Nutr* 37 (3): 211-228. 1997.
35. Fan A.M., Kizer K.W. Selenium. Nutritional, toxicologic, and clinical aspects. *West J Med* 15 (2): 160-167. 1990.
36. Lobanov A.V., Hatfield D.L., Gladyshev V.N. Eukaryotic selenoproteins and selenoproteomes. *Biochimica et Biophysica Acta* 1790: 1424-1428. 2009.
37. Holben D.H., Smith A.M. The diverse role of selenium within selenoproteins: a review. *J Am Diet Assoc.* 99(7): 836-843. 1999.
38. Wingler K., Brigeilus-Flohe R. Gastrointestinal glutathione peroxidase. *Biofactors.* 10: 245-249. 1999.
39. Takahashi K., Akasaka M, Yamamoto Y., Kabayashi C., Mizoguchi J., Koyama J. Primary structure of human plasma glutathione peroxidase deduced from cDNA sequence. *J Biochem.* 108: 145-148. 1990.
40. Thomas J.P., Girroti A.W. Peroxidation of cell membranes in the presence of hematoporphyrin derivative: reactivity of phospholipid and cholesterol hydroperoxidase with glutathione peroxidase. *Biochim Biophys Acta.* 962: 297-307. 1988.
41. Pfeifer H., Conrad M., Roethlein D., Kyriakopoulos A., Brielmeier M., Bornkamm G.W., Behne D. Identification of a specific sperm nuclei selenoenzyme necessary for protamine thiol cross-linking during sperm maturation. *FASEB J.* 15: 1236-1238. 2001.
42. Kryukov G.V., Castellano S., Novoselov S.V., Lobanov A.V., Zehtab O., Guigo R., Gladyshev V.N. Characterisation of mammalian selenoproteomes. *Science.* 300: 1439-1443. 2003.

43. Bianco A.C., Salvatore D., Gereben B., Berry M.J., Larsen P.R. Biochemistry, cellular and molecular biology and physiological roles of the iodothyronine selenodeiodinase. *Endocr. Rev.* 23: 38-89. 2002.
44. Mustacich D, Powis G. Thioredoxin reductase. *Biochem J.* 346 (1): 1-8. 2000.
45. Hill K.E., Lloyd R.S., Yang J.G., Read R., Burk R.F. The cDNA for rat selenoprotein P contains 10 TGA codons in the open reading frame. *J Biol Chem.* 266: 10050-10053. 1991.
46. Gladyshev V.N., Jeang K.T., Wootton J.C., Hatfield D.L. A new human selenium-containing proteins. Purification, characterization and cDNA sequence. *J Bio Chem.* 273: 8910-8915. 1998.
47. Lescure A., Guastheret D., Carbon P. Novel selenoproteins identified in silico and in vivo by using conserved RNA structural motif. *J Biol Chem.* 274: 38147-38154. 1999.
48. Peti E., Lescure A., Roderstorff M., Krol A., Moghadaszadeh B., Wawer U.M., guicheney P. Selenoprotein N: an endoplasmic reticulum glycoprotein with an early development expression pattern. *Hum Mol Genet.* 12: 1045-1053. 2003.
49. Beilstein M.A., Vendeland S.C., Barofsky E., Jensen O.N., Whanger P.D. Selenoprotein W of rat muscle binds glutathione and an unknown small molecular weight moiety. *J Inorg Biochem.* 61: 117-124. 1996.
50. Guimaraes M.J., Peterson D., Vicary A., Cocks B.G., Copeland N.G., Gilbert D.J., Jenkins N.A., Ferrick D.A., Kastelein R.A., Bazan J.F., Zlotnik A. Identification of a novel sel D homolog from eucariotes, bacteria, and archaea: is there an autoregulatory mechanism in selenocystein metabolism? *Proc Natl Acad Sci USA.* 93:15086-15091. 1996.
51. Kryukov G.V., Kumar R.A., Koc A., Sun Z., Gladyshev V.N. Selenoprotein R is a zinc-containing stereo-specific methionine sulfoxide reductase. *Proc Natl Acad Sci USA.* 99: 4245-4250. 2002.
52. Lu C., Qiu F., Zhou H., Peng Y., Hao W., Xu J., Yuan J., Wang S., Qiang B., Xu c., Peng X. Identification and characterization of selenoprotein K: an antioxidant in cardiomyocytes. *FEBS Lett.* 580: 5189-5197. 2006.
53. Rowett H.G.Q. The rat as a small mammal. Ed.: John Murray, Fifty Albemarle Street London 1974.
54. Hames B.D., Hooper N.M. Notes in Biochemistry. Ed.: BIOS Scientific Publishers 2000.

55. Jackson M.J., O'Farrell S. Free radicals and muscle damage. In: Free radical in medicine. P: 630-641. Ed.: Cheeseman K.H, Slater T.F. The British Council 1993.
56. Hebel R., Stromberg M.W. in: Anatomy and embryology of the laboratory rat. Bio Med Verlag. 1986.
57. Barnes P.J. Reactive oxygen species and airway inflammation. Free Radic Biol Med. 9: 235-243. 1990.
58. Faux S.P., Tai T., Thorne D., Xu Y., Breheny D., GacaM. The role of oxidative stress in the biological responses of lung epithelial cells to cigarette smoke. Biomarkers. 14 (1): 90-96. 2009.
59. Ryrfeldt A., Bannenberg G. Moldeus P. Free radicals and lung disease. In: Free radical in medicine. P: 588-603. Ed.: Cheeseman K.H, Slater T.F. The British Council 1993.
60. Hinton R.H., Mullock B.M. Isolation of subcellular fractions, in: Subcellular fractionation. P: 41-43. Ed.: Graham J.M., Rickwood D. Information Press, Ltd, UK. 1996.
61. Windell C.C., Tata J.R. Biochem. J. 92: 313-317. 1964.
62. Wilkie G.S., Schirmer E., C. Purification of nuclei and preparation of nuclear envelopes from skeletal muscle, in: The nucleus. Nuclei and nuclear components. P: 23-43 Ed.: Hancock R. Hummana Press, USA. 2008.
63. Bradford M.M. A rapid and sensitive method for the quantitation of microgram quantities of protein utilizing the principle of protein-dye binding. Anal. Biochem. 72: 248-254. 1976.
64. Laemmli U.K. Cleavage of structural proteins during the assembly of the head of bacteriophage T4. Nature. 227: 680-685. 1970.
65. O'Farrell P.H. High resolution two-dimensional electrophoresis of proteins. J Biol Chem 250 (10): 4007-4021. 1975.
66. Blum H., Beier H., Gross H.J. Improved silver staining of plant proteins, RNA and DNA in polyacrylamide gels. Electrophoresis 8: 93-99, 1987.
67. Amemiya Y., Miyahara J. Application of imaging plate. Nature: 89-93. 1988.
68. Flohe L., Gumel W.A. assays of glutathione peroxidase. Methodes Enzymol 105:114.121. 1984.
69. Ra R., Pellegrini N., Proteggente A., Pannala A., Yang M., Rice-Evans C. Antioxidant activity applying an improved ABTS radical cation decolorization assay. Free Radical Biology and Medicine 26:1231-123. 1999.

70. Golmanesh L., Mehrani H., Tabei M. Simple procedures for purification and stabilization of human serum Paraoxonase-1. *Biochemical and Biophysical Methods* 70:1037-1042. 2008.
71. Mackness, M.I., Durrington, P.N. HDL, its enzymes and its potential to influence lipid peroxidation. *Atherosclerosis* 115, 243-253. 1995.
72. Bode P. Instrumental and organizational aspect of a neutron activation analysis laboratory. Ed.: Delft. 1996.
73. Bray T.M., Kubow S., Bettger, W.J. Effect of dietary zinc on endogenous free radical production in rat lung microsomes. *J.Nutr.* 116: 1054 – 1060. 1986.
74. Xu X., Thompson L. V., Navratil M., Arriaga E. A. Analysis of Superoxide Production in Single Skeletal Muscle Fibers. *Anal Chem.* 82: 4570 – 4576. 2010.
75. MacNee W. Oxidative stress and lung inflammation in airways diseases. *European J of Pharmacology.* 429: 195 – 207. 2001.
76. Behne D., Kyriakopoulos A. Mamalian selenium-containing proteins. *Annu. Rev. Nutr.* 21: 453-473. 2001.
77. Kryukov G. V., Castellano S., Novoselov S.V., Zehtag O., Guigo R., Gladyshev V. N. Characterization of Mammalian Selenoproteomes. *Science* 300: 1439-1443. 2003.
78. Zohng L., Arner E.S., Holmgren A. Structure and mechanism of mammalian thioredoxin reductase: the active site is a redox-active selenolthiol/selenenylsulfide formed from the conserved cysteine-selenocysteine sequence. *Proc Natl Acad Sci USA* 97 (11): 5854-5859. 2000.
79. Flohe L., Gunzler W.A., Schock H.H. Glutathione peroxidase a selenoenzyme. *FEBS Lett* 32: 132-134. 1973.
80. Thakahashi K., avissar n., Whitin J., Cohen H. Purification and characterization of human plasma glutathione peroxidase: a selenoprotein distinct from the known cellular enzyme. *Arch Biochem Biophys* 256: 677-689. 1987.
81. Pushpa-Rekha T.R., Burdsall A.L., Oleksa L.M., Chisolm G.M., Driscoll D.M. Rat phospholipid-hydroperoxide glutathione peroxidase, cDNA cloning and identification of multiple transcription and translation start sites. *J Biol Chem.* 270 (45): 26993-26999. 1995.
82. Behne D., Kyriakopoulos A., Kalcklosch M., Weiss-Nowak C., Pfeifer H., Gessner H., Hamel C. Two new selenoproteins found in the prostatic glandular epithelium and in the spermatid nuclei. *Biomed Environ Sci* 10: 340-345. 1997.



83. Gu Q.P., Beilstein M.A., Barofsky E., Ream W., Whanger P.D. Purification, characterization, and glutathione binding to selenoprotein W from monkey muscle. *Arch Biochem Biophys* 361: 25-33. 1999.
84. Murphy M.P. How mitochondria produce reactive oxygen species. *Biochem. J.* 417: 1-13. 2009.
85. Banerjee K. A., Mandal A., Chanda D., Chakraborti S. Oxidant, antioxidant and physical exercise. *Molecular and Cellular Biochemistry* 253: 307 – 312. 2003.
86. Halliwell B. Reactive species and antioxidants. Redox biology is a fundamental theme of aerobic life. *Plant Physiol.* 141 (2): 312 – 322. 2006.
87. Nordberg J., Arner E.S.J. Reactive oxygen species, antioxidants, and the mammalian thioredoxin system. *Free Radical Biology and Medicine.* 31: 1287 – 1312. 2001.
88. Forstrom J.W., Zakowski J. J., Tappel A. L. Identification of the catalytic side of rat liver Glutathione peroxidase as selenocysteine. *Biochemistry* 17: 2639-2644. 1978.
89. Gladyshev V.N., Jeang K.T., Stadtman T.C. Selenocysteine identified as the penultimate C-terminal residue in human T-cell thioredoxin reductase, corresponds to TGA in the human placental gene. *Proc. Natl. Acad. Sci.* 93: 6146-6151. 1996.
90. Zhong L., Arner E.S., Holmgren A. Structure and mechanism of mammalian thioredoxin reductase : the active site is a redox-active selenolthiol /selenenylsulfide formed from the conserved cysteine-selenocysteine sequence. *Proc. Natl. Acad. Sci.* 97:5854-5859. 2000.
91. Rubertelli A., Bajetto A., Allavena G., Wollman E., Sitia R. Secretion of thioredoxin by normal and neoplastic cells through a leaderless secretion pathway. *J. Biol. Chem.* 267: 24161-24164. 1992.
92. Kasaikina M.V., Dmitri E. Fomenko D.E., Vyacheslav M. Labunskyy V.M., Salil A. Lachke S.A., Qiu W., Moncaster J.A., Zhang J., Mark W. Wojnarowicz M.W., Sathish K. Natarajan S.K., Malinouski M., Schweizer U., Petra A. Tsuji P.A., Carlson B.A., Richard L. Maas R.L., Marjorie F. Lou M.F., Goldstein L.E., Hatfield D.L., Gladyshev V.N. 15 kDa selenoprotein (Sep15) knockout mice: roles of Sep15 in redox homeostasis and cataract development. *J.Biol. Chem.* 2011.
93. Irons R., Tsuji P.A., Carlson B.A., Ouyang P., Yoo M.H., Xu X.M., Hatfield D.L., Gladyshev V.N., Davis C.D. Deficiency in the 15 kDa Selenoprotein Inhibits Tumorigenicity and Metastasis of Colon Cancer Cells. *Cancer Prev Res (Phila)* 3 (5): 630-639. 2010.

94. Kumaraswamy E., Malykh A., Korotkov K.V., Kozyavkin S., Hu Y., Kwon S.Y., Moustafa M.E., Carlson B.A., Berry M.J., Lee B.J., Hatfield D.L., Diamond A.M., Gladyshev V.N. Structure-expression relationships of the 15-kDa selenoprotein gene. Possible role of the protein in cancer etiology. *Endocrinology* 143 (12): 4897-4906. 2002.
95. Shopova V.L., Dancheva V.Y., Salovsky P.T., Stojanova A.M. Protective effects of a superoxide dismutase/catalase mimetic compound against paraquat pneumotoxicity in rat lung. *Respirology* 14:504-510.2009.
96. McCord J.M., Fridovich I. Superoxid dismutase, an enzymic function for erythrocyte. *J. Biol. Chem.* 244: 6049 – 6055. 1969.
97. Weisiger R.A., Fridovich I. Mitochondrial superoxid dismutase. Site of synthesis and intramitochondrial localization. *J. Biol. Chem.* 248: 4793-4796. 1973.
98. Chelikani, P., Fita, I. and Loewen, P. C. Diversity of structures and properties among catalases. *Cell. Mol. Life. Sci.* 61: 192-208. 2004.
99. Billecke S., Dragonov D., Counsell R., Stetson P., Watson C., Hsu C., La Du B. N. Human serum paraoxonase (PON 1) isozymes Q and R hydrolyze lactones and cyclic carbonate esters. *Drug Metab. Dispos.* 28: 1335 – 1342. 2000.
100. Marsillach J., Mackness M., Mackness M., Riu F., Beltran R. Immunohistochemical analysis of paraoxonase-1,3 and 3 expression in normal mouse tissues. *Free Radical Biology and Medicine.* 45: 146 – 157. 2008.
101. Costa L.G., Cole T.B., Vitalone A., Furlong C. E. Measurement of Paraoxonase (PON 1) status as a potential biomarker of susceptibility to organophosphate toxicity. *Clin. Chim. Acta.* 325: 37 – 47. 2005.
102. Macknes B., Quarck R., Verreth W., Mackness M., Holvoet P. Human paraoxonase-1 overexpression inhibits atherosclerosis in mouse model of metabolic syndrome. *Arterioscler. Thromb. Vasc. Biol.* 26: 1545 – 1550. 2006.
103. Ng C.J., Hama S.Y., Bourquard N., Navab N., Reddy S.T. Adenovirus mediated expression of human Paraoxonase 2 protect again development of atherosclerosis in apolipoprotein E-deficient mice. *Mol. Genet. Metab.* 89: 368 – 373. 2006.
104. Shih D.M., Xia Y.R., Wang X.P. Wang S.S., Bourquard N., Fogekman A.M., Lusis A.J., Reddy S.T. Decreased obesity and atherosclerosis in human paraoxonase 3 transgenic mice. *Circ. Res.* 100: 1200 – 1207. 2007.

105. Ganther H.E. Selenium metabolism, selenoproteins and mechanisms of cancer prevention: complexities with thioredoxin reductase. *Carcinogenesis* 20 (9): 1657-1666. 1999.
106. Saito Y., Yoshida Y., Akazawa T., Takahashi K., Niki E. Cell death caused by selenium deficiency and protective effect of antioxidants. *The Journal of Biological Chemistry*. 278 (41): 39428-39434. 2003.
107. Rederstorff M., Krol A., Lescure A. Understanding the importance of selenium and selenoproteins in muscle function. *Cell. Mol. Life Sci.* 63: 52 – 59. 2006.
108. Yoo M.H., Xu X.M., Carlson B.A., Gladyshev V.N., Hatfield D.L. Thioredoxin reductase 1 deficiency reverses tumor phenotype and thmorigenicity of lung carcinoma cells. *The Journal of Biological Chemistry*. 281: 13005-13008. 2006.
109. Brown K.M., Arthur J.R., Selenium, selenoproteins and human health: a review. *Public Health Nutr* 4 (2B): 593-599. 2001.
110. Behne, D., Wolters, W. Distribution of selenium and glutathione peroxidase in the rat. *J. Natur.* 114:1289 – 1296. 1983.
111. Behne, D., Scheid, S., Kyriakopoulos, A., Hilmert, H. Subcellular distribution of selenoproteins in the liver of the rat. *Biochemica et Biophysica Acta* 1033:219-225. 1990.
112. Rikiishi, H. Apoptotic cellular events for selenium compounds involved in cancer prevention. *J Bioenerg Biomembr* 39: 91-98. 2007.
113. Zhang Z., Kochan G.T., Ng S.S., Kavanagh K.L., Oppermann U., Schofield C.J., McDoough M.A. Crystal structure of PHYHD!A, a OG oxygenase related to phytanoyl-CoA hydroxylase. *Biochem Biophys Res Commun.* 408 (4): 553-558. 2011.
114. Hjalmarsson K., Marklund S.L., Engstroem A., Edlund T. Isolation and sequence of complementary DNA encoding human extracellular superoxide dismutase. *Proc. Natl. Acad. Sci.* 84: 6340-6344. 1984.
115. Baechner D., Kreienkamp H.J., Richter D. MIZIP, a highly conserved, vertebrate specific melanin-concentrating hormone receptor 1 interacting zinc-finger protein. *FEBS Lett.* 526: 124-128. 2002.
116. Da Cruz e Silva E.F., Fox C.A., Ouimet C.C., Gustafson E., Watson S.J., Greengard P. Differential expression of protein phosphatase 1 isoforms in mammalian brain. *J. Neurosci.* 15: 3375-3389. 1995.

117. Watt R.K., Ludden P.W. Nickel-binding proteins. *Cell. Mol. Life Sci.* 58: 604-625. 1999.
118. Koihe K., Kobayashi M., Yaginuma K., Toira M., Yoshida E., Imai M. Nucleotide sequence and evaluation of the rat mitochondrial cytochrome b gene containing the ochre termination codon. *Gene.* 20 (2): 177-185. 1982.
119. Samuelson E., Hedberg C., Nilsson S., Behboudi A. Molecular classification of spontaneous endometrial adenocarcinomas in BDII rats. *Endocrine-Related Cancer.* 16:99-111.2009.
120. 120. Gibbs,R.A and all. The status, quality, and expansion of the NIH full-length cDNA project: the Mammalian Gene Collection (MGC). *Genome Res.* 14: 2121-127. 2004.
121. Arner E.S., Holmgren A. Physiological function of thioredoxin and thioredoxin reductase. *Eur J Biochem.* 267: 6102-6109. 2000.
122. Whanger P.D. Selenoprotein W: a review. *CMLS, Cell.Mol.Life Sci.* 57: 1846-1852. 2000.
123. Gutteridge J.M.C. Biological Origin of free radicals, and mechanisms of antioxidant protection. *Chemico-Biological Interactions* 91 (2-3): 133-140. 1994.
124. Arthur J.R., McKenzie R.C., Beckett G.J. Selenium in the immune system. *J Nutr* 133 (5): 14575-14595. 2003.
125. Mackness M.I., Arrol S., Durrington P.N. Paraoxonase prevents accumulation of lipoperoxides in low-density lipoprotein. *FEBS Letters* 286: 152 – 154. 1991.
126. Watson A.D., Berliner J.A., Hama S.Y., La Du B.N., Faull K.F., Fogelman A.M., Navab M. Protective effect of high density lipoprotein associated paraoxonase. Inhibition of the biological activity of minimally oxidized low density lipoprotein. *J. Clin. Invest.* 96: 2882 – 2891.1995.
127. Chevallez m., Luche S., Rabilloud T. Silver steining of proteins in polyacrylamide gels. *Nat Protoc.* 1 (4): 1852-1858. 2006.
128. Blatter M.C., James R.W., Messmer S., Barja F., Pometta D. Identification of a distinct human high-density lipoprotein subspecies defined by a lipoprotein-associated protein, K-45. Identity of K-45 with paraoxonase. *Eur J Biochem.* 211 (1): 871-879. 1993.
129. Pidcock E. Moore G.R. Structural characteristics of protein binding sites for calcium and lanthanide ions. *J Biol Inorg Chem.* 6: 479-489. 2001.
130. Lusis A.J., Atherosclerosis. *Nature* 407: 233-241. 2000.

131. James R.W., Deakin S. P. The importance of high-density lipoproteins for Paraoxonase-1 secretion, stability and activity. *Free Radic. Biol. Med.* 37 (12): 1986-1994. 2004.
132. Dragonov D.I., La Du B.N. Pharmacogenetics of paraoxonases: a brief review. *Naunyn-Schmiedeberg's Arch Pharmacol.* 369: 78-88. 2004.
133. Costa L.G., Cole T.B., Jarvik G.P., Furlong C.E. Functional genomics of the Paraoxonase (PON1) polymorphism: effects on pesticide sensitivity, cardiovascular disease and drug metabolism. *Annu. Rev. Med.* 54: 371-392. 2003.
134. Husain M.H., Dick J.A., Kaplan Y.S. Rare earth pneumoconiosis. *Occup. Med.* 30: 15-19. 1980.
135. Stohs S.J., Bagchi D. Oxidative mechanisms in the toxicity of metal ions. *Free Radical Biology and Medicine* 18: 321-336. 1995.
136. Beaugé L A., Sjodin R. A. Transport of cesium in frog muscle. *J Physiol.* 194 (1): 105-123. 1968.
137. Chesters J.K., Will M. Zinc transport proteins in plasma. *Br J Nutr.* 46 (1): 111-118. 1981.
138. Rink L., Gabriel P. Zinc and the immune system. *Proc Nutr Soc.* 59 (4): 541-552. 2000.
139. Behne D., Wolters W. Distribution of selenium and glutathione peroxidase in the rat. *J Nutr.* 113 (2): 456-461. 1983.
140. Koster J.F., Slee R.G. Ferritin, a physiological iron donor for microsomal lipid peroxidation. *FEBS.* 199 (1): 85-88. 1986.
141. Williams Ch.H., Arscott L.D., Müller S., Lennon B.W., Ludwig M.L., Wang P.F., Veine D.M., Becker K., Schirmer R.H. Thioredoxin reductase. *FEBS* 267 (20): 6110-6117. 2000.
142. Epp O., Ladenstein R., Wendel A. "The refined structure of the selenoenzyme glutathione peroxidase at 0.2-nm resolution". *Eur J Biochem* 133 (1): 51-69. 1983.
143. Rotruck J.T., Pope A.L., Ganther H.E., Swanson A.B., Hafeman D.G., Hoekstra W.G. Selenium: Biochemical Role as Component of Glutathione Peroxidase. *Science* 179:588-590. 1973.
144. Shchedrina V.A., Zhang Y., Labunskyy V.M., Hatfield D.L., Gladyshev V.N. Structure-function, relations, physiological roles, and evolution of mammalian ER-resident selenoproteins. *Antioxidand redox Signal.* 12 (7): 839-849. 2010.

145. Whanger P.D. Selenoprotein expression and function – selenoprotein W. *Biochim Biophys Acta* 1790 (11): 1448-1452. 2009.
146. Ferguson D.A., Labunskyy V. M., Fomenko D. E., Arac D., Chelliah Y., Amezua C.A., Rizo J., Gladyshev V.N., Deisenhofer j. NMR structures of the selenoproteins Sel15 and SelM reveal redox activity of a new thioredoxin-like family. *J Biol Chem.* 281: 3536-3543. 2006.
147. Apostolou S., Klein J.O., Mitsuuchi Y., Shelter J.N., Poulikakos P.J., Jhanwar S.C., Kruger W.D., Testa J.R. Growth inhibition and induction of apoptosis in mesothelioma cells by selenium and dependence on selenoprotein SEP 15. *Oncogene.* 23: 5032–5040. 2004.
148. Imai H., Nakagawa Y. Biological significance of phospholipide hydroperoxide glutathione peroxidase ((PHGPx, GPx4) in mammalian cells. *Free Radic Biol Med.* 34: 145-169. 2003.
149. Ursini F., Maiorino M., Roveri A. Phospholipid hydroperoxide glutathione peroxidase (PHGPx): more than an antioxidant enzyme? *Biomed Environ Sci.* 10 (2-3): 327-332. 1997.
150. Hidioglou M., Carson R.B., Brossard G.A. Problems associated with selenium deficiency in beef calves. *Can J Physiol Pharmacol.* 46: 853-858. 1968.
151. Tripp M.J., Whanger P.D., Schmitz J.A. Calcium uptake and ATPase activity of sarcoplasmic reticulum vesicles isolated from control and selenium deficient lambs. *J Trace Elem Electrolytes Health Dis.* 7: 75-82. 1993.
152. Papp L.V., Lu J., Holmgren A., Khanna K.K. From selenium to selenoproteins: synthesis, identity and the role in human health. *Antioxidants and Redox Signaling.* 7(9): 775-806. 2007.
153. Rayman M.P. The importance of selenium to human health. *Lancet.* 356: 233-241. 2000.
154. Hawkes W.C., Wilhelmsen E.C., Tappel A.L. Abundance and tissue distribution of selenocystein-containing proteins in the rat. *J Inorg Biochem.* 23: 77-92. 1985.
155. Dewberry K, Fox JS, Stewart J et al: Lanthanum carbonate: a novel non-calcium containing phosphate binder. *J Am Soc Nephrol.* 8:A2610. 1997.
156. Klotz L.O., Kröncke K.D., Buchczyk D.P., Sis H. Role of copper, zinc, selenium and tellurium in the cellular defence against oxidative and nitrosative stress. *J. Nutr.* 133: 1448-1451. 2003.

## 9 Appendix

### 9.1 List of abbreviations

2D	two-dimensional
AA	acrylamide
ABTS	2,2'-Azino- di-(3-ethylbenzthiazoline sulphonate)
AOS	active oxygen species
APS	ammonium persulfate
ARDS	adult respiratory distress syndrome
BA	N,N'-methylenebisacrylamide
BER II	Berliner-Experimentier-Reaktor
BSA	bovine serum albumin
CHAPS	3-[(3-Cholamidopropyl)dimethylammonium]-1-propanesulfonate
cpm	counts per minute
Da	Dalton
DMEM	Dulbecco's Modified Eagle Medium
DNA	deoxyribonucleic acid
DSMZ	Deutsche Sammlung von Mikroorganismen und Zellen
DTT	dithiothreitol
EDTA	ethylenediaminetetraacetic acid
FBS	fetal bovine serum
g	acceleration of gravity
Hepes	2-[4-(2-hydroxyethyl)piperazin-1-yl]ethanesulfonic acid
HPLC	high performance liquid chromatography
ICP-MS	inductively coupled plasma mass spectrometry
IgG	immunoglobulin G
INAA	Instrumental Neutron Activation Analysis
MW	molecular weight
NEpHGE	Non-Equilibrium-pH Gradient Electrophoresis
NP-40	Nonidet P-40
PAGE	polyacrylamide gel electrophoresis
PBS	phosphate buffer saline
pI	isoelectric point
PMN	polymorphonuclear leukocyte
PMSF	phenylmethylsulfonyl fluoride
RF	radio frequency
RNA	ribonucleic acid
SEC	size exclusion chromatography
SDS	sodium dodecyl sulfate
TEMED	N,N,N',N'-tetramethyl-ethane-1,2-diamine
Tris	2-amino-2-hydroxymethyl-propane-1,3-diol
tRNA	transfer ribonucleic acid
v/v	volume per volume
w/v	weight per volume

## 9.2 Publications

**Charkiewicz E.** et al.

Study on the distribution of trace element containing proteins in the skeletal muscle of rat and mouse myoblast cell line. In preparation

**Charkiewicz E., Bartel J., Bartel J., Plotnikov A., Kyriakopoulos A.**

The Role of Selenium in the Antioxidative Defence System of Skeletal Muscle. Proceedings of the European Conference on Metallobiomics, 2008, München: Utz ISBN 978-3-8316-0982-6, p. 21-26

**Bartel J., Charkiewicz E., Bartz T., Bartel J., Schmidt D., Grabavac I., Kyriakopoulos A.**

Metalloproteome of the prostate: carcinoma cell line DU-145 in comparison to healthy rat tissue. Cancer Genomics Proteomics 7(2): 81-86. 2010

**Bartel J., Charkiewicz E., Bartel J., Bartz T., Kyriakopoulos A.**

Studies about the Deubiquitinating Enzyme UCH-L3 in the Metabolism of selenium. Proceedings of the European Conference on Metallobiomics, 2008, München: Utz ISBN 978-3-8316-0982-6, p. 8-16

**Bartz T., Charkiewicz E., Bartel J., Soete A., Kyriakopoulos A.,**

Molybdän im Dickdarm und in der Dickdarmkarzinomzelllinie Ht9. Experimentelle Modelle der Spurenelementforschung, 2008, München, Herbert Utz verlag.

**Kajikhina E., Schmidt D., Charkiewicz E., Bartel J., Bartel J., Pohl T., Kyriakopoulos A.**

Localisation of the metallothionein and the 15 kDa-selenoprotein in the brain and prostate and determination of the total antioxidant capacity of the tissues in action. Proceedings of the European Conference on Metallobiomics, 2008, München: Utz ISBN 978-3-8316-0982-6, p. 33-43



**Bartz T., Schmidt D., Charkiewicz E., Bartel J., Kyriakopoulos A.**

Investigation of metal- and metalloid binding proteins in the tongue of the rat by means of SECI-ICP-MS. Proceedings of the European Conference on Metallobiomics, 2008, München: Utz ISBN 978-3-8316-0982-6, p.

**Kyriakopoulos A., Schmidt D., Kajikhina E., Charkiewicz E., Plotnikov A., Bartel J.**

Characterization of antioxidative effecting proteins in the brain, prostate and cell lines by combination of analytical and biochemical procedures. Proceedings of the European Conference on Metallobiomics, 2008, München: Utz ISBN 978-3-8316-0982-6, p. 63-72

**Bartz T., Bartel J., Soete A., Charkiewicz E., Kyriakopoulos A.**

Expression Pattern of the Ubiquitin C-terminal Hydrolase in Rat Colon and in the Human Colon Carcinoma Cell line HT-29. Anticancer Research. 28: 3207. 2008

**Poster:**

**Charkiewicz E., Bartel J., Bartel J., Plotnikov A., Kyriakopoulos A.**

The Role of Selenium in the Antioxidative Defence System of Skeletal Muscle of the Rat.

2<sup>nd</sup> European Conference on Metallobiomics 2008 Berlin

**Bartel J., Charkiewicz E., Bartel J., Bartz T., Kyriakopoulos A.**

Studies about the Deubiquitinating Enzyme UCH-L3 in the Metabolism of selenium.

2<sup>nd</sup> European Conference on Metallobiomics 2008 Berlin

**Bartz T., Charkiewicz E., Bartel J., Soete A., Kyriakopoulos A.,**

Molibdenum in Rat Colon and the Human Colon Carcinoma Cell line HT29.

24. Jahrestagung der GMS 2008 Berlin

**Bartz T., Bartel J., Soete A., Charkiewicz E., Kyriakopoulos A.**

Expression Pattern of the Ubiquitin C-terminal Hydrolase in Rat Colon and in the Human Colon Carcinoma Cell line HT-29.

8<sup>th</sup> International Conference of Anticancer Research 2008 Kos

**Oral Communication:**

Antioxidantien - Status im Skelettmuskel und in der Lunge der Ratte und Zelllinien.

4<sup>th</sup> Workshop on Coordination Chemistry of Metals with Medicals Relevance and Supramolecular Building Blocks, 2011 Berlin

## 9.3 Acknowledgements

This dissertation is the fruit of my three-year PhD work. The study would not have been completed without the support, guidance and patience of many people. That is why I would like to express my deepest gratitude to the following individuals.

I am sincerely and heartily grateful to Dr. Antonios Kyriakopoulos, for the support and guidance he showed me throughout my dissertation writing.

I would like to thank Prof. Dr. Ulrich Abram for the numerous of tips while writing the dissertation and for the external supervision and reviewing my thesis.

I would also like to thank Prof. Dr. Nora Graf for reviewing my thesis.

I would also like to thank the INAA team: Dr. Dorothea Alber, Gregor Bukalis and Brigitte Stanik for the samples measurement, gamma ray spectrums evaluation and for introducing me to this interesting analytical methods.

Special thanks goes to Jürgen Bartel for supporting me during my experiments, for the patience – with my never ending questions and for the help in solving technical problems.

Many thanks to Alexandra Graebert for numerous tips in cell experiments.

I would also like to thank Dr. Alexei Plotnikov for the help in solving computer problems and to Dr. Dennis Schmidt for all the useful conversations.

To all members of F-A1: Thank you very much for the friendly atmosphere in the workplace.

Many thanks to Kasia for always supporting me and for being helpful in my work.

Finally, I would like to thank Kai for all the encouragement and profound understanding, the support and constant patience.

## **9.4 Curriculum Vitae**

For reasons of data protection,  
the curriculum vitae is not included in the online version

## **9.5 Selbständigkeitserklärung**

Hiermit versichere ich gemäß §6 (4), dass ich die vorliegende Arbeit selbständig und mit keinem anderem als den angegebenen Hilfsmitteln angefertigt habe.

Elzbieta Charkiewicz